ドリフト分岐とその応用

I ：ドリフト分岐と進行波解
II : ドリフト分岐が生じる具体例
III: ドリフト分岐点近傍における反射現象

栄 伸一郎
明治大学，城西大学

Ⅰ　：ドリフト分岐と進行波解

反応拡散型モデル方程式系
Reaction-diffusion systems

$$\mathbf{u}_\mathbf{t} = \mathbf{D}\Delta\mathbf{u} + \mathbf{F}(\mathbf{u}), \quad t > 0, x \in \Omega \subset \mathbf{R}^n$$

$$\mathbf{D} = \begin{pmatrix} d_1 & \cdots & 0 \\ & \ddots & \\ 0 & \cdots & d_N \end{pmatrix}, \quad \mathbf{u} \in \mathbf{R}^N, \quad \mathbf{F} : \mathbf{R}^N \to \mathbf{R}^N$$

$\mathbf{u}_\mathbf{t} = \mathbf{D}\Delta\mathbf{u}$, 拡散(Diffusion)

$\mathbf{u}_\mathbf{t} = \mathbf{F}(\mathbf{u})$, 反応(Kinetics)

反応拡散
Reaction-diffusion

$\mathbf{u} = \mathbf{u}(t, x)$ の時間 t, 及び空間 x に関する依存性を調べる.
Dependence on time t, space x

パターン形成のメカニズム
Mechanism of pattern formation

様々な現象と反応拡散モデル方程式
Various reaction-diffusion model systems

・BZ reaction, Keener-Tyson model

$$\begin{cases} u_t = \varepsilon d_1 \Delta u + u(1-u) - \dfrac{bv(u-a)}{u+a}, \\ v_t = \varepsilon(d_2 \Delta v + u - v), \end{cases}$$





・燃焼方程式 (combustion model)

$$\begin{cases} T_t = & d_1 \Delta T + \beta n f(T), \\ n_t = & d_2 \Delta n - \beta n f(T), \end{cases}$$

$$f(T) = e^{\frac{1}{\varepsilon}\left(1 - \frac{1}{1+\alpha(T-1)}\right)}$$

・結晶成長,Phase-Field model (Kobayashi)

$$\begin{cases} \tau p_t = & div\{d(x)\nabla p\} + f(p,T), \\ T_t = & d_2 \Delta T - \kappa p_t, \end{cases}$$

$$f(p,T) = p(1-p)(p-a(T))$$

- 形態形成Gierer-Meinhardt model

$$\begin{cases} u_t &= d_1 \Delta u - u + \dfrac{u^p}{v^q}, \\ \tau v_t &= d_2 \Delta v - v + \dfrac{u^r}{v^s}, \end{cases} \quad t>0,\ x \in \Omega,\ p>1,\ 0<\frac{p-1}{q}<\frac{r}{s+1}$$

Regeneration of hydra

$$\Omega \subset \mathbf{R}^1, \mathbf{R}^2, \quad 0 < d_1 << 1$$

Ecology of Hydra

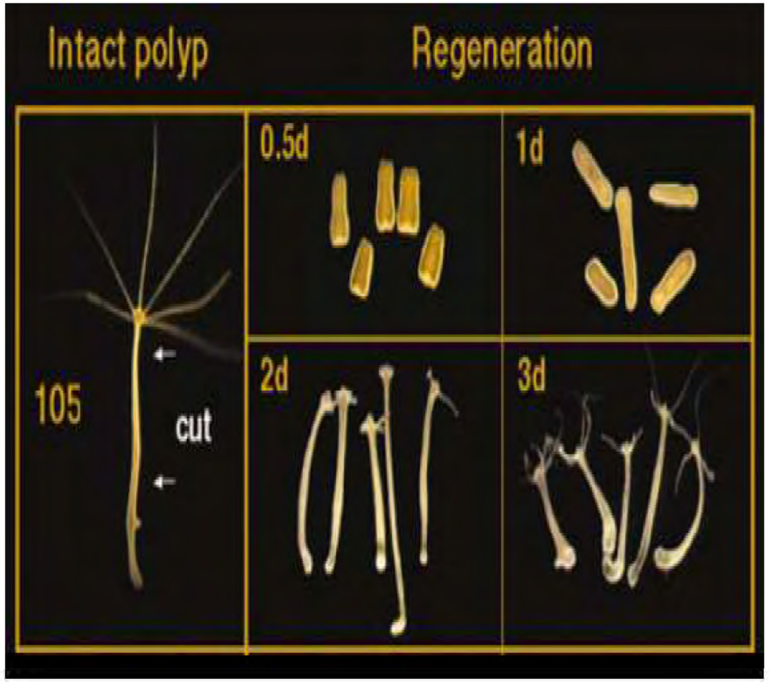

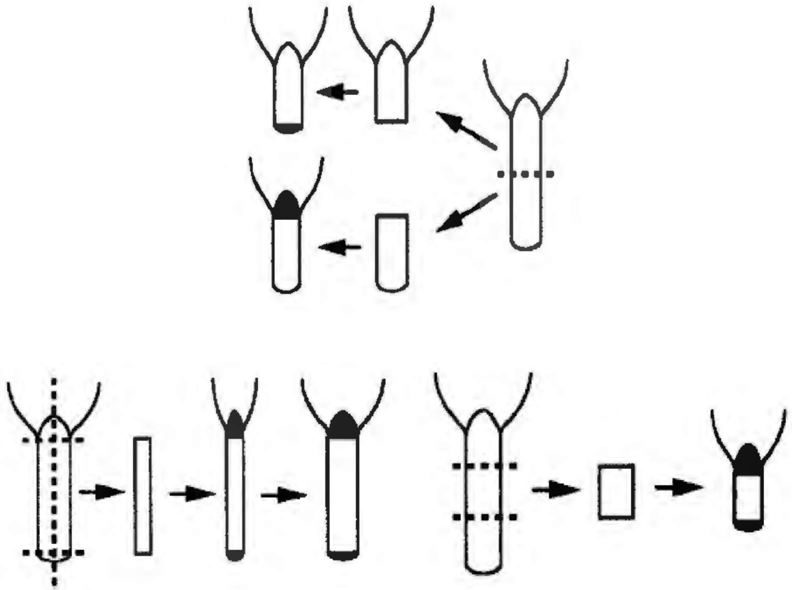

- nerve impulse, FitzHugh-Nagumo model

$$\begin{cases} u_t = u_{xx} + f(u) - v, \\ v_t = \varepsilon(u - \gamma v), \end{cases} \quad t > 0, x \in \mathbf{R}^1$$

$$f(u) = u(1-u)(u-a)$$

$$0 < \varepsilon << 1, \ \gamma > 0$$

Existence, Hastings '76
Stability, Jones '84
Yanagida '85

Traveling solution

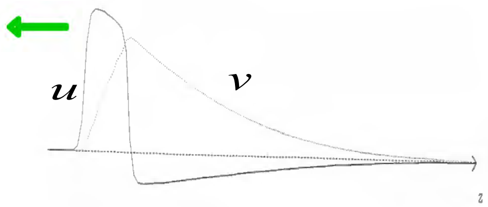

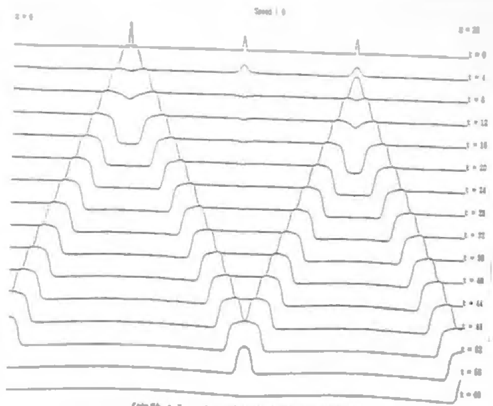
[実験1] インパルスの発生と悉無律

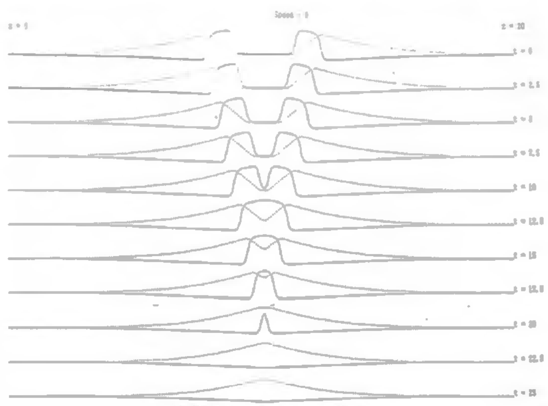
[実験3] インパルスの衝突

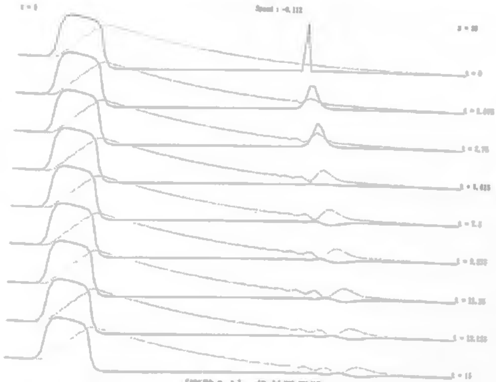
[実験2.1] 絶対不応期

Reaction-diffusion systems

$$\mathbf{u}_{\mathbf{t}} = \mathbf{D}\Delta\mathbf{u} + \mathbf{F}(\mathbf{u}), \quad t > 0, x \in \Omega \subset \mathbf{R}^n$$

$$\mathbf{D} = \begin{pmatrix} d_1 & \cdots & 0 \\ & \ddots & \\ 0 & \cdots & d_N \end{pmatrix}, \quad \mathbf{u} \in \mathbf{R}^N, \quad \mathbf{F} : \mathbf{R}^N \to \mathbf{R}^N$$

パルス状局在解 (pulse like localized solutions)

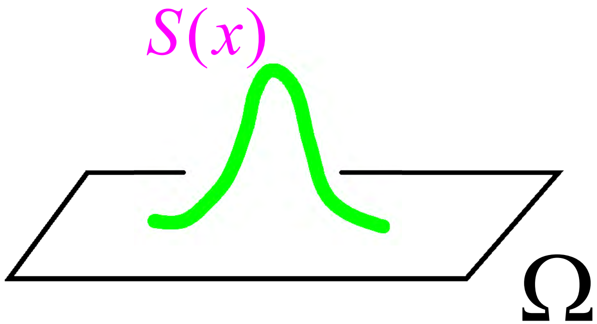

$$S(x) \to \mathbf{0} \quad (|x| \to \infty)$$

Ex.神経パルス, FitzHugh-Nagumo model

$$\begin{cases} u_t = u_{xx} + f(u) - v, \\ v_t = \varepsilon(u - \gamma v), \end{cases} \quad t > 0, x \in \mathbf{R}^1$$

$$f(u) = u(1-u)(u-a)$$

$$0 < \varepsilon << 1,\ \gamma > 0,\ 0 < a < \frac{1}{2}$$

Existence, Hastings ‘76
Stability, Jones ‘84
Yanagida ‘85

Stable Traveling pulse solution

進行波

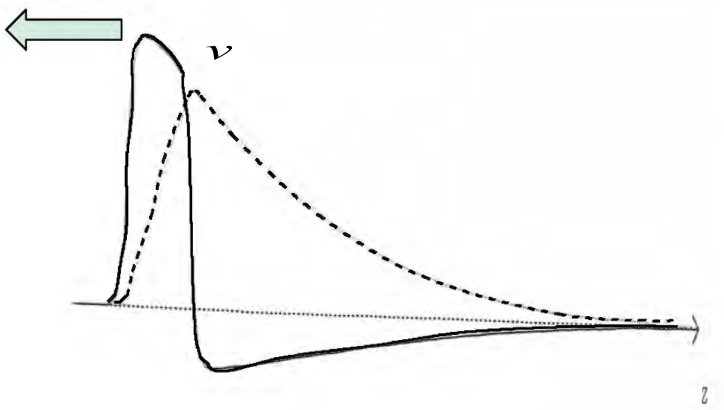

Ex. Gierer-Meinhardt model

$$\begin{cases} u_t = d_1 \Delta u - u + \dfrac{u^p}{v^q}, \\ \tau v_t = d_2 \Delta v - v + \dfrac{u^r}{v^s}, \end{cases} \quad t>0, x \in \Omega, \quad p>1, 0<\frac{p-1}{q}<\frac{r}{s+1}$$

$$\Omega \subset \mathbf{R}^1, \mathbf{R}^2, \quad 0 < d_1 << 1$$

$d_1 = \varepsilon^2 << 1,\ 0 \le \tau << 1$ ⟹

Pulse-like localized Spike solutions　スパイク解

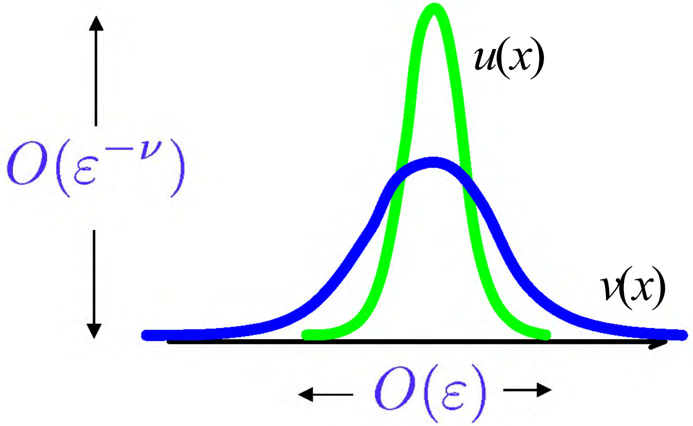

Ni, Takagi '91
Ni, Takagi, Yanagida '99
Ei, Wei '02

1D
stationary

2D

Spike solution of Gierer-Meinhardt

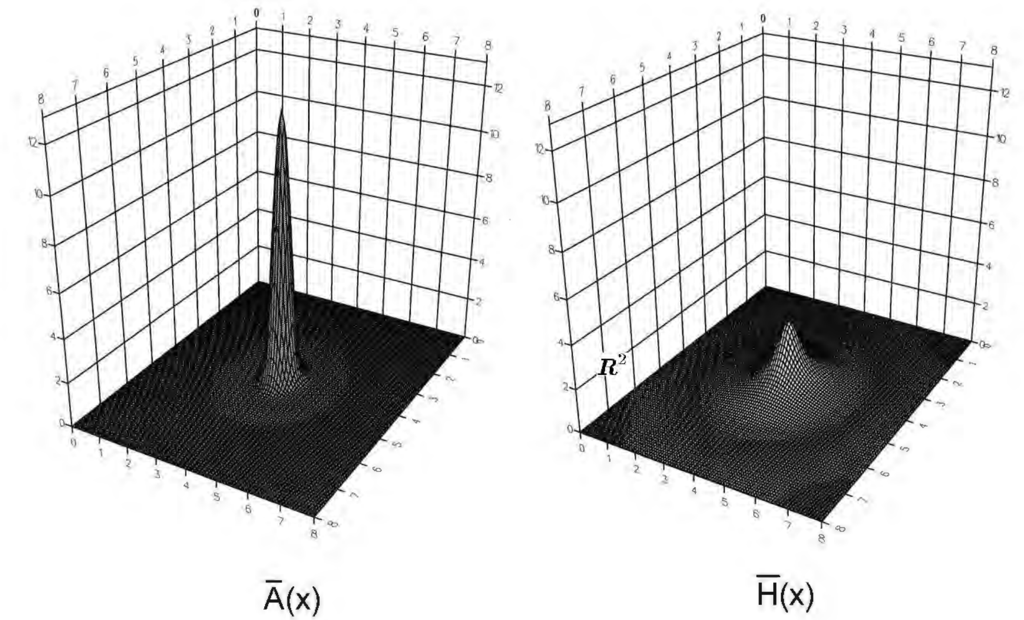

Stationary spike solution in $\boldsymbol{R}^2$
(Radially symmetric)
(E. Wei 02)

Ex. Gray-Scott model

$$\begin{cases} u_t = d_1 \Delta u - uv^2 + A(1-u), \\ v_t = d_2 \Delta v + uv^2 - (A+k)v, \end{cases} \quad t > 0, x \in \Omega \subset \mathbf{R}^1, \mathbf{R}^2$$

Pulse-like localized Spike solutions　スパイク解

$$(u(x), v(x)) \to (1,0) \ (|x| \to \infty)$$

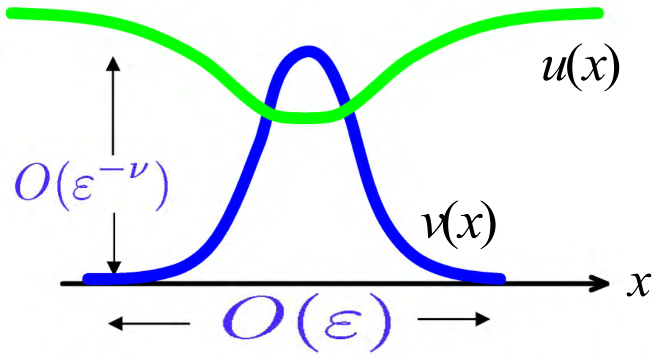

$$d_2 = \varepsilon^2,\ A = \varepsilon^2 a,\ k = \varepsilon^\mu b \ (0 < \mu < 1)$$

Stationary in $\boldsymbol{R}^1$
(Doelman et.al.99)

(Wei'01)

2 D

Spike solution of Gray-Scott model

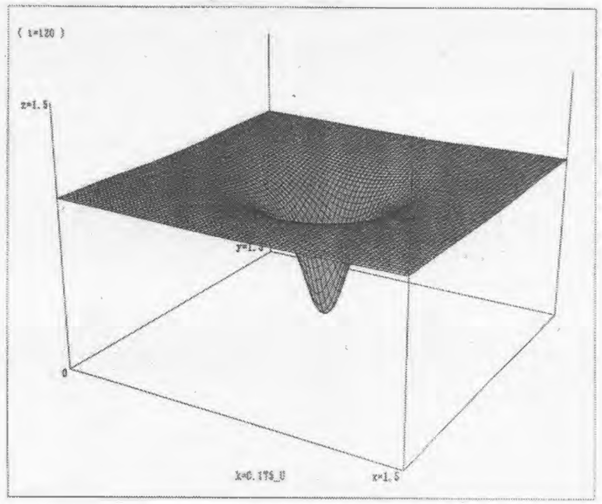

u 成分

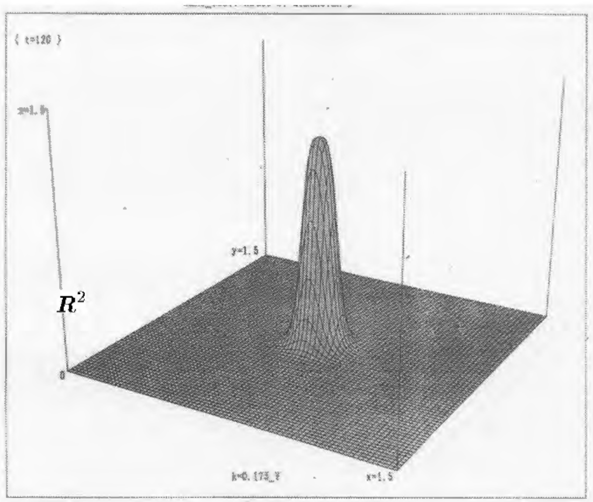

v 成分

Stationary solution in $\boldsymbol{R}^2$
(Wei 01)

Reaction-diffusion systems

$$\mathbf{u}_{\mathbf{t}} = \mathbf{D}\Delta\mathbf{u} + \mathbf{F}(\mathbf{u}), \quad t > 0, x \in \Omega \subset \mathbf{R}^{n}$$

$$\mathbf{D} = \begin{pmatrix} d_1 & \cdots & 0 \\ & \ddots & \\ 0 & \cdots & d_N \end{pmatrix}, \quad \mathbf{u} \in \mathbf{R}^{N}, \quad \mathbf{F} : \mathbf{R}^{N} \to \mathbf{R}^{N}$$

パルス状局在解 (pulse like localized solutions)

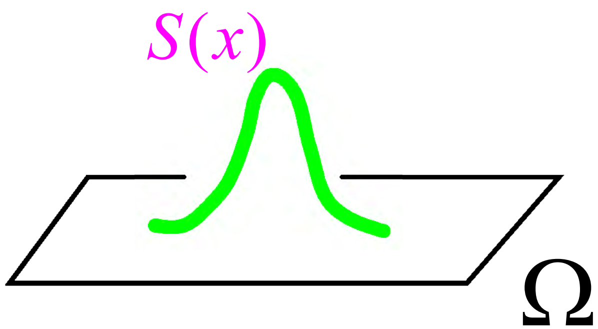

$$S(x) \to \mathbf{0} \quad (|x| \to \infty)$$

進行パルスの分岐: ドリフト分岐

$$\mathbf{u}_t = D\Delta\mathbf{u} + \mathbf{F}(\mathbf{u}; k)$$

方程式にパラメータ ***k*** を導入

Traveling pulses 進行波解

Standing pulses 定常解 (偶関数と仮定)

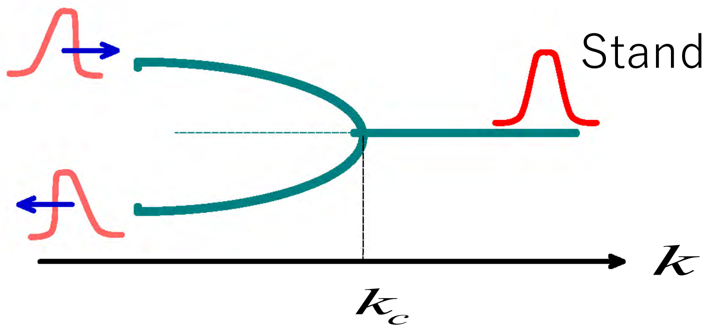

$k = k_c$; 分岐点 (ドリフト分岐点)

ドリフト分岐の例

E., Mimura,Nagayama 01

$$\begin{cases} u_t = d_1 u_{xx} + \dfrac{1}{\varepsilon} f(u,v), \\ v_t = d_2 v_{xx} + g(u,v), \end{cases} \quad t > 0, x \in \mathbf{R}^1$$

$$f(u,v) = -au + \exp(u/(1+u/c))v,$$

$$g(u,v) = h(v^* - v) - \exp(u/(1+u/c))v$$

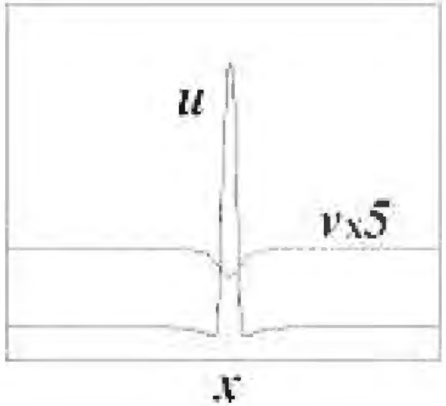

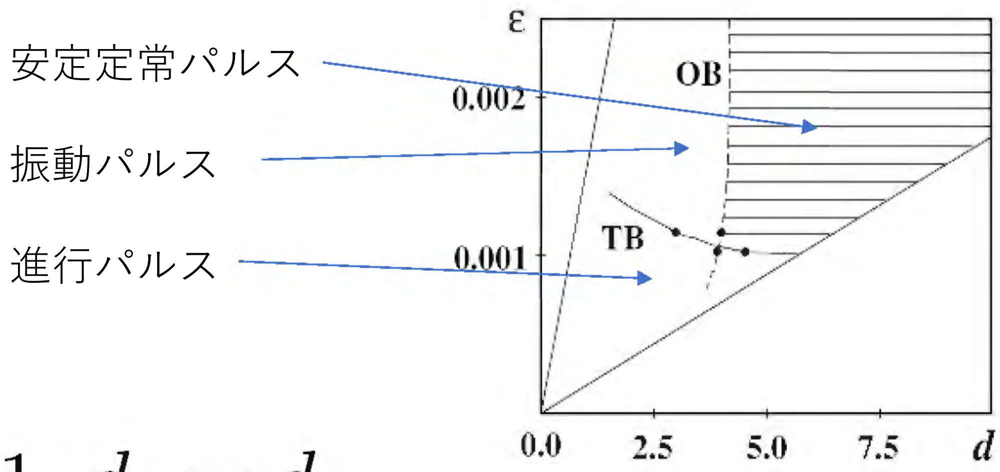

(a)

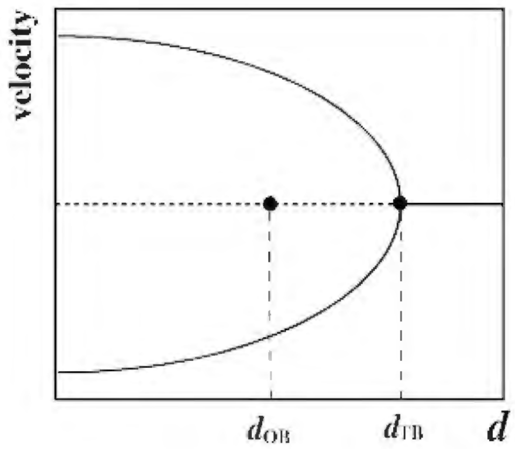

(b)

$$d_1 = 1,\ d_2 = d$$

Kawaguchi-Mimura Model 98

$$\begin{cases} \sigma u_t = \varepsilon \Delta u + \varepsilon^{-1} f(u,v,w), \\ v_t = \Delta v + u - v + h_1, \\ \tau w_t = d\Delta w + u - w + h_2 \end{cases} \qquad t > 0, x \in \Omega \subset \mathbf{R}^2,$$

$$f(u,v,w) = ru - u^3 - k_1 v - k_2 w.$$

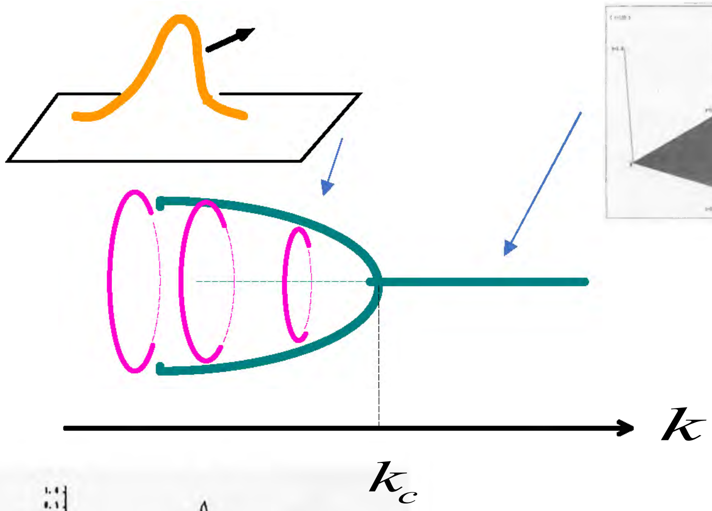

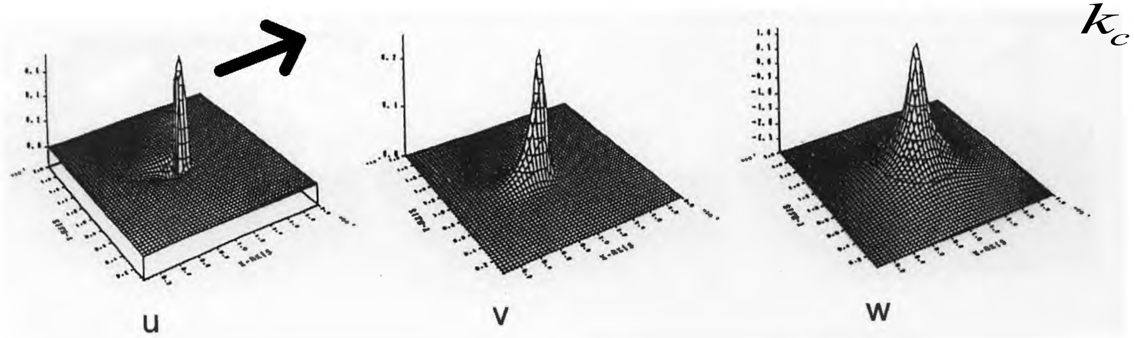

$\varepsilon = 0.1, \sigma = 0.04, r = 1.5, k_1 = 1.0, k_2 = 5.0,$
$h_1 = 1.0, h_2 = 0.8, \tau = 0.01, d = 7.0$

ドリフト分岐点の構造
-ジョルダンブロック型退化-

例: $L = \begin{pmatrix} 0 & 1 \\ 0 & 0 \end{pmatrix}$

固有方程式 $\lambda^2 = 0$

$$\Phi_0 = \begin{pmatrix} 1 \\ 0 \end{pmatrix},\ L\Phi_0 = \mathbf{0},\ \dim KerL = 1$$

$$\Phi_1 = \begin{pmatrix} 0 \\ 1 \end{pmatrix},\ L\Phi_1 = \Phi_0,\ KerL^2 = \mathbb{R}^2$$

退化:
0 固有値を持つこと
(実部 0 の固有値を持つこと)

ジョルダンブロック型:

$$KerL^2 \underset{\neq}{\supset} KerL$$

$$^\exists\Phi_1 \text{ s.t. } L\Phi_1 = \Phi_0$$

半単純: $KerL^2 = KerL$

単純: $\dim KerL = \dim KerL^2 = 1$

進行パルスの分岐

$$U_t = D\partial_x^2 U + F(U;k),\ -\infty < x < +\infty$$ 方程式にパラメータ ***k*** を導入

$$U \in \mathbb{R}^N,\ D = diag\{d_1, \cdots, d_N\}$$

Traveling pulses

Standing pulse ***S***(x), even

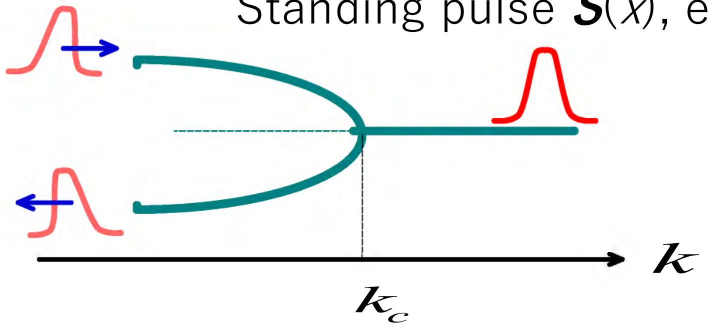

$k = k_c$; 分岐点 (ドリフト分岐点)

$$L = D\partial_x^2 + F'(S(x);k_c)$$ 線形化作用素

$$\begin{aligned} U_t &= DU_{xx} + F(U) + \eta G(U)\ (= F(U;k_c+\eta)) \\ &= \mathcal{L}(U) + \eta G(U) \end{aligned}$$

平行移動の自由度

命題: 0 が単純固有値なら k_c は分岐点でない

$$\mathcal{L}(S(x)) = 0 \Rightarrow \underbrace{\mathcal{L}'(S(x))}_{L} S_x = 0 \Rightarrow LS_x = 0$$ 退化？

単純固有値である場合の命題

平行移動の自由度 $LS_x = 0$

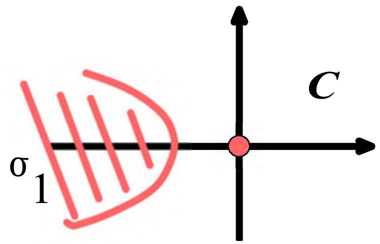

命題. 0 が *L* の単純固有値で

$$\sigma(L) = \sigma_1 \cup \{0\},\ \sigma_1 \subset \{Re(\lambda) < -\gamma < 0\}$$

ならば初期値が *S*(*x*) に十分近い

$$U_t = D\partial_x^2 U + F(U),\ -\infty < x < +\infty$$

の解 *U*(*t*,*x*) に対して, ある *b* があって

$$|U(t,x) - S(x-b)| \to 0\ (t \to \infty)$$

となる. $\Longrightarrow$ *S*(*x*) は線形安定, という

Dynamics of pulses near singularity

- Properties of the linearized operator L

1. L has always the zero eigenvalue

$$LS_x = \mathbf{0} \quad (LS_y = \mathbf{0})$$

2. L has another singularity

- Jordan Block (odd) $L\psi_1 = -S_x \ (L\psi_2 = -S_y)$
- Another zero eigenfunctions
  (symmetric, even) $L\psi_j = \mathbf{0}$
- Hopf point (symmetric, even)
- ・・・・・ $L\psi_1 = -\mu\psi_2, \quad L\psi_2 = \mu\psi_1 \quad (\mu > 0)$

Center Manifold Theory

$$\boldsymbol{u} \sim S(x-p) + \sum q_j \psi_j (x-p)$$

Jordan Block (1D case) (bifurcation diagram)

E., Mimura,Nagayama 01

$$LS_x = 0, \quad L\psi = -S_x \qquad \mathbf{u} \approx S(x-p) + q\psi(x-p)$$

$$\begin{cases} u_t = d_1 u_{xx} + \dfrac{1}{\varepsilon} f(u,v), \\ v_t = d_2 v_{xx} + g(u,v), \end{cases} \quad t > 0, x \in \mathbf{R}^1$$

$$f(u,v) = -au + \exp(u/(1+u/c))v,$$

$$g(u,v) = h(v^* - v) - \exp(u/(1+u/c))v$$

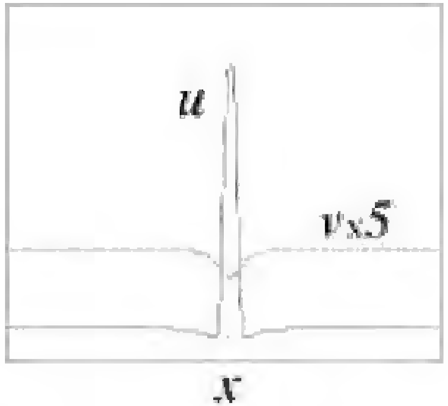

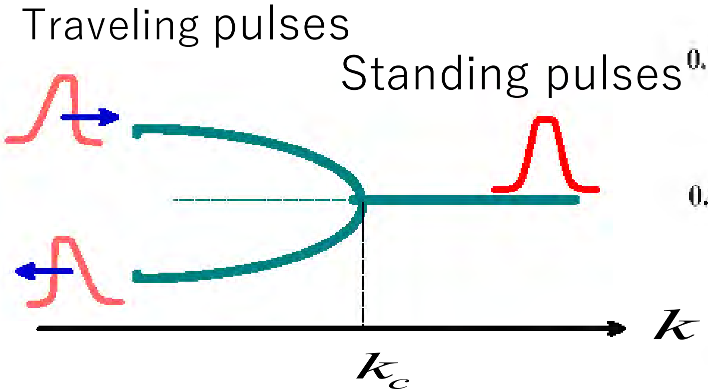

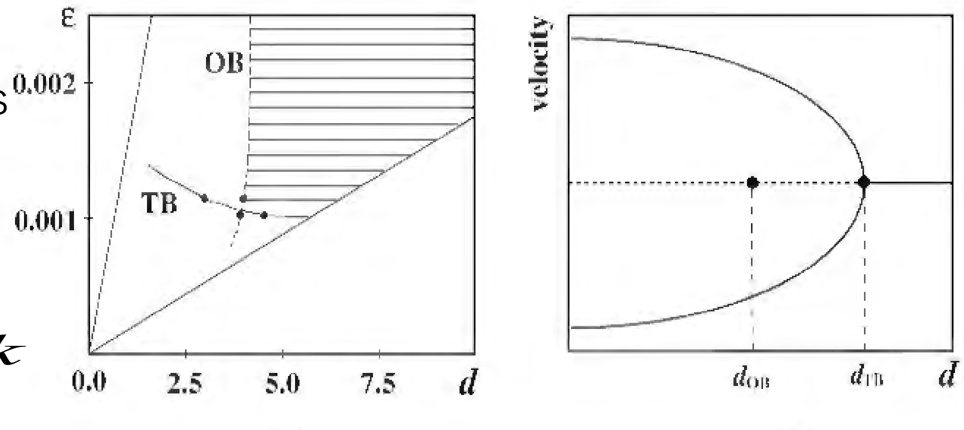

(a) (b)

Construction of traveling pulses

$$\begin{aligned} \boldsymbol{u}_t &= D\boldsymbol{u}_{xx} + F(\boldsymbol{u}) + \eta g(\boldsymbol{u}) \ (= F(\boldsymbol{u}; k_c + \eta)) \\ &= \mathcal{L}(\boldsymbol{u}) + \eta g(\boldsymbol{u}) \end{aligned}$$

$$X = L^2(\boldsymbol{R}^1)$$

Assume:

$$* \ {}^{\exists}S(x) \ s.t. \ \mathcal{L}(S(x)) \equiv 0$$

$$* \ L = \mathcal{L}'(S), \ LS_x = 0, \ L^{\exists}\psi = -S_x$$

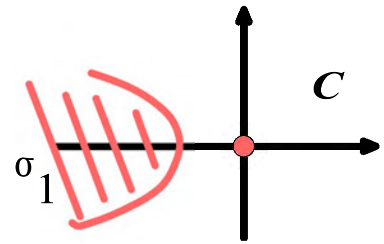

$$* \ \sigma(L) = \sigma_1 \cup \{0\}, \ \sigma_1 \subset \{Re(\lambda) < -\gamma < 0\}$$

Let $Q = \frac{1}{2\pi i}\int_C (\lambda - L)^{-1} d\lambda, \ R = Id - Q$ $\qquad L = D\partial_x^2 + F'(S(x))$

$$* \ QX = KerL^2 = span\{S_x, \ \psi\} = E \qquad RX = E^{\perp}$$

REM. $QX = span\{S_x\} \Rightarrow S(x)$; stable in linearized sense.

$$\mathcal{M} := \{S(\cdot - p)\ ;\ {}^{\forall} p \in \boldsymbol{R}^1\}$$

<u>Proposition</u>

$dist(\boldsymbol{u},\ \mathcal{M}) < \delta\ \Rightarrow {}^{\exists}p,\ q \in \boldsymbol{R}^1,\ {}^{\exists}\boldsymbol{w} \in E^{\perp}$

s.t. $\boldsymbol{u} = S(x-p) + q\psi(x-p) + \boldsymbol{w}(x-p)$

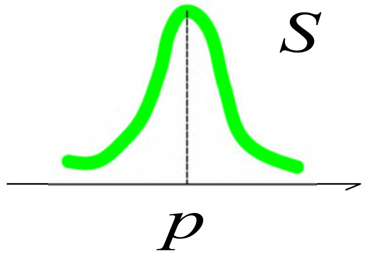

For $\boldsymbol{u}$ nbd. of $\mathcal{M}$, $\boldsymbol{u} \iff (p, q, \boldsymbol{w}) \in \boldsymbol{R} \times \boldsymbol{R} \times E^{\perp}$

<u>Theorem</u> (c.f. E. Wei '02)

$$\boldsymbol{u}_t = \mathcal{L}(\boldsymbol{u}) + \eta g(\boldsymbol{u}) \iff \left\{ \begin{array}{lcl} \dot{p} & = & H_1(q,\boldsymbol{w}) + \eta G_1(q,\boldsymbol{w}), \\ \dot{q} & = & H_2(q,\boldsymbol{w}) + \eta G_2(q,\boldsymbol{w}), \\ \boldsymbol{w}_t & = & L\boldsymbol{w} + H_3(q,\boldsymbol{w}) + \eta G_3(q,\boldsymbol{w}) \end{array} \right.$$

${}^{\exists}$*Localy attractive invariant manifold,*

$$\boldsymbol{w} = \sigma(q;\eta)\ \ : \to E^{\perp} \text{ s.t. } \|\sigma\|_{\omega} \le O(q^2 + |\eta|) \quad (X^{\omega} \hookrightarrow C^1(\boldsymbol{R}))$$

$$\boldsymbol{u}(t,x) = S(x-p) + q\psi(x-p) + \sigma(q;\eta)(x-p)$$

Dynamics of *q*

$$\begin{aligned} \boldsymbol{u}_t &= D\boldsymbol{u}_{xx} + F(\boldsymbol{u}) + \eta g(\boldsymbol{u}) \ (= F(\boldsymbol{u}; k_c + \eta)) \\ &= \mathcal{L}(\boldsymbol{u}) + \eta g(\boldsymbol{u}) \end{aligned}$$

$$\mathcal{A}(S(x)) = 0$$

$$\mathbf{u} = \begin{pmatrix} u \\ v \end{pmatrix}$$

$$\mathbf{u}(t,x) = S(x-p) + q\psi(x-p) + q^2\xi(x-p)$$
$$+\eta\varsigma(x-p) + \underline{\mathbf{v}(t,x-p)}$$

$$\xi, \varsigma, \mathbf{v} \in E^{\perp}$$

$$\approx O(q^3 + \eta^2)$$

$$(E^{\perp} = RX)$$

$$L = \mathcal{L}'(S), \ LS_x = 0, \ L^{\exists}\psi = -S_x$$

$$L^*\varphi^* = 0, \quad L^*\psi^* = -\varphi^*$$

All odd

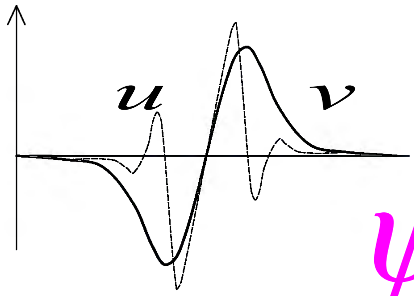

ψ ;odd

$$\boxed{\begin{aligned} &<\psi, S_x> = <\psi, \psi^*> = 0, < S_x, \psi^*> = 1, \\ &<\psi, \varphi^*> = 1, < S_x, \varphi^*> = 0 \end{aligned}}$$

$$E^{\perp} = \{\mathbf{v}; <\mathbf{v}, \psi^*> = <\mathbf{v}, \varphi^*> = 0\} \ni (\textit{even functions})$$

$$\mathbf{u}_{\mathbf{t}}(t,x) = \dot{p}S_x(x-p) + \dot{q}\psi(x-p) - \dot{p}q\psi_x(x-p) + \cdots$$

$$\mathcal{A}(\mathbf{u}) + \eta g(\mathbf{u}) = L\mathbf{v}(t,x-p) - qS_x(x-p) + \eta g(S(x-p)) + \cdots$$

$$x - p \Rightarrow x$$

$$\begin{aligned} &-\dot{p}S_x + \dot{q}\psi - \dot{p}q\psi_x + 2q\dot{q}\xi - q^2\dot{p}\xi_x - \eta\dot{p}\zeta_x - \dot{p}\boldsymbol{v}_x + \boldsymbol{v}_t \\ &= L\boldsymbol{v} + q^2L\xi + \eta L\zeta - qS_x + \eta g(S) + \tfrac{1}{2}q^2F''(S)\psi^2 + \eta q g'(S)\psi + O(\eta^2 + q^3) \end{aligned}$$

$$\langle \cdot, \psi^* \rangle$$

$$\dot{p}(1 + O(|q| + |\eta|)) = q + O(q^2 + \eta^2)$$

$$\therefore \quad \dot{p} = q + O(q^2 + \eta^2)$$

$$\langle \cdot, \varphi^* \rangle$$

$$\dot{q}(1 + O(q^2 + \eta^2)) = O(q^2 + \eta^2)$$

$$\therefore \quad \dot{q} = O(q^2 + \eta^2)$$

$$\dot{p} = q + O(q^2 + \eta^2)$$
$$\dot{q} = O(q^2 + \eta^2)$$
$$\|\boldsymbol{v}\|_\omega \le O(q^2 + |\eta|)$$
$$|\eta q| \le O(|q|^3 + |\eta|^{3/2})$$

$$-\cancel{\dot{p}}S_x + \dot{q}\psi - \dot{p}q\psi_x + 2q\dot{q}\xi - q^2\dot{p}\xi_x - \eta\dot{p}\zeta_x - \dot{p}\boldsymbol{v}_x + \boldsymbol{v}_t$$
$$= L\boldsymbol{v} + q^2 L\xi + \eta L\zeta - \cancel{qS_x} + \eta g(S) + \tfrac{1}{2}q^2 F''(S)\psi^2 + \eta q g'(S)\psi + O(\eta^2 + q^3)$$

$$\Downarrow$$

$$O(q^2 + \eta^2)S_x + \dot{q}\psi - q^2\psi_x + qO(q^2 + \eta^2)\psi_x + 2q\dot{q}\xi$$
$$-q^3\xi_x + q^2 O(q^2 + \eta^2)\xi_x - \eta q\zeta_x + \eta O(q^2 + \eta^2)\zeta_x - q\boldsymbol{v}_x + \boldsymbol{v}_t$$
$$= L\boldsymbol{v} + q^2\{L\xi + \tfrac{1}{2}F''(S)\psi^2\} + \eta\{L\zeta + g(S)\} + O(|q|^3 + |\eta|^{3/2})$$

$$\Downarrow$$

In $E^\perp$

$$-q^2\psi_x + \boldsymbol{v}_t = L\boldsymbol{v} + q^2\{L\xi + \tfrac{1}{2}F''(S)\psi^2\} + \eta\{L\zeta + g(S)\} + O(|q|^3 + |\eta|^{3/2})$$

q^2; $-\psi_x = L\xi + \dfrac{1}{2}F''(S)\psi^2$ $\quad\Downarrow\quad$ η; $\quad 0 = L\varsigma + g(S)$

$$\boldsymbol{v}_t = L\boldsymbol{v} + O(|q|^3 + |\eta|^{3/2}) \quad \text{In } E^\perp$$

$$\Downarrow$$

$$\boldsymbol{v} = O(|q|^3 + |\eta|^{3/2})$$

$$\dot{q}\psi + qO(q^2+\eta^2)\psi_x + 2q\dot{q}\xi - q^3\xi_x - \eta q\zeta_x + \boldsymbol{v}_t$$
$$= L\boldsymbol{v} + q^3\{F''(S)\psi\xi + \tfrac{1}{6}F'''(S)\psi^3\} + \eta q\{F''(S)\psi\zeta + g'(S)\psi\} + O(q^4+|\eta|^{3/2})$$

$$F(S+q\psi+q^2\xi+\eta\zeta)$$
$$= F(S)+F'(S)(q\psi+q^2\xi+\eta\zeta)+\tfrac{1}{2}F''(S)(q\psi+q^2\xi+\eta\zeta)^2+\tfrac{1}{6}F'''(S)(q\psi+q^2\xi+\eta\zeta)^3$$
$$= \cdots + q^3\{F''(S)\psi\xi+\tfrac{1}{6}F'''(S)\psi^3\} + \eta qF''(S)\psi\zeta + O(q^4+|\eta|^{3/2})$$

$$\eta g(S+q\psi+\cdots) = \eta g(S) + \eta q g'(S)\psi + O(q^4+|\eta|^{3/2})$$

$$\langle\ \cdot, \varphi^*\ \rangle$$

$$\boxed{\dot{q} = -M_1 q^3 + M_2\eta q + O(q^4+\eta^{3/2})}$$

$$M_1 = -<\xi_x + F''(S)\psi\xi + \frac{1}{6}F'''(S)\psi^3, \varphi^*>$$
$$M_2 = <\varsigma_x + F''(S)\psi\varsigma + g'(S)\psi, \varphi^*>

不変多様体の存在

$^{\exists}$*Localy attractive invariant manifold,*

$$\boldsymbol{w} = \sigma(q;\eta) \ : \to RX \text{ s.t. } \|\sigma\|_{\omega} \le O(q^3 + |\eta|^{3/2})$$

$$U(t,x) = S(x-p) + q\psi(x-p) + q^2\xi(x-p) + \eta\zeta(x-p) + \sigma(q;\eta)(x-p)$$

$$\therefore \boxed{\begin{aligned} \dot{p} &= q + O(q^2 + \eta^2) \\ \dot{q} &= -M_1 q^3 + M_2 \eta q + O(q^4 + \eta^{3/2}) \end{aligned}}$$

$$M_1 = -< \xi_x + F''(S)\psi\xi + \frac{1}{6}F'''(S)\psi^3, \varphi^* >$$

$$M_2 = < \varsigma_x + F''(S)\psi\varsigma + g'(S)\psi, \varphi^* >$$

$$q^2 ; -\psi_x = L\xi + \frac{1}{2}F''(S)\psi^2$$

$$\eta ; \quad 0 = L\varsigma + g(S)$$

進行パルスの分岐

$$U_t = D\partial_x^2 U + F(U;k),\ -\infty < x < +\infty$$ 方程式にパラメータ ***k*** を導入

$$U \in \mathbb{R}^N,\ D = diag\{d_1, \cdots, d_N\}$$

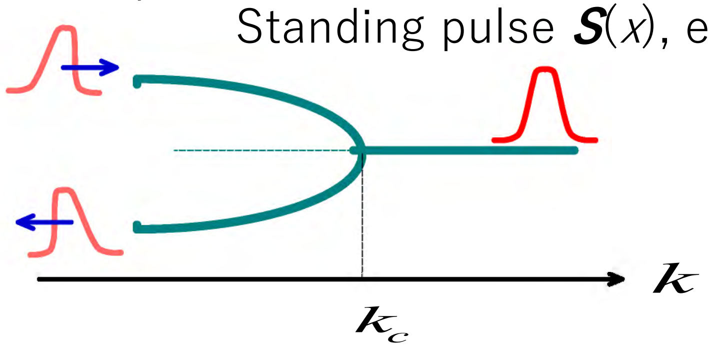

$k = k_c$; 分岐点 (ドリフト分岐点)

$$L = D\partial_x^2 + F'(S(x);k_c)$$ 線形化作用素

$$\begin{aligned} U_t &= DU_{xx} + F(U) + \eta G(U)\ (= F(U;k_c+\eta)) \\ &= \mathcal{L}(U) + \eta G(U) \end{aligned}$$

命題: 0 が単純固有値なら *kc* は分岐点でない

平行移動の自由度

$$\mathcal{L}(S(x)) = 0 \Rightarrow \underbrace{\mathcal{L}'(S(x))}_{L} S_x = 0 \Rightarrow LS_x = 0$$

$LS_x = 0,\quad L\psi = -S_x$

Jordan Block型縮退

$$\dot{p} = q$$

$$\dot{q} = -M_1 q^3 + M_2 \eta q$$

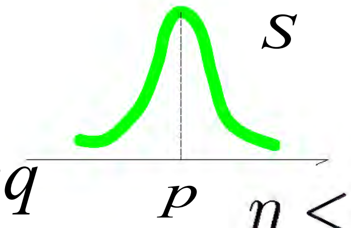

$$k = k_c + \eta$$

$$q = \pm\sqrt{\frac{M_2 \eta}{M_1}}$$

$\eta < 0$ $\eta > 0$

$M_1,\ M_2 > 0 \Rightarrow$

$M_1 < 0,\ M_2 > 0 \Rightarrow$

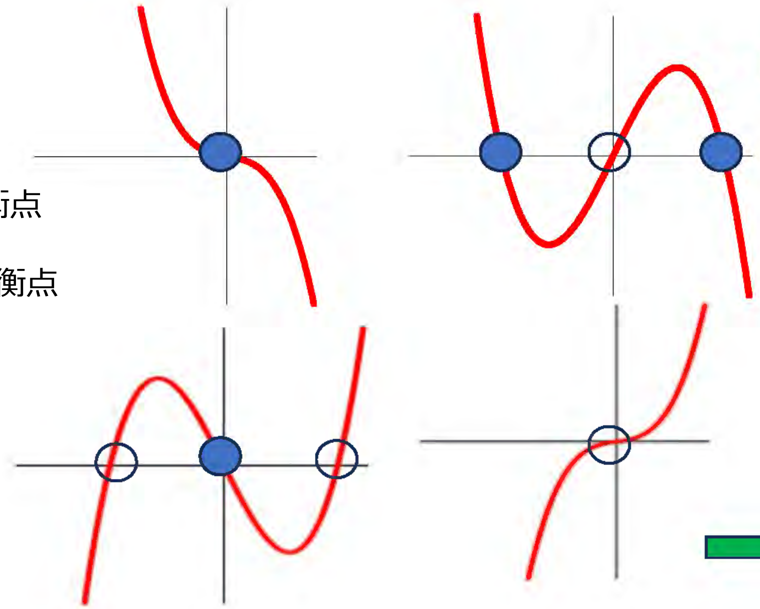

● 安定平衡点

○ 不安定平衡点

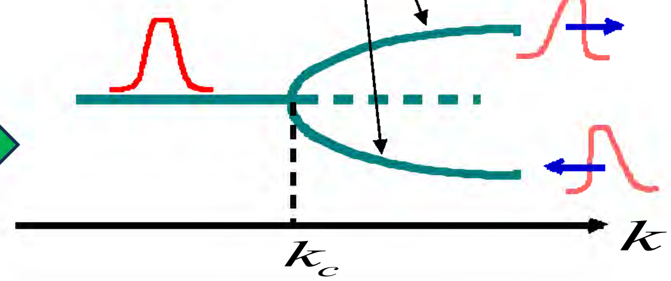

Super-critical分岐
超臨界分岐

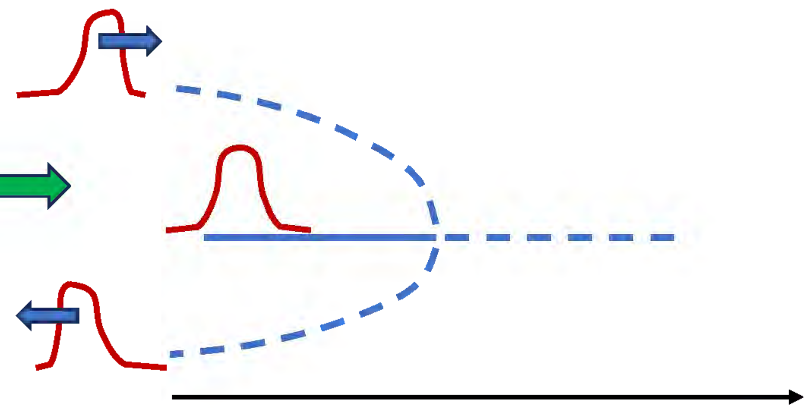

Sub-critical 分岐
劣臨界分岐

※ M_2 の符号はパラメータ ***k*** の方向を決める

Example of Drift Bifurcation

E.,Ikeda, Kawana 08

$$\begin{cases} \varepsilon\tau u_t = \varepsilon^2 u_{xx} + f(u,v), \\ v_t = d v_{xx} + g(u,v), \end{cases} \quad t > 0,\ x \in \boldsymbol{R}.$$

$$f(u,v) = u(1-u)(u - \frac{1}{2}v - \frac{1}{2}),\ g(u,v) = u - v,$$

$$\dot{p} = q$$

$$\dot{q} = -M_1 q^3 + M_2 \eta q$$

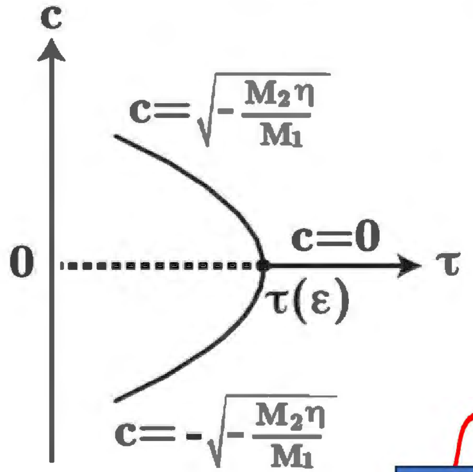

$$M_1 = \frac{1}{6d} + O(\varepsilon) > 0, \quad M_2 = -\frac{4}{3\tau_0} + O(\varepsilon + |\eta|) < 0$$

$$\tau(\varepsilon) = \tau_0 + O(\varepsilon) = \frac{1}{4\sqrt{2d}} + O(\varepsilon)$$

$$\tau = \tau(\varepsilon) + \eta$$

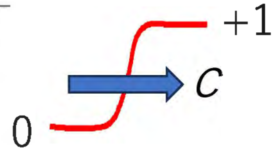

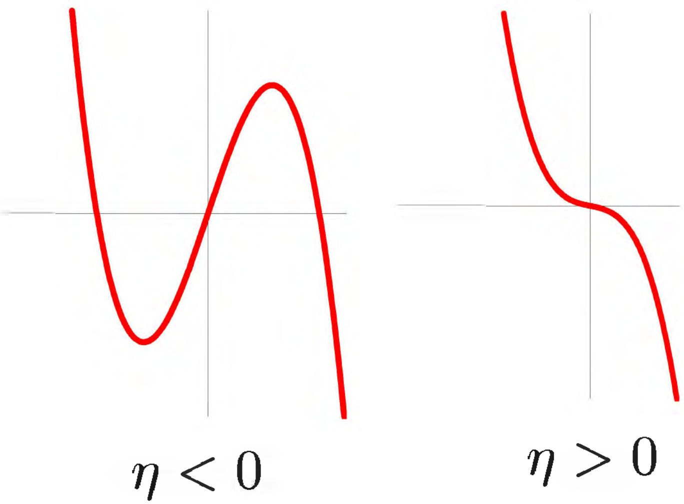

参考文献

係数の計算方法

$$\dot{p} = q$$
$$\dot{q} = -M_1 q^3 + M_2 \eta q$$

$$M_1 = -< \xi_x + F''(S)\psi\xi + \frac{1}{6}F'''(S)\psi^3, \varphi^* >$$
$$M_2 =< \varsigma_x + F''(S)\psi\varsigma + g'(S)\psi, \varphi^* >$$

$$q^2;\ -\psi_x = L\xi + \frac{1}{2}F''(S)\psi^2$$
$$\eta;\quad 0 = L\varsigma + g(S)$$

池田: 特異摂動により臨界固有値を計算できる

自明解の臨界固有値 $\sim \quad M_2\eta$

分岐解の構成 $\quad \sim \quad \sqrt{\frac{M_2\eta}{M_1}}$ ⇨ $M_1,\ M_2$ の決定

2D case drift bifurcation

Kawaguchi-Mimura Model 98

$$\begin{cases} \sigma u_t = \varepsilon \Delta u + \varepsilon^{-1} f(u,v,w), & \\ v_t = \Delta v + u - v + h_1, & t > 0, x \in \Omega \subset \mathbf{R}^2, \\ \tau w_t = d \Delta w + u - w + h_2 & \end{cases}$$

$$f(u,v,w) = ru - u^3 - k_1 v - k_2 w.$$

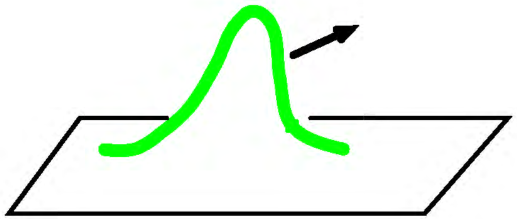

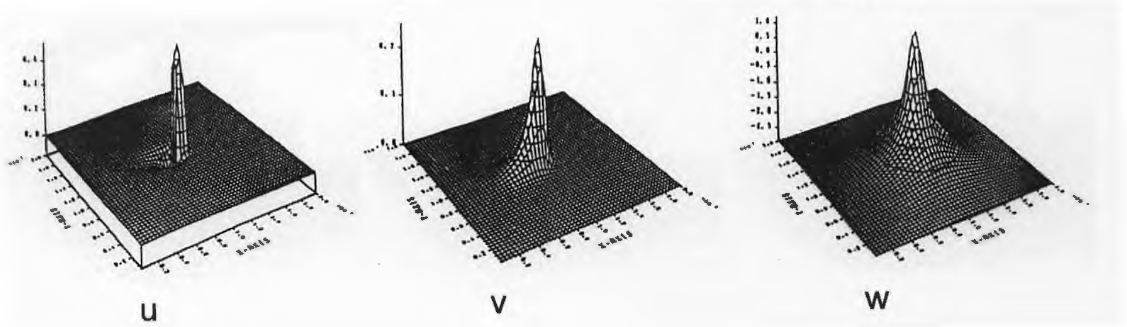

$\varepsilon = 0.1, \sigma = 0.04, r = 1.5, k_1 = 1.0, k_2 = 5.0,$
$h_1 = 1.0, h_2 = 0.8, \tau = 0.01, d = 7.0$

2次元のドリフト分岐

$$\mathbf{u}_t = D\Delta\mathbf{u} + \mathbf{F}(\mathbf{u};k) \;=\; \mathcal{L}(u;k)$$

$S(x)$

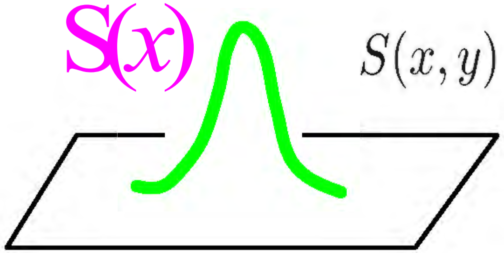

$$S(x,y) = S(r) \;\; (r = \sqrt{x^2+y^2})$$

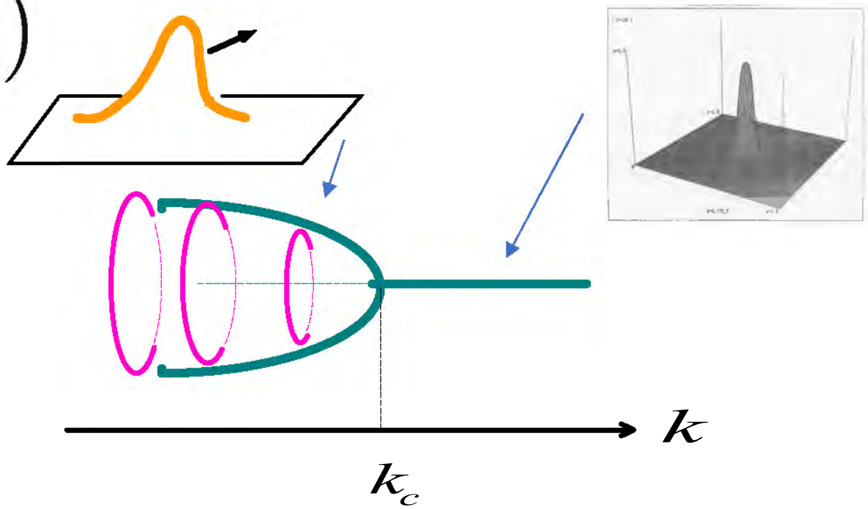

球対称性を仮定

$$(LS_x = \mathbf{0},\, LS_y = \mathbf{0})$$

dim *Ker L* = 2

半単純性 $KerL^2 = KerL$

半単純固有値である場合の命題

平行移動の自由度　$LS_x = 0,\ LS_y = 0$

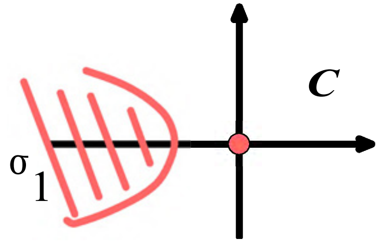

命題. 0 が L の半単純固有値で

$$\sigma(L) = \sigma_1 \cup \{0\},\ \sigma_1 \subset \{Re(\lambda) < -\gamma < 0\}$$

$$\boldsymbol{x} = (x, y) \in \boldsymbol{R}^2$$

ならば初期値が $S(\boldsymbol{x})$ に十分近い

$$U_t = D\Delta U + F(U),\ (x, y) \in \boldsymbol{R}^2$$

の解 $U(t,x,y)$ に対して, ある $\boldsymbol{b} \in \boldsymbol{R}^2$ があって

$$|U(t, \boldsymbol{x}) - S(\boldsymbol{x} - \boldsymbol{b})| \to 0\ (t \to \infty)$$

となる.　⟹　$S(\boldsymbol{x})$ は線形安定, という

Construction of a traveling spot
(as the bifurcating solution)

Assume Jordan Block E., Mimura,Nagayama 02

$$L^{\exists}\psi_1 = -S_x,\ L^{\exists}\psi_2 = -S_y \quad (LS_x = \mathbf{0},\ LS_y = \mathbf{0})$$

$$\begin{aligned} \boldsymbol{u}_t &= D\Delta\boldsymbol{u} + F(\boldsymbol{u}; k_c + \eta = D\Delta\boldsymbol{u} + F_c(\boldsymbol{u}) + \eta G(\boldsymbol{u}) \\ &= \mathcal{L}_c(\boldsymbol{u}) + \eta G(\boldsymbol{u}) \end{aligned}$$

$\boldsymbol{x} = (x, y) \in \boldsymbol{R}^2,\ \boldsymbol{u} \in \boldsymbol{R}^N$

$\mathcal{L}_c(S(\boldsymbol{x})) = 0$; stationary solution of $\boldsymbol{u}_t = \mathcal{L}(\boldsymbol{u}; k)$

$L = \mathcal{L}_c'(S) = D\Delta + F_c'(S(\boldsymbol{x}))$

$S(x)$;radially symmetric

$S(x) \to \mathbf{0}\ (|x| \to \infty)$

$S(x)$

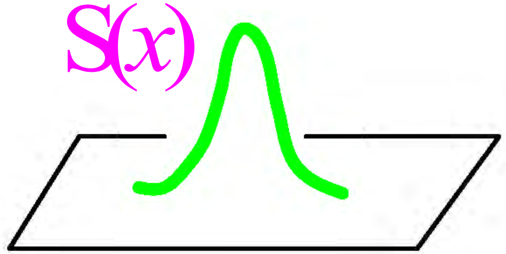

Assumptions

1) The speturum of L

$$\Sigma(L)=\Sigma_0\cup\Sigma_1,\ \Sigma_0=\{0\}\quad \Sigma_1\subset\{\mathrm{Re}\,z<-\gamma_0\}$$

Q, R; Projections of Σ_0, Σ_1

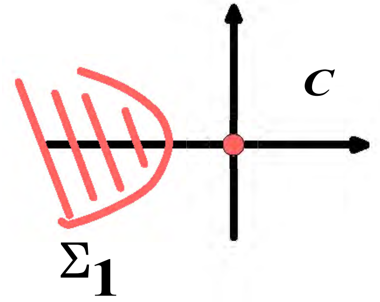

2) $QX = span\{S_x, S_y, \psi_1, \psi_2\}$

$$L\psi_1=-S_x,\ L\psi_2=-S_y$$

$$(LS_x=\mathbf{0},\ LS_y=\mathbf{0})$$

$$L^*\phi_1^*=0,\ L\phi_2^*=0,\ L^*\psi_1^*=-\phi_1^*,\ L^*\psi_2^*=-\phi_2^*$$

Theorem[12]

$$\boldsymbol{u}(t,\boldsymbol{x}) = S(\boldsymbol{x}-P) + \zeta_1\psi_1(\boldsymbol{x}-P) + \zeta_2\psi_2(\boldsymbol{x}-P) + O(|\boldsymbol{\zeta}|^2 + |\eta|)$$

$$\dot P = \varsigma + O(|\varsigma|^3 + |\eta|^{\frac{3}{2}}),$$

$$\dot\varsigma = -\nabla_\varsigma W(\varsigma) + O(|\varsigma|^4 + |\eta|^2)$$

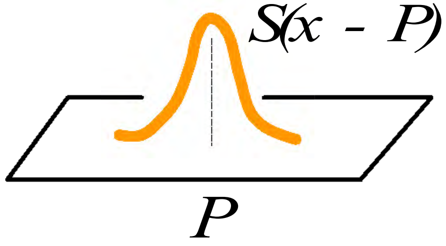

as long as $|\varsigma| < \varsigma^*, |\eta| < \eta^*, {}^\forall P \in \mathbf{R}^2$, where

$$\boldsymbol{x} = (x,y),\ \boldsymbol{\zeta} = (\zeta_1,\zeta_2),\ W(\boldsymbol{\zeta}) = \frac{1}{4}M_1|\boldsymbol{\zeta}|^4 + \frac{1}{2}M_2\eta|\boldsymbol{\zeta}|^2$$

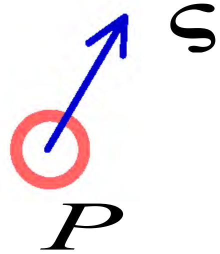

Proof: construct an exponentially attractive invariant manifold

$$\mathcal{M} = \{S(\boldsymbol{x}-P) + \zeta_1\psi_1(\boldsymbol{x}-P) + \zeta_2\psi_2(\boldsymbol{x}-P) +^{\exists} \sigma(\boldsymbol{\zeta},\eta)(\boldsymbol{x}-P);$$
$$|\boldsymbol{\zeta}| < \zeta^*,\ |\eta| < \eta^*,\ P \in \boldsymbol{R}^2\}$$

$$E^{\perp} = \{\boldsymbol{v};\ \langle\, \boldsymbol{v}, \phi_j^* \,\rangle_2 = \langle\, \boldsymbol{v}, \psi_j^* \,\rangle_2 = 0\ \ (j = 1,\ 2)\}$$

$$\langle\, \psi_1^*, \phi_1^* \,\rangle_2\, M_1 = -\left\{ \frac{1}{6} \langle\, F_c'''(S(r))\psi_1^3, \phi_1^* \,\rangle_2 + \langle\, F_c''(S(r))\psi_1 V_1, \phi_1^* \,\rangle_2 + \langle\, \partial_x V_1, \phi_1^* \,\rangle_2 \right\}$$

$$\langle\, \psi_1^*, \phi_1^* \,\rangle_2\, M_2 = -\{\langle\, G'(S(r))\psi_1, \phi_1^* \,\rangle_2 + \langle\, F_c''(S(r))\psi_1 V_2, \phi_1^* \,\rangle_2 + \langle\, \partial_x V_2, \phi_1^* \,\rangle_2\}$$

$$V_1,\ V_2 \in E^{\perp} \qquad -LV_1 = \frac{1}{2} F_c''(S(r))\psi_1^2 + \partial_x \psi_1,\ -LV_2 = G(S(r))$$

$$LS_x = 0,\ LS_y = 0,\ L\psi_1 = -S_x,\ L\psi_2 = -S_y$$

$$L^*\phi_1^* = 0,\ L^*\phi_2^* = 0,\ L^*\psi_1^* = -\phi_1^*,\ L^*\psi_2^* = -\phi_2^*$$

Rem: $\psi_1(x,y) = {}^{\exists}\psi(r)\cos\theta,\ \psi_2(x,y) = \psi(r)\sin\theta$

$\phi_1^*(x,y) = {}^{\exists}\phi^*(r)\cos\theta,\ \phi_2^*(x,y) = \phi^*(r)\sin\theta$

$\psi_1^*(x,y) = {}^{\exists}\psi^*(r)\cos\theta,\ \psi_2^*(x,y) = \psi^*(r)\sin\theta$

Roles of $\varsigma = (\varsigma_1, \varsigma_2)$

$$\mathbf{u}_t = D\Delta\mathbf{u} + \mathbf{F}(\mathbf{u}; k_c + \eta) = \underline{\underline{D\Delta\mathbf{u} + \mathbf{F}(\mathbf{u})}} + \eta g(\mathbf{u})$$

$$= \underline{\underline{L(\mathbf{u})}} + \eta g(\mathbf{u}),\ x \in \mathbf{R}^2,\ \mathbf{u} \in \mathbf{R}^N$$

$$\mathbf{u}(t,x) = \underbrace{S(x-P)}_{\text{(radial)}} + \varsigma_1\psi_1(x-P) + \varsigma_2\psi_2(x-P),$$

$$\begin{cases} \dot{P} = \varsigma, \\ \dot{\varsigma} = -\nabla_{\varsigma} W(\varsigma), \end{cases}$$

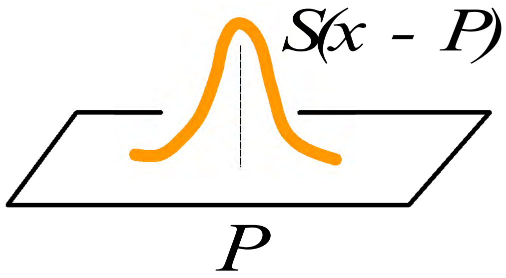

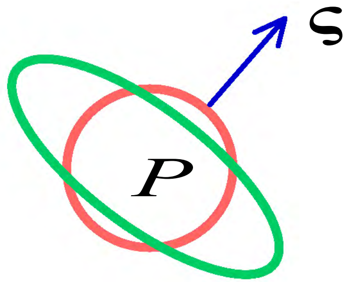

- Velocity of spot
- Deformation of spot from radial symmetry

Dynamics of solutions

$$W(\varsigma) = \frac{1}{4} M_1 |\varsigma|^4 + \frac{1}{2} M_2 \eta |\varsigma|^2 \quad M_1, M_2 > 0 \Rightarrow$$

$$\begin{cases} \dot{P} = \varsigma, \\ \dot{\varsigma} = -\nabla_{\varsigma} W(\varsigma), \end{cases}$$

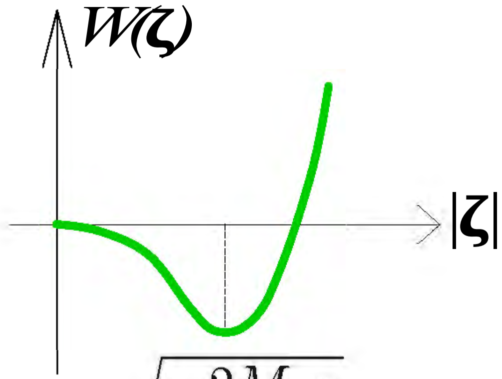

$\eta < 0$ $\quad \sqrt{-\frac{2M_2\eta}{M_1}}$

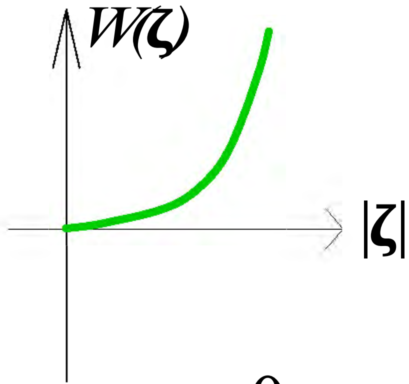

$\eta > 0$

$k = k_c + \eta$

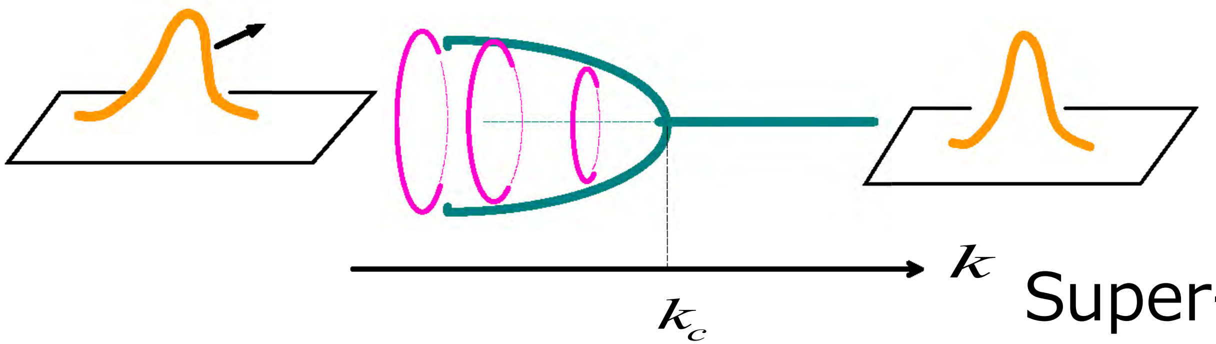

Super-critical bifurcation

Kawaguchi-Mimura Model 98

$$\begin{cases} \sigma u_t = \varepsilon \Delta u + \varepsilon^{-1} f(u,v,w), \\ v_t = \Delta v + u - v + h_1, & t>0, x \in \Omega \subset \mathbf{R}^2, \\ \tau w_t = d\Delta w + u - w + h_2 \end{cases}$$

$$f(u,v,w) = ru - u^3 - k_1 v - k_2 w.$$

$$\Rightarrow M_1, M_2 > 0$$

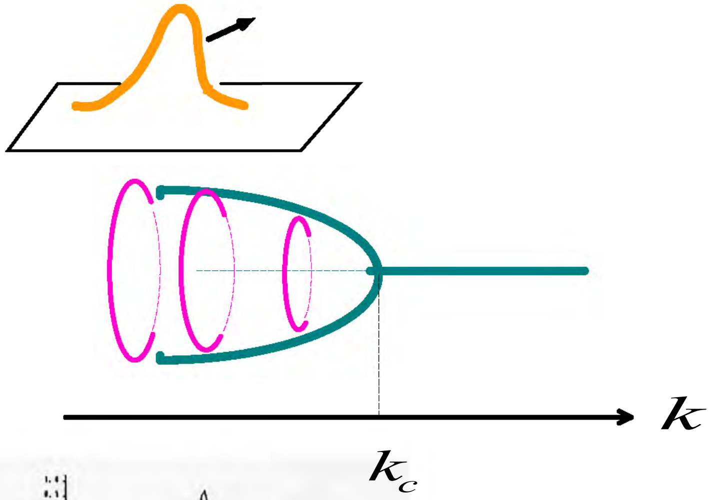

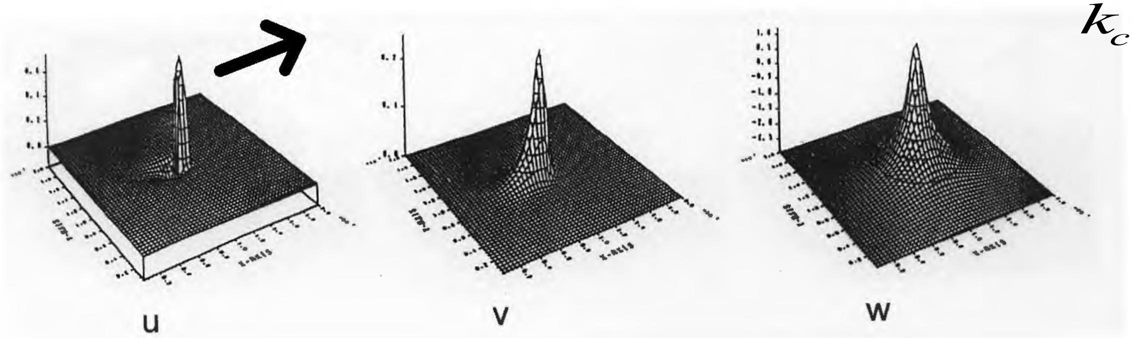

$\varepsilon = 0.1, \sigma = 0.04, r = 1.5, k_1 = 1.0, k_2 = 5.0,$
$h_1 = 1.0, h_2 = 0.8, \tau = 0.01, d = 7.0$

II：ドリフト分岐が生じる具体例
Proof of Drift bifurcation

Tomoyuki Miyaji, Shin-Ichiro Ei
Masayasu Mimura

A Billiard Problem in Nonlinear Dissipative Systems

March 29, 2025

-Monograph- Springer 2025

Springer

文献

II：ドリフト分岐が生じる具体例
Proof of Drift bifurcation
by Chen, E, Mimura 2009

7　樟脳片の運動　Camphor motion

ドリフト分岐が起きている例は数値的には多くのモデル方程式で観察されている．しかし．数学的に厳密に示された例は殆どない．[17], [1] は数少ない厳密に示された例である．[17] のフロント解のドリフト分岐を示しているが, この章ではスポット解に注目するために, 文献 [1] にもとづいて結果の紹介を行う．前章で速度の遅い進行パルスはドリフト分岐点の近傍で捉えられることを示した．しかし, 実際にドリフト分岐が起きていることを, モデル方程式において厳密に示すのは難しく, 数値的に確認されている結果が殆どである．それに対して, 樟脳円板のモデルではドリフト分岐が起きていることが [1] において厳密に示された．樟脳円板の数理モデルはドリフト分岐を厳密に示すことができた数少ない例の一つとなっている．

English version

Moving boundary (MB) model for camphor disk

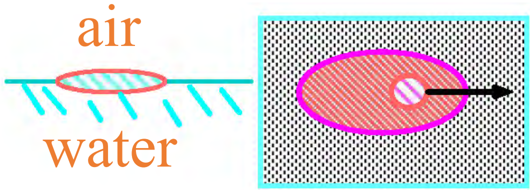

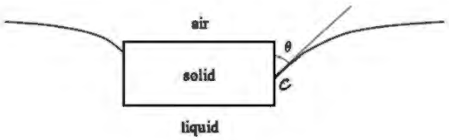

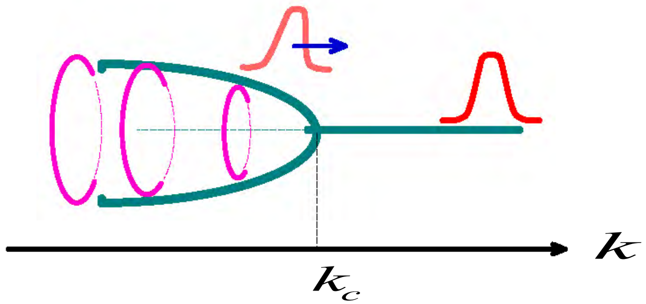

$$
\begin{cases}
\dfrac{dP}{dt} &= \displaystyle\int_{\partial\Omega_c} \gamma(u)\boldsymbol{n}\,dl, \\
u_t &= \Delta u - u + f(\boldsymbol{x}, P),
\end{cases}
$$

Chen, E, Mimura 2009

$$
f(\boldsymbol{x}, P) = \begin{cases} f_0, & \boldsymbol{x} \in \overline{\Omega}_c, \\ 0, & \boldsymbol{x} \in \Omega \backslash \overline{\Omega}_c, \end{cases}
$$

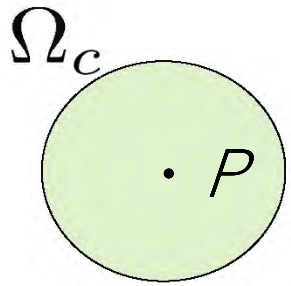

First rigorous result
for drift bifurcation and 2D reflection

MB model which can be rigorously treated.

文献[1]

Experiment for camphor disk

By Kanda (02, Hiroshima Univ.)

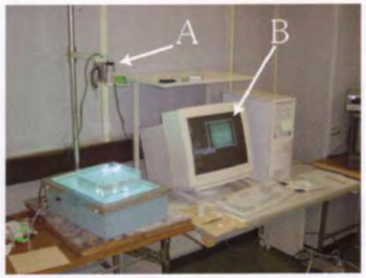

Recorded by the video camera at A and monitored by the display at B to produce a movie.

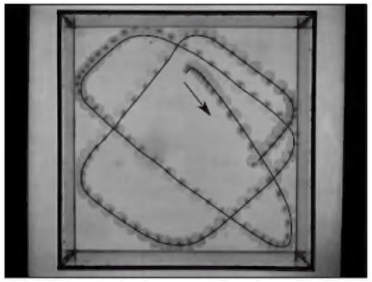

A trajectory of a camphor disk of an experiment

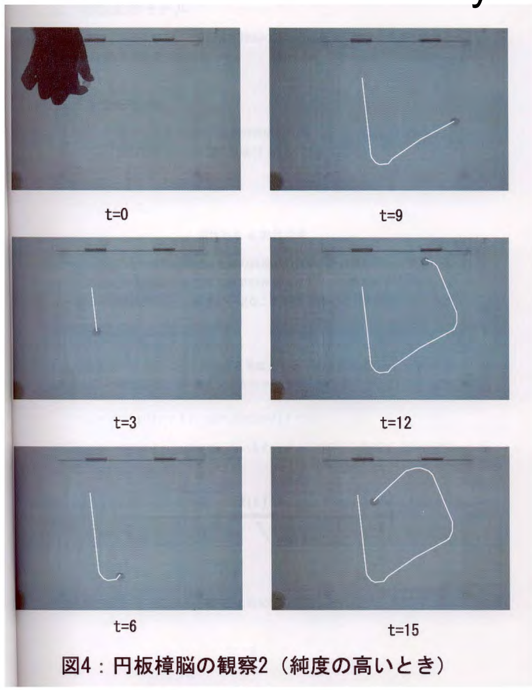

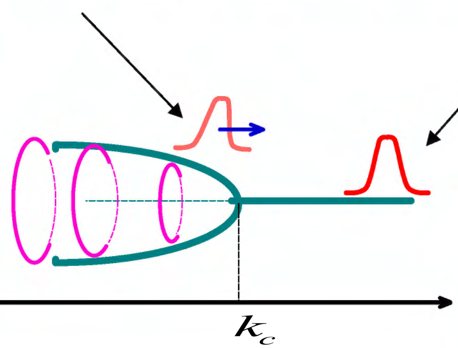

k = 1/(content rate of camphor)

Camphor disk problem is a nice example both from models and phenomena !

7.1　樟脳円板の数理モデルと定常スポット解

文献 [24, 25] によい解説があるので参照されたい．

樟脳片が完全な円板 $B(P, r_0) := \{|x-P| \le r_0\}$ として

$$
\begin{cases} \dfrac{dP}{dt} &= \beta \displaystyle\int_{\partial B(P,r_0)} \Gamma(c)\boldsymbol{n}ds, \\ c_t &= d\Delta c - \alpha c + F(c)\chi_{B(P,r_0)} \end{cases} \tag{7.1}
$$

が提案されており, moving boundary (MB) モデルと呼ばれている．ここで c は水面に溶けた樟脳分子の濃度, $\Gamma(c)$ は溶けた樟脳分子 c が表面張力に関わる関数であり, 一般に c に関して単調減少が仮定される．$\boldsymbol{n}$ は $\partial B(P, r_0)$ 上の外向き単位法線ベクトルである．また $F(c)$ は樟脳円板から水面に供給される樟脳分子の量を表しており, これも一般に非負の単調減少関数が採用される．多くの場合, 定数関数 $F(c) = a_0 > 0$ が使われる．

仮定:

1) $\Gamma(c) > 0$, $\Gamma'(c) < 0$ for $c > 0$.
2) $F(c) > 0$, $F'(c) \le 0$ for $c > 0$.

以下, (7.1) を全平面上 $\boldsymbol{R}^2$ で考えることにする．

(7.1) は Heaviside 関数 $H(\xi)$ ($H(\xi) = 0$ for $\xi < 0$ and $H(\xi) = 1$ for $\xi > 0$) を用いて

$$
\begin{cases} \dfrac{dP}{dt} &= \beta \displaystyle\int_{\partial B_0} \Gamma(c(P+x))\boldsymbol{n}ds, \\ c_t &= d\Delta c - \alpha c + F(c)H(r_0 - |x-P|) \end{cases} \tag{7.2}
$$

と表されることに注意しておく．ここで $B_0 := B(O, r_0)$ である．

(7.2) において，$y = x - P(t)$, $u(t,y) = c(t, P(t)+y)$ とすると，第 2 項が

$$u_t = d\Delta u - \alpha u + \langle\, \dot{P}, \nabla u\,\rangle + F(u)H(r_0 - |y|)$$

となることから, 結局

$$u_t = d\Delta u - \alpha u + \langle\, \beta \int_{\partial B_0} \Gamma(u)\boldsymbol{n}ds, \nabla u\,\rangle + F(u)H(r_0 - |y|) \tag{7.3}$$

のみを考えれば $P(t)$ は

$$\frac{dP}{dt} = \beta \int_{\partial B_0} \Gamma(u(t,x))\boldsymbol{n}ds$$

によって与えられることになる．

(7.3) における球対称な定常スポット解を構成する．定常解を $S(r) = S(|y|)$ とおけば (7.3) より

$$\begin{cases} d(S_{rr} + \dfrac{1}{r}S_r) - \alpha S + F(S)H(r_0 - r) = 0,\ r > 0, \\ S_r(0) = 0,\ S(\infty) = 0 \end{cases} \tag{7.4}$$

となる．定常解より $\dot{P} = 0$ であることに注意しておく．

以下, (7.4) の解 $S(r)$ が存在するとしてその安定性を調べていくが, 実際, $F = a_0$ (定数) など, F が具体的に与えられれば解くことができる．

$S(r)$ の安定性を調べるために (7.3) において, $S(r)$ に関する線形化作用素 L を考えると

$$L\phi = \{d\Delta - \alpha + F'(S)H(r_0 - |y|)\}\phi + \langle\, \beta\Gamma'(S(r_0))\nabla S, \int_{\partial B_0} \phi\boldsymbol{n}ds\,\rangle$$

となる．

今, $\boldsymbol{v} = (v_1, v_2) = \beta\Gamma'(S(r_0)) \int_{\partial B_0} \phi \boldsymbol{n} ds$ とおくと, 固有値問題 $L\phi = \lambda\phi$ は

$$(7.5) \qquad \begin{cases} \boldsymbol{v} = \beta\Gamma'(S(r_0)) \displaystyle\int_{\partial B_0} \phi \boldsymbol{n} ds, \\ \{d\Delta - \alpha + F'(S)H(r_0 - |y|) - \lambda\}\phi = -\langle\, \boldsymbol{v}, \nabla S\,\rangle \end{cases}$$

となる. $F' \leq 0$ より上記第 2 式左辺は $\lambda \notin (-\infty, -\alpha]$ に対して逆写像をもつから, 与えられた $\boldsymbol{v}$ に対して一意の解 ϕ が存在する. また極座標 $y = (r\cos\theta, r\sin\theta)$ に対して, 右辺 $\langle\, \boldsymbol{v}, \nabla S\,\rangle = (v_1\cos\theta + v_2\sin\theta)S_r$ より,

$$\phi(r,\theta) = \psi(r)(v_1\cos\theta + v_2\sin\theta)$$

とおいて (7.5) 第 2 式に代入すると,

$$(7.6) \qquad \begin{cases} (L_R - \lambda)\psi = -S_r,\ r > 0, \\ \psi_r(0) = \psi(\infty) = 0 \end{cases}$$

となる. ここで

$$L_R := d(\partial_r^2 + \frac{1}{r}\partial_r - \frac{1}{r^2}) + F'(S(r))H(r_0 - r) - \alpha$$

である. L_R は球対称関数から成る空間 $L^2_R(\boldsymbol{R}^2)$ において, $\lambda \notin (-\infty, -\alpha]$ に対して逆像が存在するから, (7.5) より $\psi = -(L_R - \lambda)^{-1}S_r \leq 0$ として解くことができる. $\psi(r;\lambda) := -\{(L_R - \lambda)^{-1}S_r\}(r)$ とする. この $\psi(r;\lambda)$ に対して $\phi(r,\theta;\lambda) = \psi(r;\lambda)(v_1\cos\theta + v_2\sin\theta)$ を (7.5) 第 1 式に代入すると

$$\boldsymbol{v} = \beta\Gamma'(S(r_0)) \cdot \pi r_0 \psi(r_0;\lambda)\boldsymbol{v}$$

となる. 以上より, Γ' ≤ 0 に注意すると, 次の補題を得る.

Lemma 7.1. $\lambda \notin (-\infty, -\alpha]$ が L の固有値であるのは

$$-\psi(r_0;\lambda) = b := \frac{1}{\pi r_0 \beta |\Gamma'(S(r_0))|}$$

が成り立つとき, かつそのときに限る.

Lemma 7.2. L のすべての固有値は実数である.

Proof. $L^2_R(\boldsymbol{R}^2)$ における内積 $\langle\, \psi_1, \psi_2 \,\rangle_R := 2\pi \int_0^\infty r\psi_1(r)\overline{\psi}_2(r)dr$ に対して L_R は負定値であることに注意しておく. また (7.4) の第 1 式を r で微分することにより,

$$L_R S_r = F(S(r_0))\delta_{r_0}$$

となる. ここで $\delta_{r_0}(r) := \delta(r_0 - r)$ は $r = r_0$ にサポートをもつディラック関数である. (7.6) の両辺と ψ および S_r との内積をとるが

$$\langle\, L_R\psi, S_r \,\rangle_R = \langle\, \psi, L_R S_r \,\rangle_R = 2\pi r_0 \psi(r_0;\lambda)F(S(r_0))$$

に注意して

$$\lambda \|\psi\|_R^2 = \langle\, L_R\psi, \psi \,\rangle_R + \langle\, S_r, \psi \,\rangle_R$$

および

$$\lambda \langle\, \psi, S_r \,\rangle_R = \langle\, L_R\psi, S_r \,\rangle_R + \|S_r\|_R^2 = 2\pi r_0 \psi(r_0;\lambda)F(S(r_0)) + \|S_r\|_R^2$$

を得る. よって

$$(7.7)\quad \begin{aligned} |\lambda|^2\|\psi\|_R^2 &= \overline{\lambda}\langle\, L_R\psi, \psi \,\rangle_R + \overline{\lambda}\langle\, S_r, \psi \,\rangle_R \\ &= \overline{\lambda}\langle\, L_R\psi, \psi \,\rangle_R + 2\pi r_0\overline{\psi(r_0;\lambda)}F(S(r_0)) + \|S_r\|_R^2 \end{aligned}$$

となるが, $\langle\, L_R\psi, \psi \,\rangle_R$ は負の実数で, $\psi(r_0;\lambda) = -b$ は実数であるから, λ も実数でなければない. ∎

Lemma 7.3. L のスペクトルを $\sigma(L)$ とすると

$$\sigma(L) = (-\infty, -\alpha] \cup \{\lambda^*(b)\}$$

となる．ここで $\lambda^*(b)$ は $-\psi(r_0;\lambda) = b$ の解である．さらに，

$$b^* := \frac{\|S_r\|_R^2}{2\pi r_0 F(S(r_0))}$$

と定義すると，$\lambda^*(b) > 0$ *(*$b < b^*$*)*, $\lambda^*(b^*) = 0$, $\dfrac{d\lambda^*}{db}(b^*) < 0$, $\lambda^*(b) < 0$ *(*$b > b^*$*)* が成り立つ．

Proof. $L_R S_r = F(S(r_0))\delta_{r_0}$ より $S_r < 0$ $({}^\forall r > 0)$ である．したがって $\lambda > -\alpha$ であれば (7.6) より $\psi(r;\lambda) < 0$ $({}^\forall r > 0)$ であり，また $|\psi(r_0;\lambda)|$ は λ に関して単調減少で $\lim_{\lambda\to\infty} |\psi(r_0;\lambda)| = 0$ である．実際 $\psi_j(r) = \psi(r;\lambda_j)$ として，(7.6) より $(L_R - \lambda_1)(\psi_1 - \psi_2) = (\lambda_1 - \lambda_2)\psi_2$ となるから，$\lambda_1 < \lambda_2$ ならば $(L_R - \lambda_1)(\psi_1 - \psi_2) > 0$，したがって $\psi_1(r) < \psi_2(r)$ となるが $\psi_j(r) < 0$ よりこれは $|\psi_1(r)| > |\psi_2(r)|$ を示している．

以上より任意の $b > 0$ に対して $-\psi(r_0;\lambda) = |\psi(r_0;\lambda)| = b$ となる $\lambda = \lambda^*(b)$ がただ一つ定まる．ただし $b > |\psi(r_0;-\alpha)|$ なる b に対しては $\lambda^*(b) = -\alpha$ と定めることとする．

また (7.7) において $\lambda = 0$ とおくことにより，$-\psi(r_0;0) = |\psi(r_0;0)| = b^*$ となる．これは $\lambda^*(b^*) = 0$, $\lambda^*(b) < 0$ $(b > b^*)$, $\lambda^*(b) > 0$ $(b < b^*)$ を示している．

最後に (7.7) で λ が実数であることを考慮して両辺 λ で微分し $\lambda = 0$ とおくことにより

$$0 = \langle\, L_R\psi_0, \psi_0 \,\rangle_R + 2\pi r_0 \partial_\lambda \psi(r_0;0) F(S(r_0))$$

を得る．ただし $\psi_0(r) = \psi(r;0)$ である．よって

$$\partial_\lambda \psi(r_0;0) = -\frac{\langle\, L_R\psi_0, \psi_0 \,\rangle_R}{2\pi r_0 F(S(r_0))} > 0$$

となる．$-\psi(r_0;\lambda^*(b))=b$ より

$$\frac{d\lambda^*}{db}(b^*)=-\frac{1}{\partial_\lambda\psi(r_0;\lambda^*(b^*))}=-\frac{1}{\partial_\lambda\psi(r_0;0)}<0$$

となり証明できた. ∎

(7.3) において $b:=\dfrac{1}{\pi r_0\beta|\Gamma'(S(r_0))|}$ であったから,

$$b \underset{<}{\overset{>}{=}} b^* \iff \frac{1}{\pi r_0\beta|\Gamma'(S(r_0))|} \underset{<}{\overset{>}{=}} b^* \iff \beta \underset{>}{\overset{<}{=}} \beta^* := \frac{1}{\pi r_0|\Gamma'(S(r_0))|b^*}$$

となり, 例えば β を分岐パラメータと考えることにより

$$\lambda^*(\beta)<0\ (\beta<\beta^*),\ \lambda^*(\beta^*)=0,\ \lambda^*(\beta)>0\ (\beta>\beta^*)$$

となる.

$$b^*:=\frac{\|S_r\|_R^2}{2\pi r_0F(S(r_0))}$$

であったことを考慮すると, β 以外には樟脳の供給項 F の係数を変えれば, b^* が変化することから, やはり不安定化を起こすことができると考えられる.

実際, $F(c)=f_0>0$ (定数) とおくと $S(r)$ の定義式 (7.4) より $S(r)=f_0S_0(r)$, $S_0(r)$ は (7.4) において $F\equiv 1$ としたときの解, と表される．この場合,

$$b=\frac{1}{\pi r_0\beta|\Gamma'(f_0S_0(r_0))|},\ b^*=\frac{f_0\|\partial_rS_0\|_R^2}{2\pi r_0}$$

となるから, 仮に $|\Gamma'(f_0S_0(r_0))|$ が f_0 に関してあまり変化しないと考えれば, f_0 が大きくなると b^* も大きくなり, 不安定化すると考えられる.

7.2 樟脳片のドリフト分岐

前節より, $b=b^*$ において定常スポット解 $S(r)$ $(r=\sqrt{x^2+y^2})$ が不安定化することがわかった．この節では元の問題 (7.2) に戻って, 不安定化に関わる特異点の構造を調べる．

(7.2) を定常スポット解 $\boldsymbol{S}(r):=(\boldsymbol{0},S(r))$ の周りで線形化した作用素 $\boldsymbol{L}$ は (7.2) の解 (P,c) を考慮して

$$\boldsymbol{L}\Phi=\boldsymbol{L}\begin{pmatrix}\boldsymbol{q}\\ \phi\end{pmatrix}=\begin{pmatrix}\beta\Gamma'(S(r_0))[\pi r_0 S_r(r_0)\boldsymbol{q}+\displaystyle\int_{\partial B_0}\phi\boldsymbol{n}ds]\\ (d\Delta-\alpha+F'(S)H)\phi+F(S(r_0))\delta_{\partial B_0}\langle\,\boldsymbol{e}(\theta),\boldsymbol{q}\,\rangle\end{pmatrix}$$

for $(\boldsymbol{q},\phi)\in\boldsymbol{R}^2\times H^2(\boldsymbol{R}^2)$. ただし $H=H(r_0-r)$, $\boldsymbol{e}(\theta):={}^t(\cos\theta,\sin\theta)$ であり極座標 $\boldsymbol{x}=(x,y)=r\boldsymbol{e}(\theta)$ で考えている．

固有値問題 $\boldsymbol{L}\Phi=\lambda\Phi$ を考える．まず 連続スペクトルは $(-\infty,-\alpha]$ であることに注意して, $\lambda\notin(-\infty,-\alpha]$ となる固有値のみ考える．また平行移動の自由度がある, すなわち ${}^\forall P\in\boldsymbol{R}^2$ に対して $(P,S(|\boldsymbol{x}-P|))$ も定常スポット解となることから, $\Phi_1:={}^t(-\boldsymbol{e}_1,S_r\cos\theta)$ と $\Phi_2:={}^t(-\boldsymbol{e}_2,S_r\sin\theta)$ は $\boldsymbol{L}\Phi_j=0$ を満たす．ここで $\boldsymbol{e}_1:={}^t(1,0)$, $\boldsymbol{e}_2:={}^t(0,1)$ である．

今, $\boldsymbol{q}=(q_1,q_2)$, $\phi(r,\theta)=\psi(r)\langle\,\boldsymbol{e}(\theta),\boldsymbol{q}\,\rangle$ とおいて, 固有値問題 $\boldsymbol{L}\Phi=\lambda\Phi$ に代入すると

$$\boldsymbol{L}\begin{pmatrix}\boldsymbol{q}\\ \phi\end{pmatrix}=\begin{pmatrix}\beta\Gamma'(S(r_0))[\pi r_0 S_r(r_0)\boldsymbol{q}+\pi r_0\psi(r_0)\boldsymbol{q}]\\ \{L_R\psi+F(S(r_0))\delta(r_0-r)\}\langle\,\boldsymbol{e}(\theta),\boldsymbol{q}\,\rangle\end{pmatrix}=\lambda\begin{pmatrix}\boldsymbol{q}\\ \psi\langle\,\boldsymbol{e}(\theta),\boldsymbol{q}\,\rangle\end{pmatrix}$$

となるから 第 2 式より $\psi=\widetilde{\psi}(\cdot;\lambda):=-F(S(r_0))(L_R-\lambda)^{-1}\delta_{r_0}$ となり, これを第 1 式に代入することにより, b を補題 7.1 で定義された量として, $S_r(r_0)+\widetilde{\psi}(r_0)=-\lambda b$ を得る．すなわち λ が $\boldsymbol{L}$ の固有値であるための必要十分条件は

$$\psi=\widetilde{\psi}(\lambda)=-F(S(r_0))(L_R-\lambda)^{-1}\delta_{r_0},\ \lambda b+S_r(r_0)+\widetilde{\psi}(r_0)=0 \tag{7.8}$$

である．(7.8) の第 1 式と $\widetilde{\psi}$ との内積をとって

$$-2\pi r_0 F(S(r_0))\overline{\widetilde{\psi}(r_0)} = \langle\, L_R\widetilde{\psi}, \widetilde{\psi}\,\rangle_R - \lambda\|\widetilde{\psi}\|_R^2, \tag{7.9}$$

また S_r との内積をとって

$$\lambda\langle\, \widetilde{\psi}, S_r\,\rangle_R = \langle\, L_R\widetilde{\psi}, S_r\,\rangle_R + 2\pi r_0 F(S(r_0))S_r(r_0)$$

であるが, 補題 7.2 にあるように $L_R S_r = F(S(r_0))\delta_{r_0}$ より

$$\langle\, L_R\widetilde{\psi}, S_r\,\rangle_R = \langle\, \widetilde{\psi}, L_R S_r\,\rangle_R = F(S(r_0))\cdot 2\pi r_0\widetilde{\psi}(r_0)$$

となる．よって

$$\lambda\langle\, \widetilde{\psi}, S_r\,\rangle_R = 2\pi r_0 F(S(r_0))\{\widetilde{\psi}(r_0) + S_r(r_0)\} \tag{7.10}$$

を得る．(7.10) に (7.8) 第 2 式を代入することにより

$$\lambda\{\langle\, \widetilde{\psi}, S_r\,\rangle_R + 2\pi r_0 F(S(r_0))b\} = 0 \tag{7.11}$$

となる．

※ (7.11) より $\lambda \neq 0$ ならば

$$\langle\, \widetilde{\psi}, S_r\,\rangle_R + 2\pi r_0 F(S(r_0))b = 0 \tag{7.12}$$

でなくてはならない．特に $\langle\, \widetilde{\psi}, S_r\,\rangle_R \in \boldsymbol{R}$ でなくてはならない．これより $\lambda \in \boldsymbol{R}$ である． ※※

$\lambda > -\alpha$ ならば $S_r < 0$, $\widetilde{\psi}(r;\lambda) > 0$, $\widetilde{\psi}(r;\lambda)$ は λ に関して単調減少などより, $-\langle\, \widetilde{\psi}(\cdot;\lambda), S_r\,\rangle_R$ は λ に関して単調減少である．$-\langle\, \widetilde{\psi}(\cdot;-\alpha), S_r\,\rangle_R < 2\pi r_0 F(S(r_0))b$ ならば $\widetilde{\lambda}^*(b) = -\alpha$ と定めることにして $-\langle\, \widetilde{\psi}(\cdot;\lambda), S_r\,\rangle_R = 2\pi r_0 F(S(r_0))b$ を満たす一意の解を $\widetilde{\lambda}^*(b)$ と定義する．このとき特に $\widetilde{\lambda}^*(b^*) = 0$ となる．実際, $\widetilde{\psi}(r;0) = -S_r$ より $b = b^* = \dfrac{\|S_r\|_R^2}{2\pi r_0 F(S(r_0))}$ のとき (7.12) が満たされることがわかる．

同様に, $\widetilde{\lambda}^*(b) < 0$ for $b > b^*$, $\widetilde{\lambda}^*(b) > 0$ for $b < b^*$ が示される.

最後に $b = b^*$ のとき, $\boldsymbol{L}$ がどのようになっているか調べよう. まず (7.8) より $\boldsymbol{L}\Phi = 0$ ならば $\phi(r,\theta) = \widetilde{\psi}(r;0)\langle\, \boldsymbol{e}(\theta), \boldsymbol{q}\,\rangle$ の形でなくてはならないことがわかるから, ${}^\forall b$ に対して

$$Ker\boldsymbol{L} = span\{\Phi_1,\ \Phi_2\}$$

であることに注意しておく.

$\phi_0 := -(L_R)^{-1}S_r$ と定義する. また

$$\Psi_1(r,\theta) := {}^t(\boldsymbol{0}, \phi_0(r)\cos\theta),\ \Psi_2(r,\theta) := {}^t(\boldsymbol{0}, \phi_0(r)\sin\theta)$$

と定義する.

Lemma 7.4. $b = b^*$ のとき, $\Phi_1 := {}^t(-\boldsymbol{e}_1, S_r\cos\theta)$, $\Phi_2 := {}^t(-\boldsymbol{e}_2, S_r\sin\theta)$,

$$\Psi_1(r,\theta) := {}^t(\boldsymbol{0}, \phi_0(r)\cos\theta),\ \Psi_2(r,\theta) := {}^t(\boldsymbol{0}, \phi_0(r)\sin\theta)$$

に対して

$$\boldsymbol{L}\Phi_1 = \boldsymbol{L}\Phi_2 = 0,\ \boldsymbol{L}\Psi_1 = -\Phi_1,\ \boldsymbol{L}\Psi_2 = -\Phi_2$$

が成立する.

Outline of Proof. Ψ_1 を $\boldsymbol{L}$ に代入すると

$$\begin{aligned}
\boldsymbol{L}\Psi_1 &= \boldsymbol{L}\begin{pmatrix} \boldsymbol{0} \\ \phi_0(r)\cos\theta \end{pmatrix} = \begin{pmatrix} \beta\Gamma'(S(r_0))\phi_0(r_0)\displaystyle\int_{\partial B_0}\cos\theta\boldsymbol{n}ds \\ (L_R\phi_0)\cos\theta \end{pmatrix} \\
&= \begin{pmatrix} \beta\Gamma'(S(r_0))\phi_0(r_0)\pi r_0\boldsymbol{e}_1 \\ -S_r\cos\theta \end{pmatrix}.
\end{aligned}$$

ここで, (7.6) などより $\phi_0(r) = \psi(r;0)$ であるから, $\phi_0(r_0) = \psi(r_0;0) = -|\psi(r_0;0)| = -b^*$ (補題 7.3 の証明参照) となる. したがって

$$\beta\Gamma'(S(r_0))\phi_0(r_0)\pi r_0 = -\beta\Gamma'(S(r_0))b^*\pi r_0$$

であるが

$$b = \frac{1}{\pi r_0 \beta |\Gamma'(S(r_0))|} = b^*$$

より $\Gamma' \leq 0$ を考慮して

$$1 = \pi r_0 \beta |\Gamma'(S(r_0))| b^* = -\pi r_0 \beta \Gamma'(S(r_0)) b^*$$

となり $\boldsymbol{L}\Psi_1 = {}^t(\boldsymbol{e}_1, -S_r \cos\theta) = -\Phi_1$ を得る．他も同様である． ∎

同様に共役作用素 $\boldsymbol{L}^*$ について考える．

$$\boldsymbol{L}^*\Phi = \boldsymbol{L}\begin{pmatrix} \boldsymbol{q} \\ \phi \end{pmatrix} = \begin{pmatrix} \beta\Gamma'(S(r_0))\pi r_0 S_r(r_0)\boldsymbol{q} + F(S(r_0))\displaystyle\int_{\partial B_0} \phi \boldsymbol{n} ds \\ (d\Delta - \alpha + F'(S)H)\phi + \beta\Gamma'(S(r_0))\delta_{\partial B_0}\langle\, \boldsymbol{e}(\theta), \boldsymbol{q}\,\rangle \end{pmatrix}$$

for $\Phi = (\boldsymbol{q}, \phi) \in \boldsymbol{R}^2 \times H^2(\boldsymbol{R}^2)$ となり，以下の補題を得る．

Lemma 7.5.

$$\Phi_1^*(r,\theta) := \begin{pmatrix} -\frac{F(S(r_0))}{\beta\Gamma'(S(r_0))}\boldsymbol{e}_1 \\ S_r(r)\cos\theta \end{pmatrix},\ \Phi_2^*(r,\theta) := \begin{pmatrix} -\frac{F(S(r_0))}{\beta\Gamma'(S(r_0))}\boldsymbol{e}_2 \\ S_r(r)\sin\theta \end{pmatrix},$$

および

$$\Psi_1^*(r,\theta) := \begin{pmatrix} \frac{a_0 F(S(r_0))}{\beta\Gamma'(S(r_0))}\boldsymbol{e}_1 \\ (-a_0 S_r(r) + \phi_0(r))\cos\theta \end{pmatrix},\ \Psi_2^*(r,\theta) := \begin{pmatrix} \frac{a_0 F(S(r_0))}{\beta\Gamma'(S(r_0))}\boldsymbol{e}_2 \\ (-a_0 S_r(r) + \phi_0(r))\sin\theta \end{pmatrix},$$

$a_0 := \dfrac{\|\phi_0\|_R^2}{\langle\, S', \phi_0\,\rangle_R}$．このとき，$\boldsymbol{L}^*\Phi_j^* = 0$ と $\boldsymbol{L}^*\Psi_j^* = -\Phi_j^*$，および次の規格化が成り立つ:

$$\langle\, \Phi_j, \Phi_j^*\,\rangle_{L^2} = \langle\, \Psi_j, \Psi_j^*\,\rangle_{L^2} = 0,\ \langle\, \Psi_j, \Phi_j^*\,\rangle_{L^2} = \langle\, \Phi_j, \Psi_j^*\,\rangle_{L^2} = \frac{1}{2}\langle\, S', \phi_0\,\rangle_R > 0.$$

Φ_j と Ψ_j は $j \neq k$ のとき Φ_k^*, Ψ_k^* と直交している．

7.3 進行スポット解

前節で b が b^* を横切るとき $\boldsymbol{L}$ のゼロ固有値が Jordann 型に縮退することを示したが, 以降は β を分岐パラメータと考え, b^* に対応する β を $\beta^* := \dfrac{1}{\pi r_0|\Gamma'(S(r_0))|b^*}$ とするのは7.1節と同様である. このとき

$$\lambda^*(\beta) < 0\ (\beta < \beta^*),\ \lambda^*(\beta^*) = 0,\ \lambda^*(\beta) > 0\ (\beta > \beta^*)$$

であった.

$\boldsymbol{S}(\boldsymbol{x}; P) := (P, S(\boldsymbol{x} - P))$, Let $\mathcal{M} := \{\boldsymbol{S}(\cdot - P; P);\ P \in \boldsymbol{R}^2\}$ and $\boldsymbol{U}(y, \boldsymbol{\zeta}, P) := \boldsymbol{S}(y; P) + \zeta_1\Psi_1(y) + \zeta_2\Psi_2(y)$ $(\boldsymbol{\zeta} = (\zeta_1, \zeta_2))$. Define $E := span\{\boldsymbol{S}_1,\ \boldsymbol{S}_2,\ \Psi_1,\ \Psi_2\}$ and the orthogonal space $E^\perp := \{\boldsymbol{v};\ (\boldsymbol{v}, \Phi_j^*)_{L^2} = (\boldsymbol{v}, \Psi_j^*)_{L^2} = 0\ (j = 1, 2)\}$. Then, $\boldsymbol{u} = (u, \widehat{P})^T$ in the neighborhood of $\mathcal{M}$ is uniquely represented by $\boldsymbol{u} = \boldsymbol{U}(x - P; \zeta, P) + (v(x - P), \boldsymbol{q})$ for $P \in \boldsymbol{R}^2$ and $\boldsymbol{v} = (v(y), \boldsymbol{q})^T \in E^\perp$ by a standard manner.

By $\beta = \beta^* + \eta$, (7.1) becomes

$$(7.13)\qquad \begin{cases} c_t(y, t) = D\Delta c - \alpha\, c + F(c)H(r_0 - |y - \boldsymbol{q}|) + \dot{P}\cdot\nabla c, \\ \dfrac{d}{dt}(P + \boldsymbol{q}) = \beta^* \displaystyle\int_{C_{r_0}} \Gamma(c(\boldsymbol{q} + y))d\vec{s} + \eta \int_{C_{r_0}} \Gamma(c(\boldsymbol{q} + y))d\vec{s} \end{cases}$$

for $y = x - P \in \Omega$ and $t \in (0, \infty)$, which we write as

$$(7.14)\qquad \boldsymbol{u}_t = \boldsymbol{A}_0(\boldsymbol{u}) + \eta\boldsymbol{G}_1(\boldsymbol{u}) + \boldsymbol{G}_2(c, \dot{P}),$$

where $\boldsymbol{u} = (c(x - P, t), P + \boldsymbol{q})^T$

$$\begin{aligned} \boldsymbol{u} &= \begin{pmatrix} c \\ P + \boldsymbol{q} \end{pmatrix}, \qquad \boldsymbol{G}_2(c, \dot{P}) := \begin{pmatrix} \dot{P}\cdot\nabla c \\ 0 \end{pmatrix}, \\ \boldsymbol{A}_0(\boldsymbol{u}) &:= \begin{pmatrix} D\Delta c - \alpha\, c + F(c)H(r_0 - |y - \boldsymbol{q}|) \\ \beta^* \int_{\partial B_0} \Gamma(c(\boldsymbol{q} + y))d\vec{s} \end{pmatrix}, \\ \boldsymbol{G}_1(\boldsymbol{u}) &:= \begin{pmatrix} 0 \\ \int_{\partial B_0} \Gamma(c(\boldsymbol{q} + y))d\vec{s} \end{pmatrix}. \end{aligned}$$

By the representation of $\boldsymbol{u} = \boldsymbol{U}(y;\zeta,P)+\boldsymbol{v}$ with $\boldsymbol{v} = (v(y,t),\boldsymbol{q}) \in E^{\perp}$, (7.14) becomes

$$\begin{aligned}
\boldsymbol{v}_t &= \boldsymbol{L}_0\boldsymbol{v} + \boldsymbol{L}_0(\zeta_1\Psi_1+\zeta_2\Psi_2) - (\dot{\zeta}_1\Psi_1+\dot{\zeta}_2\Psi_2) + \frac{1}{2}\boldsymbol{A}_0''(\boldsymbol{S})(\zeta_1\Psi_1+\zeta_2\Psi_2+\boldsymbol{v})^2+\cdots \\
&\quad +\eta\boldsymbol{G}_1(\boldsymbol{U}+\boldsymbol{v}) + \boldsymbol{G}_2(U,\dot{P}) - (0,\dot{P})^T + \boldsymbol{G}_2(\boldsymbol{v},\dot{P}) \\
&= \boldsymbol{L}_0\boldsymbol{v} - (\zeta_1\boldsymbol{S}_1+\zeta_2\boldsymbol{S}_2) - (\dot{\zeta}_1\Psi_1+\dot{\zeta}_2\Psi_2) + \frac{1}{2}\boldsymbol{A}_0''(\boldsymbol{S})(\zeta_1\Psi_1+\zeta_2\Psi_2+\boldsymbol{v})^2+\cdots \\
&\quad +\eta\boldsymbol{G}_1(\boldsymbol{U}+\boldsymbol{v}) + \dot{p}_1\boldsymbol{S}_1 + \dot{p}_2\boldsymbol{S}_2 + \boldsymbol{G}_2(\zeta_1\Psi_1+\zeta_2\Psi_2,\dot{P}) + \boldsymbol{G}_2(\boldsymbol{v},\dot{P}),
\end{aligned}$$

where $\boldsymbol{L}_0 = \boldsymbol{A}_0'(\boldsymbol{S})$ and $P = (p_1,p_2)^T$. Thus, all the necessary properties of the equation for $\boldsymbol{v}$ are satisfied together with the property of $\boldsymbol{L}_0$, as in Lemma ??, so that we can apply the results of [11]. As a consequence, we have the following results corresponding to Theorem 2.2 in [11]:

Lemma 7.6. *$P(t)$ and $\zeta(t) = (\zeta_1(t),\zeta_2(t))$ satisfy*

$$\left\{\begin{array}{rcl} \dot{P} &=& \zeta + O(|\zeta|^3 + |\eta|^{\frac{3}{2}}), \\ \dot{\zeta} &=& -\nabla_\zeta W + O(|\zeta|^4+|\eta|^2) \end{array}\right. \tag{7.15}$$

as long as $|\zeta| < \zeta^*$ and $|\eta| < \eta^*$ for positive constants ζ^* and η^*, where $W = W(\zeta) := \frac{1}{4}M_1|\zeta|^4 + \frac{1}{2}M_2\eta|\zeta|^2$. M_1 and M_2 are given by

$$\begin{aligned}
M_1 &:= \frac{2}{(S',\phi_0)_R}\Bigg(-\frac{1}{8}\{\int_0^{r_0} rF'''(S(r))\phi_0^3(r)S_r(r)dr - \frac{\Gamma'''(S_0)}{\Gamma'(S_0)}\phi_0^3(r_0)F(S_0)\} \\
&\quad -\frac{1}{4}\int_0^{r_0} rF''(S(r))\phi_0(r)(V_1(r)+\frac{1}{2}W_1(r))S_r(r)dr \\
&\quad +\frac{\Gamma''(S_0)F(S_0)\phi_0(r_0)}{4\Gamma'(S_0)}(V_1(r_0)+\frac{1}{2}W_1(r_0)) \\
&\quad -\frac{1}{2}\int_0^{r_0}(2r\partial_r V_1(r) + r\partial_r W_1(r) + 2W_1(r))S_r(r)dr\Bigg), \\
M_2 &:= \frac{\phi_0(r_0)F(S_0)}{\beta^*(S',\phi_0)_R},
\end{aligned}$$

where $V_1(r)$ *and* $W_1(r)$ *are the solutions of*

$$(7.16)\quad -L_R^0 V_1 \;=\; \frac{1}{2}\left(\partial_r\phi_0 - \frac{1}{2}F''(S(r))H(r_0-r)\phi_0^2 + \frac{1}{r}\phi_0(r)\right),$$

$$(7.17)\quad -L_R^2 W_1 \;=\; \frac{1}{2}\left(\partial_r\phi_0 - \frac{1}{2}F''(S(r))H(r_0-r)\phi_0^2 - \frac{1}{r}\phi_0(r)\right),$$

respectively and $L_R^N := -D\left(\frac{d^2}{dr^2} + \frac{1}{r}\frac{d}{dr} - \frac{N^2}{r^2}\right) - F'(S(r))H(r_0-r) + \alpha.$

Proof. The proof is basically the same as that for Theorem 2.2 in [~~?~~]. 12
We simply show that the constants M_1 and M_2 are given by the above equations.

First, we shall consider M_1. From (7.15), we have

$$\dot{\zeta}_1 = -M_1(\zeta_1^2+\zeta_2^2)\zeta_1 - M_2\eta\zeta_1 + h.o.t.$$

Thus, M_1 is the coefficient of ζ_1^3 and $\zeta_2^2\zeta_1$. According to the proof of Theorem 2.2 ([11]), ζ_1^3 and $\zeta_2^2\zeta_1$ are derived from

$$(7.18)\qquad \frac{1}{6}(\boldsymbol{A}_0'''(\boldsymbol{S})(\zeta_1\Psi_1+\zeta_2\Psi_2)^3, \Phi_1^*)_{L^2},$$

$$(7.19)\qquad (\boldsymbol{A}_0''(\boldsymbol{S})(\zeta_1\Psi_1)(\zeta_1^2\boldsymbol{v}_1), \Phi_1^*)_{L^2},$$

$$(7.20)\qquad -(\partial_x\boldsymbol{v}_1, \Phi_1^*)_{L^2},$$

where the function $\boldsymbol{v}_1$ is defined by

$$-\boldsymbol{L}\boldsymbol{v}_1 = \frac{1}{2}\boldsymbol{A}_0''(\boldsymbol{S})\Psi_1^2 + \partial_{y_1}\Psi_1.$$

First, we consider the coefficient ζ_1^3 in (7.18), that is,

$$\frac{1}{6}(\boldsymbol{A}_0'''(\boldsymbol{S})\Psi_1^3, \Phi_1^*)_{L^2}.$$

We calculate

$$\begin{aligned}
&(\boldsymbol{A}_0'''(\boldsymbol{S})\Psi_1^3, \Phi_1^*)_{L^2} \\
&= (\begin{pmatrix} \cos^3\theta F'''(S(r))H(r_0-r)\phi_0^3(r) \\ \beta^*\Gamma'''(S_0)\displaystyle\int_{\partial B_0}\cos^3\theta\phi_0(r)\,d\vec{s} \end{pmatrix}, \begin{pmatrix} S_r\cos\theta \\ -\dfrac{F(S_0)}{\beta^*\Gamma'(S_0)}\boldsymbol{e}_1 \end{pmatrix})_{L^2} \\
&= \frac{3}{4}\pi M_1',
\end{aligned}$$

where

$$M_1' := \int_0^{r_0} rF'''(S(r))\phi_0^3(r)S'(r)dr - \frac{\Gamma'''(S_0)}{\Gamma'(S_0)}\phi_0^3(r_0)F(S_0).$$

Next, consider (7.19), that is,

$$(\boldsymbol{A}_0''(\boldsymbol{S})\Psi_1\cdot\boldsymbol{v}_1, \Phi_1^*)_{L^2}. \tag{7.21}$$

This requires the calculation of $\boldsymbol{v}_1$. Since the equation of $\boldsymbol{v}_1$ is written for $\boldsymbol{v}_1 = (v, \boldsymbol{q})$

$$\begin{aligned}
\boldsymbol{L}\boldsymbol{v}_1 &= \begin{pmatrix} (D\Delta - \alpha + F'(S(r))H(r_0-r)v + F(S_0)\delta(r_0-r)\boldsymbol{e}(\theta)\cdot\boldsymbol{q} \\ \beta^*\Gamma'(S_0)[\pi r_0 S'\boldsymbol{q} + \displaystyle\int_{C_{r_0}} v\,d\vec{s}] \end{pmatrix} \\
&= \begin{pmatrix} (\cos^2\theta\partial_r\phi_0 - \dfrac{\sin^2\theta}{r}\phi_0) + \dfrac{1}{2}F''(S(r))H(r_0-r)\cos^2\theta\phi_0^2(r) \\ \dfrac{1}{2}\beta^*F''(S_0)\displaystyle\int_{C_{r_0}}\cos^2\theta\phi_0^2(r)d\vec{s} \end{pmatrix} \\
&= \begin{pmatrix} (\cos^2\theta\partial_r\phi_0 + \dfrac{\sin^2\theta}{r}\phi_0) - \dfrac{1}{2}F''(S(r))H(r_0-r)\cos^2\theta\phi_0^2(r) \\ 0 \end{pmatrix},
\end{aligned}$$

$\boldsymbol{v}_1 = \begin{pmatrix} V_1(r) + \cos 2\theta W_1(r) \\ 0 \end{pmatrix}$ satisfies the above equation of $\boldsymbol{v}_1$ together with $\boldsymbol{v}_1 \in E^\perp$ if V_1 and W_1 are defined by (7.16) and (7.17). Substituting

$\boldsymbol{v}_1$ of this form into (7.21), we have

$$(\boldsymbol{A}_0''(\boldsymbol{S})\Psi_1 \cdot \boldsymbol{v}_1, \Phi_1^*)_{L^2} = \pi M_1'',$$

where

$$\begin{aligned} M_1'' &:= \int_0^{r_0} rF''(S(r))\phi_0(r)(V_1(r) + \frac{1}{2}W_1(r))S'(r)dr \\ &\quad - \frac{\Gamma''(S_0)F(S_0)\phi_0(r_0)}{4\Gamma'(S_0)}(V_1(r_0) + \frac{1}{2}W_1(r_0)). \end{aligned}$$

Finally, we obtain (7.20). Since

$$\partial_x \boldsymbol{v}_1 = \cos\theta\partial_r \boldsymbol{v}_1 + \frac{\sin\theta}{r}\partial_\theta \boldsymbol{v}_1 = \begin{pmatrix} \cos\theta\partial_r V_1 + \cos\theta\cos 2\theta\partial_r W_1 - \frac{2\sin\theta\sin 2\theta}{r}W_1 \\ 0 \end{pmatrix},$$

(7.20) is calculated as

$$\pi M_1''' := -(\partial_x \boldsymbol{v}_1, \Phi_1^*)_{L^2} = -\frac{1}{2}\pi\int_0^{r_0}(2r\partial_r V_1(r) + r\partial_r W_1(r) + 2W_1(r))S_r(r)dr.$$

Thus, the coefficient of ζ_1^3 is given by $\frac{1}{6}\cdot\frac{3}{4}\pi M_1' + \pi M_1'' + \pi M_1''' = \pi(\frac{1}{8}M_1' + M_1'' + M_1''')$. Since $(\Psi_1, \Phi_1^*)_{L^2} = \frac{1}{2}\pi(S', \phi_0)_R$ from Lemmas7.4, 7.5, M_1 is given by $M_1 = -\frac{2}{(S', \phi_0)_R}(\frac{1}{8}M_1' + M_1'' + M_1''')$, which is used in this lemma.

Similarly, M_2 is given by

$$M_2 = -\frac{2}{(S', \phi_0)_R}(\boldsymbol{G}_1'(\boldsymbol{S})\Psi_1, \Phi_1^*)_{L^2},$$

which proves this lemma. □

Remark 7.1. *By Lemma 7.6, ζ denotes the deformation of solution c from the radially symmetric solution $S(y)$ as well as the velocity of the camphor disc, because ζ gives $\dot{P}$ for the location $P(t)$.*

Remark 7.2. *Here, $\phi_0(r) \leq 0$, and $F(c)$ is positive. Hence, M_2 is a negative constant, while the sign of M_1 is not fixed and depends on various factors, such as F, Γ, and. in particular, the radius of the camphor disc, r_0.*

Remark 7.3. *The negative sign of the constant M_2 and (7.15) implies that the radially symmetric stationary solution $\boldsymbol{S}(x-P;P)$ is stable for $\eta < 0 (\beta < \beta^*)$ and unstable for $\eta > 0 (\beta > \beta^*)$, whereas the sign of M_1 determines the direction of bifurcation, that is, super-critical bifurcation occurs when $M_1 > 0$ and sub-critical bifurcation occurs when $M_1 < 0$.*

III: ドリフト分岐点近傍における反射現象 Repulsive Interaction of Pulses

$$\begin{aligned} \boldsymbol{u}_t &= D\boldsymbol{u}_{xx} + F(\boldsymbol{u}) + \eta g(\boldsymbol{u}) \ (= F(\boldsymbol{u}; k_c + \eta)) \quad -\infty < x < \infty \\ &= \mathcal{L}(\boldsymbol{u}) + \eta g(\boldsymbol{u}) \qquad \boldsymbol{u} \in \mathbb{R}^N,\ D = diag\{d_1, \cdots, d_N\}1 \end{aligned}$$

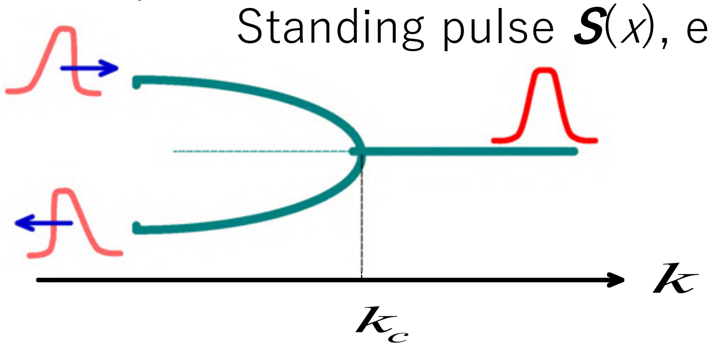

$k = k_c$; 分岐点 (ドリフト分岐点)

$$L = D\partial_x^2 + F'(S(x); k_c) \text{ 線形化作用素}$$

$$L = \mathcal{L}'(S),\ LS_x = 0,\ L^{\exists}\psi = -S_x$$

$$\boldsymbol{w} = \sigma(q;\eta) \in X^{\perp} \text{ s.t. } \|\sigma\|_{\omega} \le O(q^3 + |\eta|^{3/2})$$

$$\boldsymbol{u}(t,x) = S(x-p) + q\psi(x-p) + q^2\xi(x-p) + \eta\zeta(x-p) + \sigma(q;\eta)(x-p)$$

Repulsive Interaction of Pulses

$$\mathbf{u}(t,x) = S(x-p_1) + q_1\psi(x-p_1) + q_1{}^2\xi(x-p_1) + \eta\varsigma(x-p_1)$$

$$+S(x-p_2) + q_2\psi(x-p_2) + q_2{}^2\xi(x-p_2) + \eta\varsigma(x-p_2) + \mathbf{v}$$

$$\mathbf{v} = O(q_1{}^3 + q_2{}^3 + \eta^2 + \delta)$$

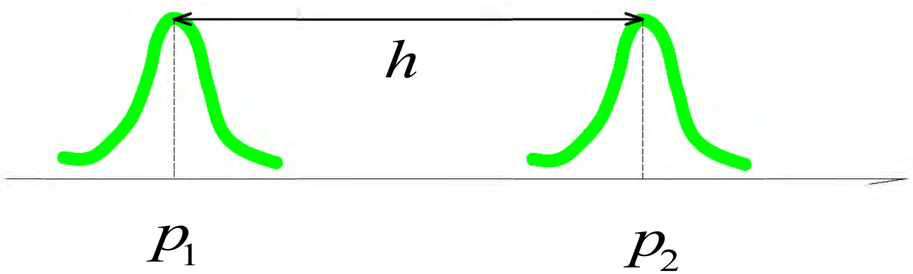

$$\delta = \delta(h) := \sup_{x\in \boldsymbol{R}} |\mathcal{L}(S(x) + S(x-h))|$$

$$\delta(h) \to 0 \text{ as } h \to \infty \ (\mathcal{L}(S(x)) \equiv 0)$$

Rem. $S(x) \to e^{-\alpha|x|}\mathbf{a} \Rightarrow \delta(h) = O(e^{-\alpha h})$

$$\mathbf{u}_t(t,x), \quad x-p_1 \Rightarrow x,\, x-p_2 \Rightarrow x-h$$

$$-\dot{p}_1 S_x + \dot{q}_1\psi - \dot{p}_1 q_1 \psi_x + 2q_1\dot{q}_1\xi - q_1{}^2\dot{p}_1\xi_x - \eta\,\dot{p}_1\varsigma_x$$

$$-(\dot{p}_1 + \dot{h})S_x(x-h) + \cdots - \dot{p}_1\mathbf{v}_x + \mathbf{v}_t$$

$$\boxed{\begin{aligned}\dot{q}_1 \quad = \quad & \langle\, \mathcal{L}(S(x)+S(x-h)), \varphi^*\,\rangle - M_1 q_1^3 + M_2\eta q_1 \\ & +O(q_1^4 + q_2^4 + \eta^{3/2} + \delta^2)\end{aligned}}$$

REM. $S(x) \to e^{-\alpha|x|}\boldsymbol{a} \Rightarrow \langle\, \mathcal{L}(S(x)+S(x-h)), \varphi^*\,\rangle \sim M_0 e^{-\alpha h}$

Equations of q_j, h and p_1

$$\langle\, \mathcal{L}(S(z)+S(z-h)), \phi_0^*(h)\,\rangle_2 = M_0 e^{-\alpha h} + O(e^{-\gamma h})\ ({}^\exists\gamma > \alpha)$$

を示す．$\phi_0^*(h) = \phi^* + O(\delta)$ と $|\mathcal{L}(S(z)+S(z-h))| \le O(\delta)$ より

$$\begin{aligned}
&\langle\, \mathcal{L}(S(z)+S(z-h)), \phi_0^*(h)\,\rangle_2 \\
&= \langle\, \mathcal{L}(S(z)+S(z-h)), \phi^*\,\rangle_2 + O(\delta^2) \\
&= \langle\, \{F(S(z)+S(z-h)) - F(S(z)) - F(S(z-h)), \phi^*(z)\,\rangle_2 + O(\delta^2) \\
&= \int_{-\infty}^{\frac{1}{2}h} \langle\, F(S(z)+S(z-h)) - F(S(z)) - F(S(z-h)), \phi^*(z)\,\rangle\, dz \\
&\quad + \int_{\frac{1}{2}h}^{\infty} \langle\, F(S(z)+S(z-h)) - F(S(z)) - F(S(z-h)), \phi^*(z)\,\rangle\, dz + O(\delta^2) \\
&= \int_{-\infty}^{\frac{1}{2}h} \langle\, \{F'(S(z)) - F'(0)\}S(z-h), \phi^*(z)\,\rangle\, dz + \int_{-\infty}^{\frac{1}{2}h} O(e^{-2\alpha|z-h|}\cdot e^{-\alpha|z|})dz \\
&\quad \int_{\frac{1}{2}h}^{\infty} \{F'(S(z-h)) - F'(0)\}S(z), \phi^*(z)\,\rangle\, dz + \int_{\frac{1}{2}h}^{\infty} O(e^{-2\alpha|z|}\cdot e^{-\alpha|z|})dz + O(\delta^2) \\
&= \int_{-\infty}^{\frac{1}{2}h} \langle\, \{F'(S(z)) - F'(0)\}S(z-h), \phi^*(z)\,\rangle\, dz \\
&\quad + \int_{\frac{1}{2}h}^{\infty} \{F'(S(z-h)) - F'(0)\}S(z), \phi^*(z)\,\rangle\, dz + O(e^{-\frac{3}{2}\alpha h}) + O(\delta^2) \\
&= \int_{-\infty}^{\frac{1}{2}h} \langle\, \{F'(S(z)) - F'(0)\}e^{-\alpha(h-z)}\boldsymbol{a}, \phi^*(z)\,\rangle\, dz \\
&\quad + \int_{\frac{1}{2}h}^{\infty} O(e^{-2\alpha|z-h|}\cdot e^{-2\alpha z})dz + O(e^{-\gamma h}) \\
&= e^{-\alpha h}\int_{-\infty}^{\frac{1}{2}h} \langle\, \{F'(S(z)) - F'(0)\}e^{\alpha z}\boldsymbol{a}, \phi^*(z)\,\rangle\, dz + O(e^{-\gamma h}).
\end{aligned}$$

ここで α が

$$\alpha^2 D\boldsymbol{a} + F'(0)\boldsymbol{a} = 0$$

を満たすことから

$$D(e^{\alpha z}\boldsymbol{a})_{zz} + F'(0)(e^{\alpha z}\boldsymbol{a}) = 0$$

が成立している．これを上記の式に代入することにより

$$D\partial_z^2\phi^* + {}^tF'(S(z))\phi^* = 0$$

$$\begin{aligned}
(\text{与式}) &= e^{-\alpha h}\int_{-\infty}^{\frac{1}{2}h}\langle\, F'(S(z))e^{\alpha z}\boldsymbol{a} + D\partial_z^2(e^{\alpha z}\boldsymbol{a}), \phi^*(z)\,\rangle\, dz + O(e^{-\gamma h}) \\
&= e^{-\alpha h}\int_{-\infty}^{\frac{1}{2}h}\{\langle\, e^{\alpha z}\boldsymbol{a}, \underline{{}^tF'(S(z))\phi^*(z)}\,\rangle + \langle\, e^{\alpha z}\boldsymbol{a}, \underline{D\partial_z^2\phi^*(z)}\,\rangle\}dz \\
&\quad + e^{-\alpha h}\left[\langle\, D(e^{\alpha z}\boldsymbol{a})_z, \phi^*(z)\,\rangle - \langle\, D(e^{\alpha z}\boldsymbol{a}), \partial_z\phi^*(z)\,\rangle\right]_{-\infty}^{\frac{1}{2}h} + O(e^{-\gamma h}) \\
&= 0 + e^{-\alpha h}\{\langle\, \alpha e^{\alpha z}D\boldsymbol{a}, e^{-\alpha z}\boldsymbol{a}^*\,\rangle - \langle\, De^{\alpha z}\boldsymbol{a}, (-\alpha)e^{-\alpha z}\boldsymbol{a}^*\,\rangle\}_{z=\frac{1}{2}h} + O(e^{-\gamma h}) \\
&= 2\alpha\langle\, D\boldsymbol{a}, \boldsymbol{a}^*\,\rangle e^{-\alpha h} + O(e^{-\gamma h})
\end{aligned}$$

となり証明できた．∎

Simple case(symmetric case)

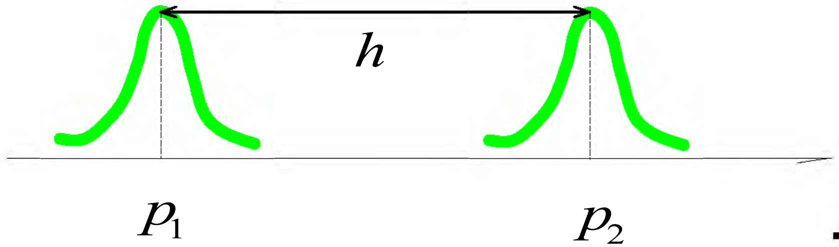

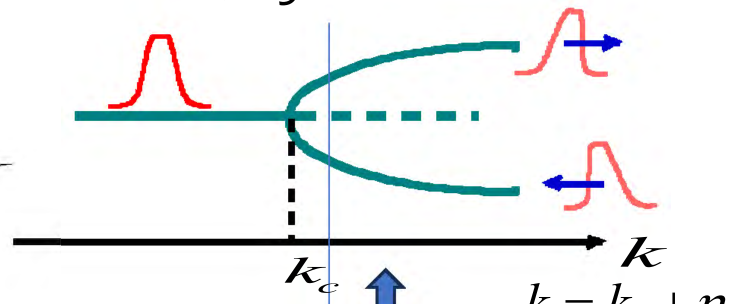

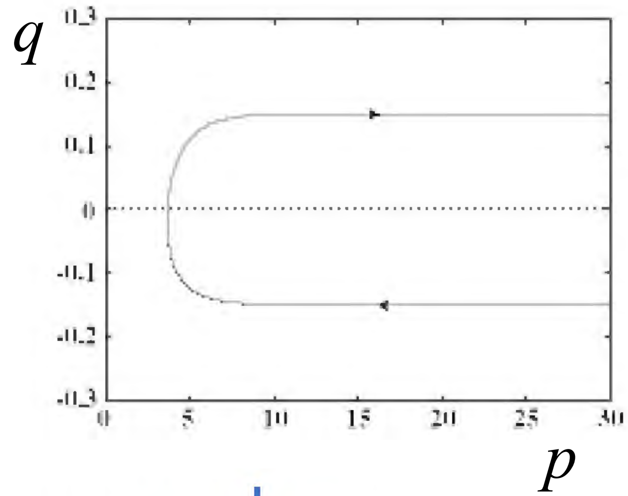

$$\begin{cases} \dot p_1 &= q_1 - \widetilde{M}_0 e^{-\alpha(p_2-p_1)}, \\ \dot q_1 &= -M_1 q_1^3 + M_2\eta q_1 - M_0 e^{-\alpha(p_2-p_1)}, \\ \dot p_2 &= q_2 + \widetilde{M}_0 e^{-\alpha(p_2-p_1)}, \\ \dot q_2 &= -M_1 q_2^3 + M_2\eta q_2 + M_0 e^{-\alpha(p_2-p_1)}, \end{cases}$$

$M_1,\ M_2 > 0$

$M_0 > 0,\ \widetilde{M}_0 > 0$

$p_2 = p,\ p_1 = -p,\ q_2 = q_1 = q$

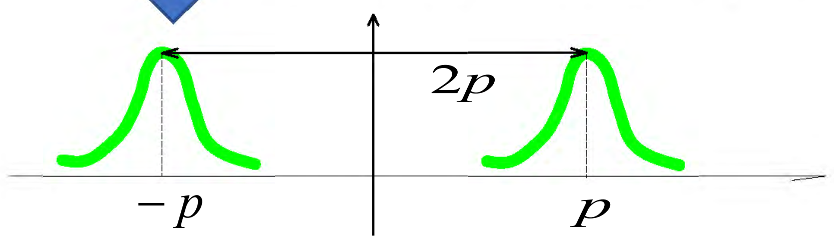

$$\dot p = q + \tilde M_0 e^{-2\alpha p}$$

$$\dot q = -M_1 q^3 + M_2 \eta q + M_0 e^{-2\alpha p}$$

$\eta > 0$

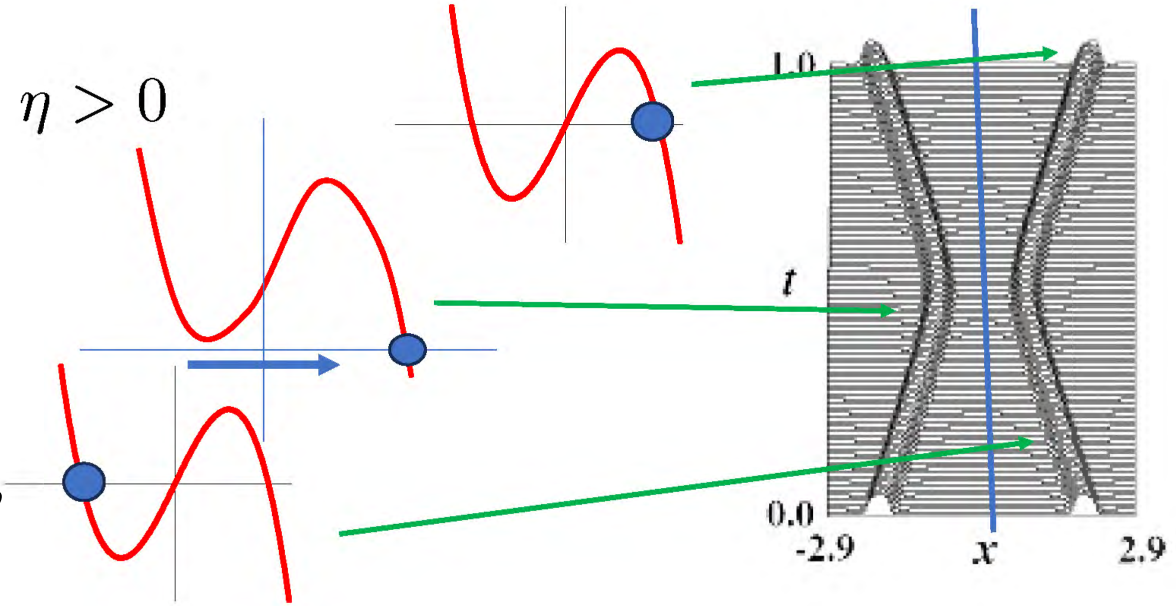

Interaction of traveling spots

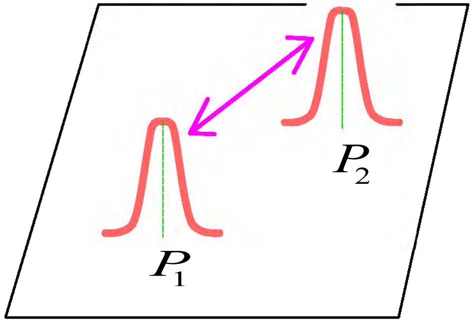

$$\mathbf{u}_t = D\Delta\mathbf{u} + \mathbf{F}(\mathbf{u}; k_c + \eta) = \underline{\underline{D\Delta\mathbf{u} + \mathbf{F}(\mathbf{u})}} + \eta g(\mathbf{u})$$

$$= \underline{\underline{L(\mathbf{u})}} + \eta g(\mathbf{u}),\ x \in \mathbf{R}^2,\ \mathbf{u} \in \mathbf{R}^N$$

Assume $S(x) \to \frac{1}{\sqrt{r}} e^{-\alpha r}\mathbf{a}\ (r = |x| \to \infty),\ \mathbf{a} \in \mathbf{R}^{\mathrm{N}}$

Define $S(x;\mathbf{h}) := S(x) + S(x - \mathbf{h}) \quad (\mathbf{h} \in \mathbf{R}^2)$

$$\delta(\mathbf{h}) := \sup_{x \in \mathbf{R}^2} |L(S(x;\mathbf{h}))| = O\left(\frac{1}{\sqrt{h}} e^{-\alpha h}\right) \quad (h = |\mathbf{h}|)$$

$$\Theta(x;\boldsymbol{\varsigma}) := S(x) + \varsigma_1\psi_1(x) + \varsigma_2\psi_2(x) \quad (\boldsymbol{\varsigma} = (\varsigma_1, \varsigma_2))$$

$$L^{\exists}\psi_1 = -S_x,\ L^{\exists}\psi_2 = -S_y$$

Theorem

$$\mathbf{u}(t,x) = \Theta(x - P_1; \varsigma_1) + \Theta(x - P_2; \varsigma_2) + O(\delta(\mathbf{h}) + |\varsigma_1|^2 + |\varsigma_2|^2 + |\eta|),$$

$$\begin{cases} \dot{P}_1 = \varsigma_1 - \dfrac{M_0}{\sqrt{h}} e^{-\alpha h} \mathbf{e} + O(\delta^2 + |\varsigma_1|^3 + |\varsigma_2|^3 + |\eta|^{3/2}), \\ \dot{P}_2 = \varsigma_2 + \dfrac{M_0}{\sqrt{h}} e^{-\alpha h} \mathbf{e} + O(\delta^2 + |\varsigma_1|^3 + |\varsigma_2|^3 + |\eta|^{3/2}), \\ \dot{\varsigma}_1 = -\nabla W(\varsigma_1) - \dfrac{M'_0}{\sqrt{h}} e^{-\alpha h} \mathbf{e} + O(\delta^2 + |\varsigma_1|^4 + |\varsigma_2|^4 + |\eta|^2), \\ \dot{\varsigma}_2 = -\nabla W(\varsigma_2) + \dfrac{M'_0}{\sqrt{h}} e^{-\alpha h} \mathbf{e} + O(\delta^2 + |\varsigma_1|^4 + |\varsigma_2|^4 + |\eta|^2), \end{cases}$$

as long as $\quad |\varsigma_j| < \varsigma^*, |\eta| < \eta^*, \ {}^\forall P_j \in \mathbf{R}^2$

$$\mathbf{h} = P_2 - P_1, h = |P_2 - P_1|, \mathbf{e} = \frac{|P_2 - P_1|}{h}$$

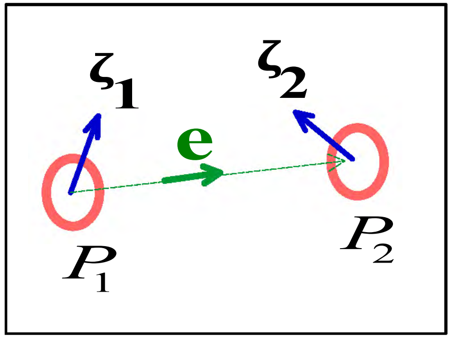

$$k = k_c + \eta$$

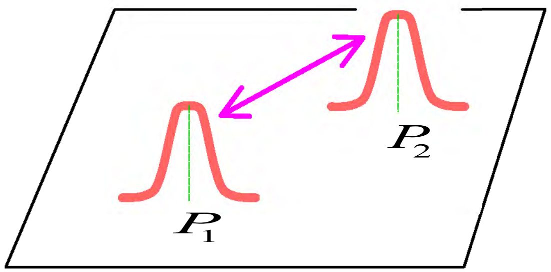

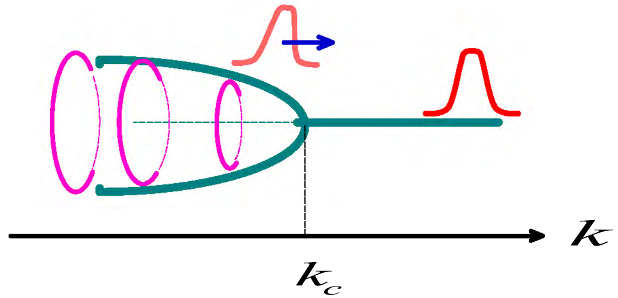

$$M_0, M'_0 > 0 \Rightarrow$$

Repulsive interaction

$$h = | P_2 - P_1 |, \mathbf{e} = \frac{| P_2 - P_1 |}{h}$$

$$\begin{cases} \dot{P}_1 = \varsigma_1 - \dfrac{M_0}{\sqrt{h}} e^{-\alpha h} \mathbf{e}, \\ \dot{P}_2 = \varsigma_2 + \dfrac{M_0}{\sqrt{h}} e^{-\alpha h} \mathbf{e}, \\ \dot{\varsigma}_1 = -\nabla W(\varsigma_1) - \dfrac{M'_0}{\sqrt{h}} e^{-\alpha h} \mathbf{e}, \\ \dot{\varsigma}_2 = -\nabla W(\varsigma_2) + \dfrac{M'_0}{\sqrt{h}} e^{-\alpha h} \mathbf{e}, \end{cases}$$

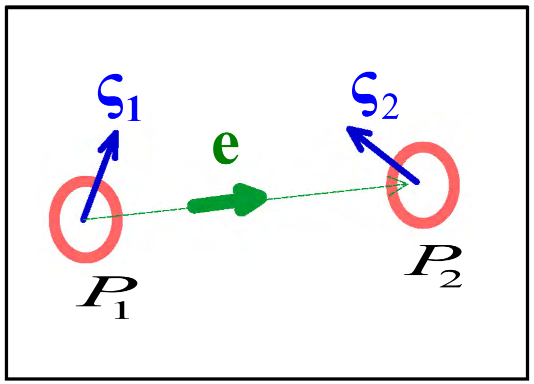

Special Cases

- On a line

$$P_j = (p_j, 0), \boldsymbol{\varsigma}_{\mathbf{j}} = (\varsigma_j, 0)$$

(E. Mimura, Nagayama 02)

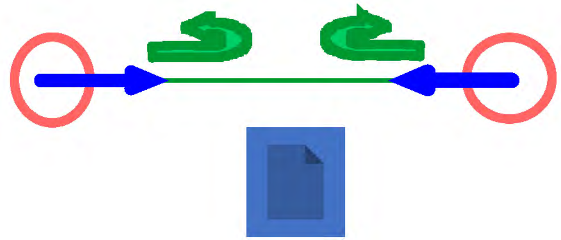

- Neuman boundary

$$P_1 = (p, q), \boldsymbol{\varsigma}_1 = (\varsigma, \xi), P_2 = (p, -q), \boldsymbol{\varsigma}_2 = (\varsigma, -\xi),$$

(Matsumoto 02)

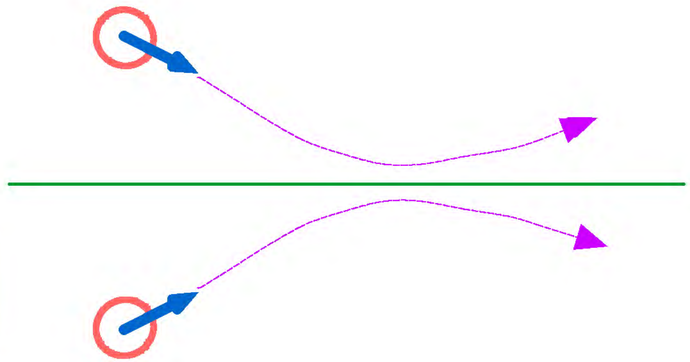

ODE1 ODE2 PDE1 PDE2

Example of 2D reflecting traveling spot

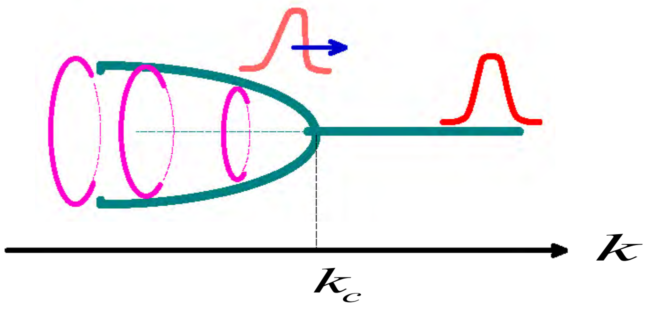

c.f. フロント解のドリフト分岐 [17]

1D reflec.

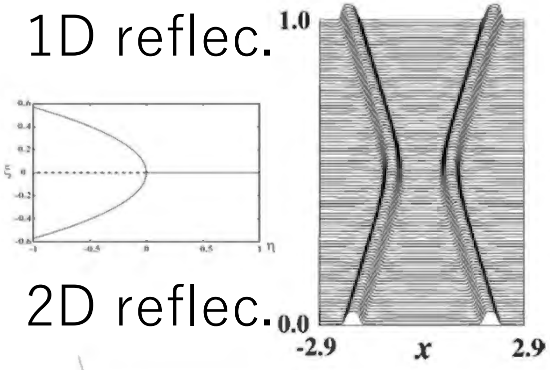

2D reflec.

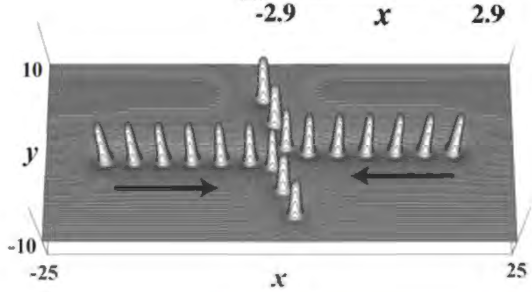

Drift bifurcation of
traveling pulse, spot

Pitch-fork type bifurcation
diagram of pulses, spots

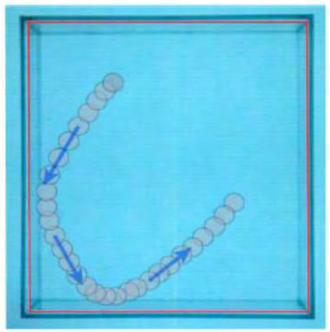

Experiment for camphor disk

By Kanda (02, Hiroshima Univ.)

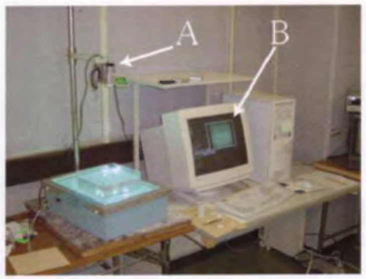

Recorded by the video camera at A and monitored by the display at B to produce a movie.

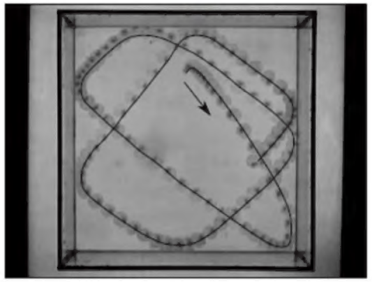

A trajectory of a camphor disk of an experiment

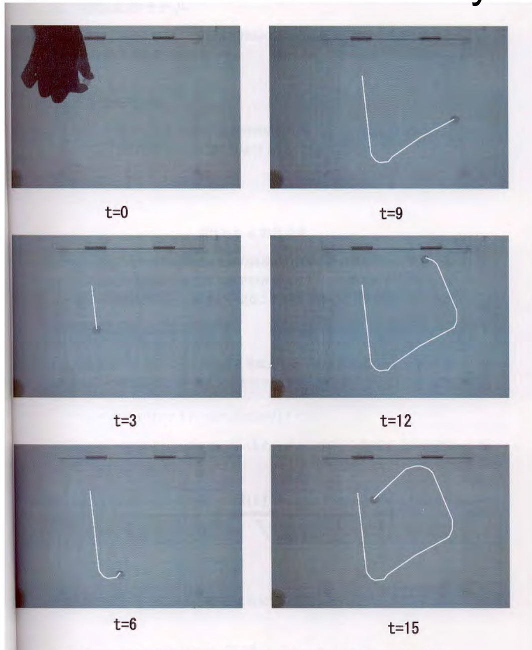

図4：円板樟脳の観察2（純度の高いとき）

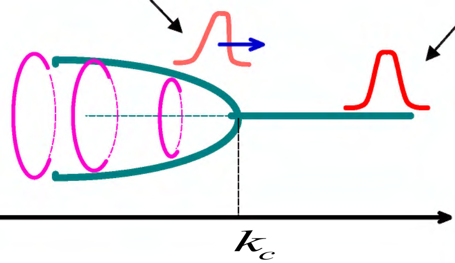

k = 1/(content rate of camphor)

Camphor disk problem is a nice example both from models and phenomena !

Camphor Layer Model(樟脳)

- Nagayama et.al.00

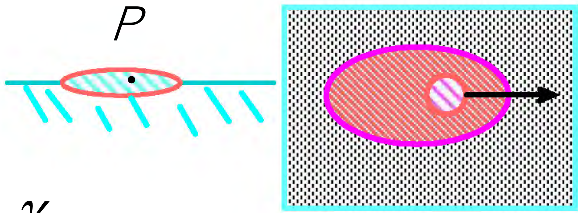

$$\begin{cases} u_t = D\Delta u - au + F(|x-P|), \\ \ddot{P} = \nabla_x \gamma(u)|_{x=P} - \mu \dot{P}, \end{cases}$$

$$\gamma(u) = \frac{\gamma_0}{1+cu}$$

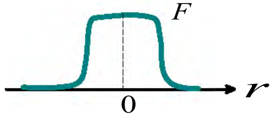

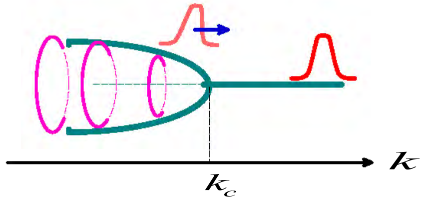

- Mimura et.al.01

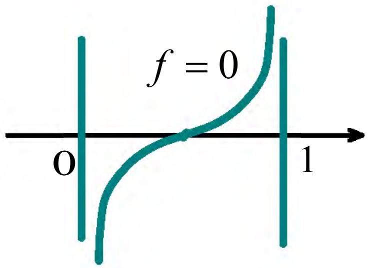

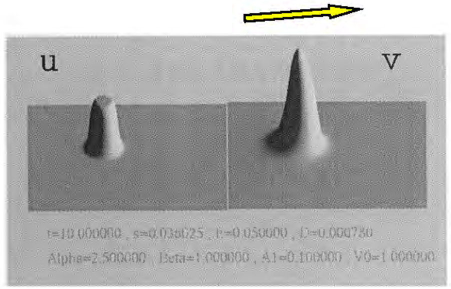

(Koya 00)

$$\begin{cases} \tau\varepsilon u_t = \varepsilon^2 \Delta u + f(u,v) - \langle f \rangle, \\ v_t = D\Delta v + au - \gamma v, \end{cases}$$

$$\langle f \rangle = \frac{1}{|\Omega|}\int f\,dx, \quad f(u,v) = u(1-u)(u-a(v)), \quad a(v) = \frac{1+\tanh v}{2}$$

Moving boundary (MB) model for camphor disk

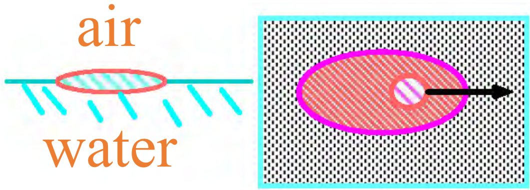

$$\begin{cases} \dfrac{dP}{dt} &= \displaystyle\int_{\partial\Omega_c} \gamma(u)\boldsymbol{n}dl, \\ u_t &= \Delta u - u + f(\boldsymbol{x}, P), \end{cases}$$

Chen, E, Mimura 2009

$$f(\boldsymbol{x}, P) = \begin{cases} f_0, & \boldsymbol{x} \in \overline{\Omega}_c, \\ 0, & \boldsymbol{x} \in \Omega \backslash \overline{\Omega}_c, \end{cases}$$

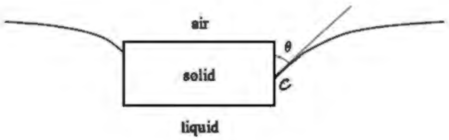

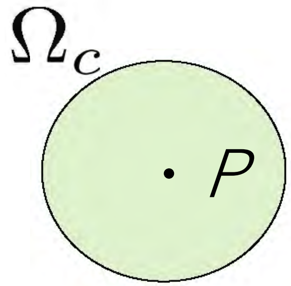

First rigorous result
for drift bifurcation and 2D reflection

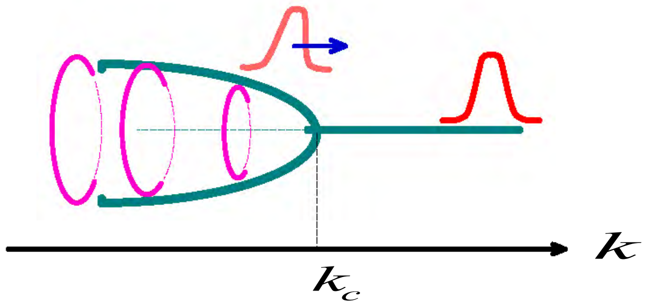

MB model which can be rigorously treated.

文献[1]

Interaction of camphor disks

$$k = k_c + \eta$$

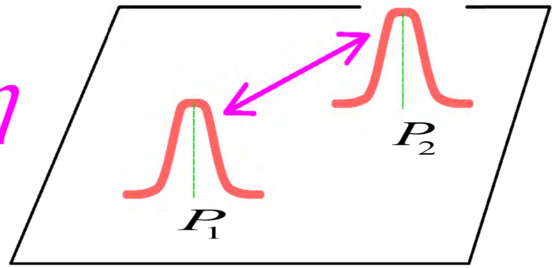

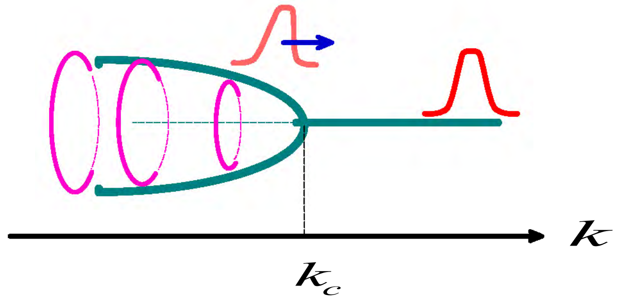

MB model

$$M_0, M'_0 > 0 \Rightarrow$$ Repulsive interaction

$$\begin{cases} \dot{P}_1 = \varsigma_1 - \dfrac{M_0}{\sqrt{h}} e^{-\alpha h} \mathbf{e}, \\ \dot{P}_2 = \varsigma_2 + \dfrac{M_0}{\sqrt{h}} e^{-\alpha h} \mathbf{e}, \\ \dot{\varsigma}_1 = -\nabla W(\varsigma_1) - \dfrac{M'_0}{\sqrt{h}} e^{-\alpha h} \mathbf{e}, \\ \dot{\varsigma}_2 = -\nabla W(\varsigma_2) + \dfrac{M'_0}{\sqrt{h}} e^{-\alpha h} \mathbf{e}, \end{cases}$$

$$h = |P_2 - P_1|, \mathbf{e} = \frac{|P_2 - P_1|}{h}$$

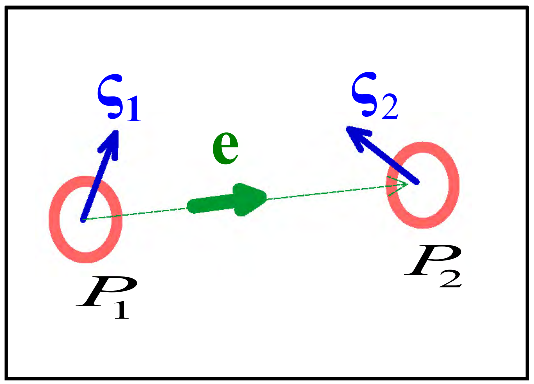

Special Cases

- On a line

$$P_j=(p_j,0),\ \boldsymbol{\varsigma}_j=(\varsigma_j,0)$$

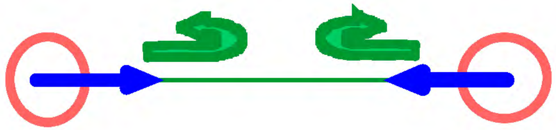

(E. Mimura, Nagayama 02)

- Neuman boundary

$$P_1=(p,q),\ \boldsymbol{\varsigma}_1=(\varsigma,\xi),\ P_2=(p,-q),\ \boldsymbol{\varsigma}_2=(\varsigma,-\xi),$$

(Matsumoto 02)

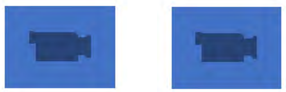

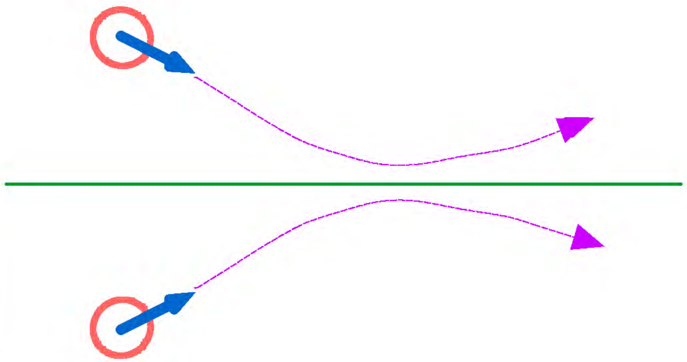

Dynamics of ODE

$$P = (p, q),\ V = (\zeta, \xi),\ P^* = (p, -q),\ V^* = (\zeta, -\xi)$$

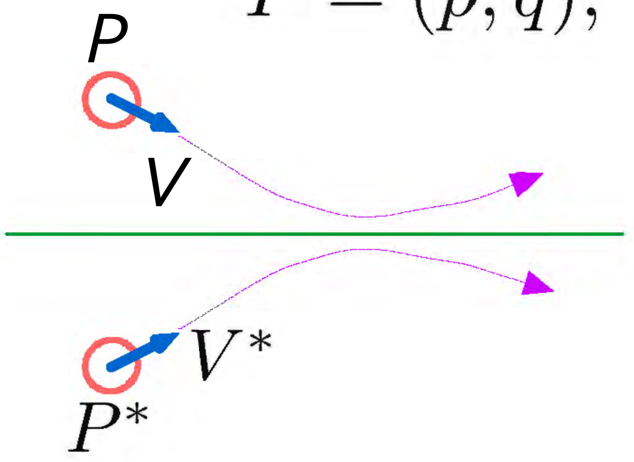

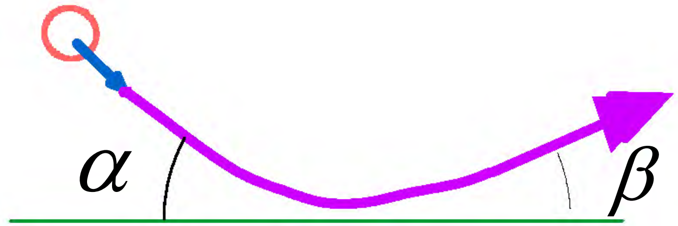

$$\beta = T(\alpha)$$

$$\alpha > \beta \ (?)$$

$(\alpha \geq \beta)$ Mimura et.al

Meaning?

difference from usual billiard problem ?

$$\begin{cases} \dot{p} &= \zeta, \\ \dot{q} &= \xi + \dfrac{M_0}{\sqrt{2q}} e^{-2\alpha q}, \\ \dot{\zeta} &= -(M_1|V|^2 + M_2\eta)\zeta, \\ \dot{\xi} &= -(M_1|V|^2 + M_2\eta)\xi + \dfrac{M_0'}{\sqrt{2q}} e^{-2\alpha q}, \end{cases}$$

Dynamics in a square region

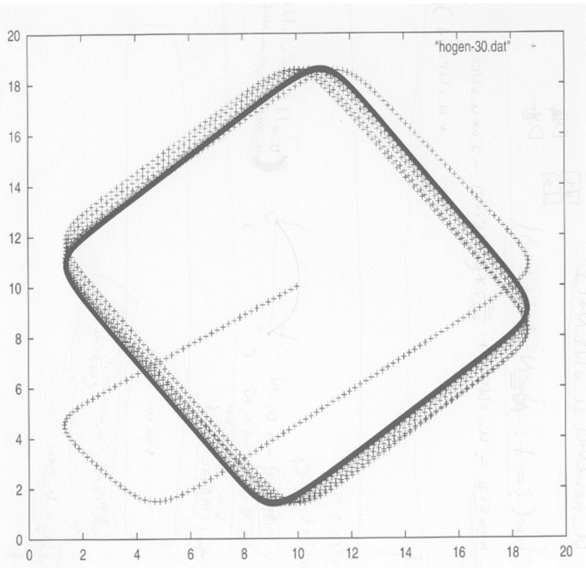

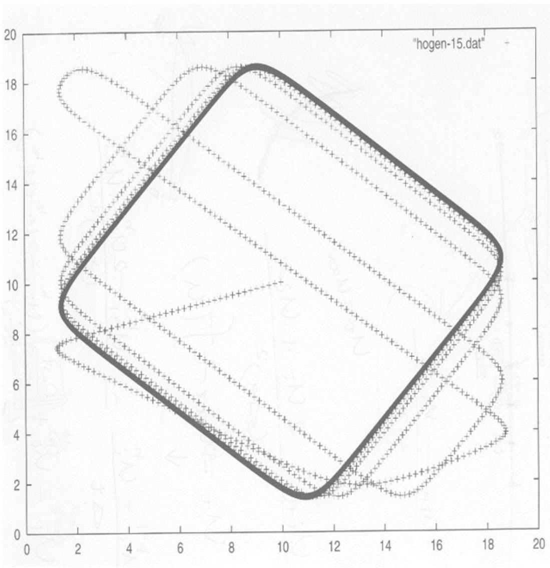

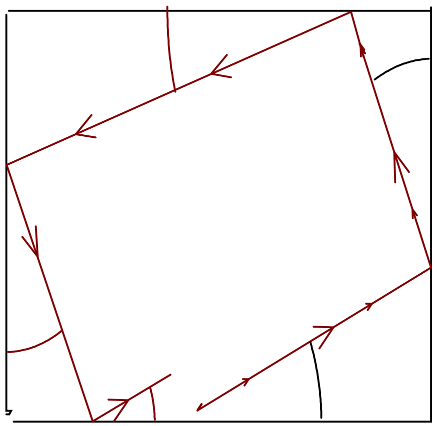

Mimura sensei discovered the stable limit cycle

c.f. Billiard problem
(Generically the region is densely filled by orbits)

Experiment in Hiroshima
by Mimura and Lab. students 2002

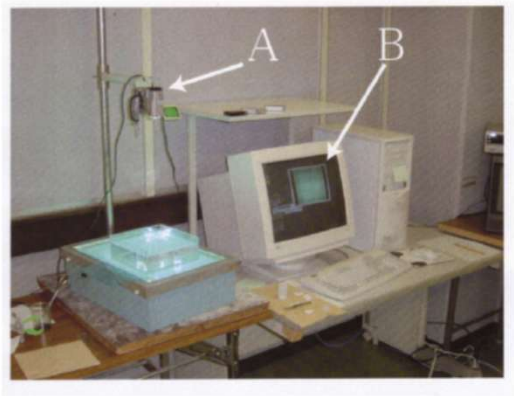

Fig. 1.1 The experimental facility by Kanda[4]. The experiment was recorded by the video camera at A and monitored by the display at B to produce a movie.

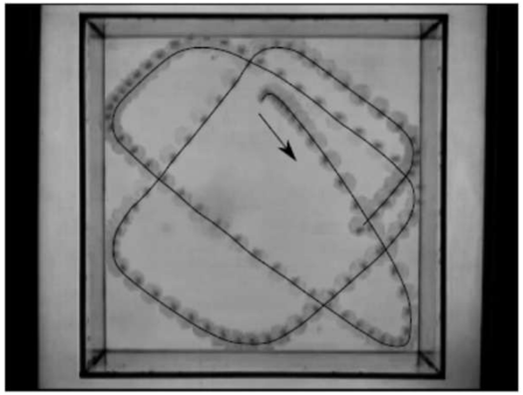

Fig. 1.2 A trajectory of a camphor disk of an experiment by [4].

Complicated motions of camphor disk

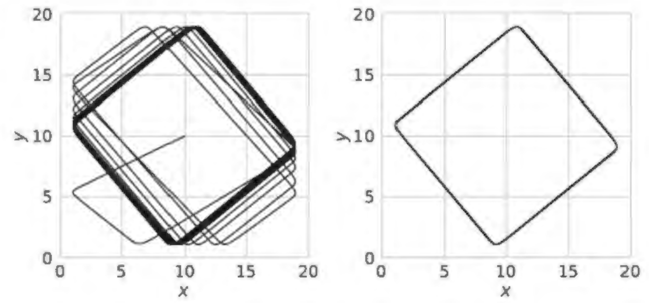

Fig. 1.9 Trajectories of the center of the disk of moving boundary model on square . Left: $0 \leq t \leq 10^4$, Right: $9.5 \times 10^3 \leq t \leq 10^4$.

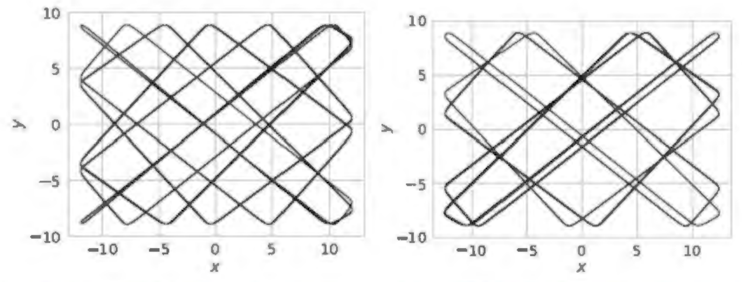

Fig. 1.11 Complicated periodic orbits for (1.11) on rectangular domains with $k = 1.3$(left) and $k = 1.35$ (right).

$$k = a/b$$

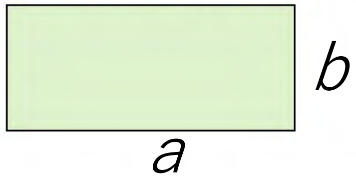

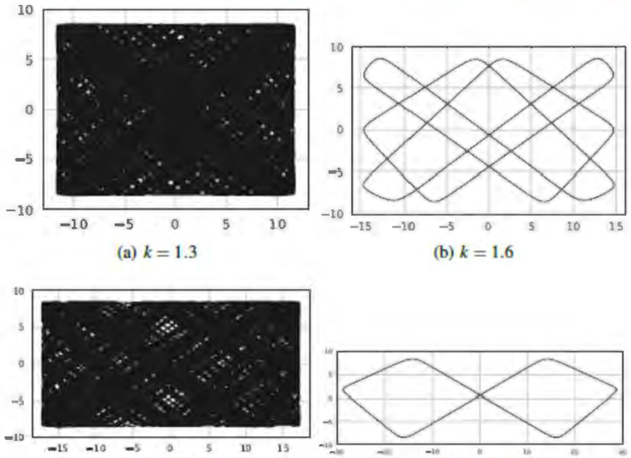

(a) $k = 1.3$ (b) $k = 1.6$

(c) $k = 1.85$ (d) $k = 3.0$

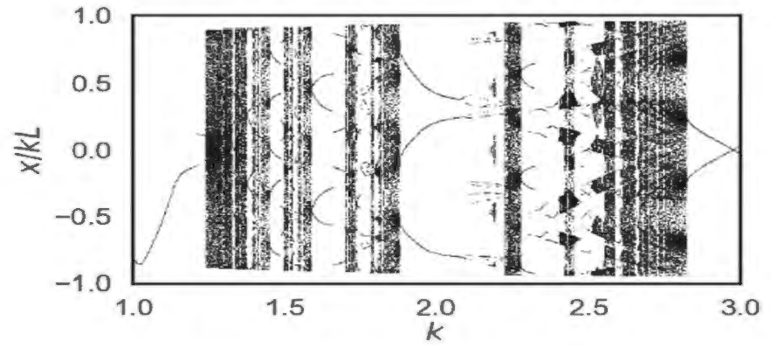

Fig. 1.15 An orbit diagram for (1.11). The horizontal and vertical axes are k and x/kL, respectively.

4. Y. Kanda. Experiments and numerical analyses for motions of a camphor disk(in Japanese). Bachelor thesis, Hiroshima University, 2002.
5. M. Mimura, T. Miyaji, and I. Ohnishi, A billiard problem in nonlinear and nonequilibrium systems, Hiroshima Math. J. 37(2007) 343–384.
6. S. Nakata, Y. Iguchi, S. Ose, M. Kuboyama, T. Ishii, and K. Yoshikawa. Self-rotation of a camphor scraping on water: new insight into the old problem. Langmuir 13 (1997) 4454–4458.
7. S. Nakata et al.(eds.) Self-organized Motion: Physicochemical Design based on Nonlinear Dynamics, Royal Society of Chemistry, 2019.
8. U. A. Rozikov, An Introduction to Mathematical Billiards, World Scientific, New Jersey, 2019
9. N. J Suematsu and S. Nakata, Evolution of Self-Propelled Objects: From the Viewpoint of Nonlinear Science, Chemistry–A European Journal 24 (2018) 6308–6324.
10. T. Vicsek et al., Novel type of phase transition in a system of self-driven particles, Phys. Rev. Lett. 75 (1995) 1226. 11. T. Vicsek and A. Zafeiris, Collective motion, Phys. Rep. 517 (2012) 71–140

Limiting problem

by considering sufficiently large region

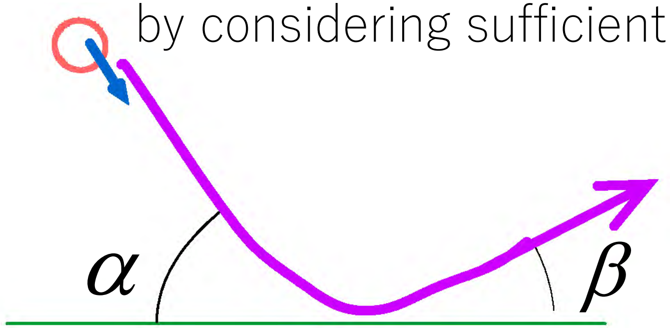

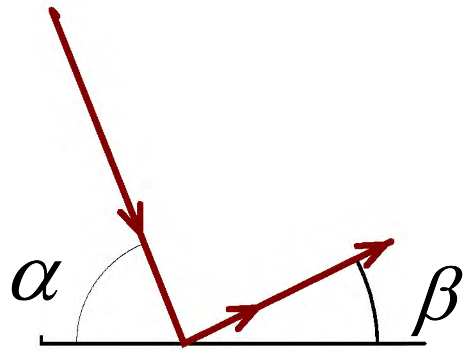

$$\beta = T(\alpha)$$

Discrete time model

Assume

$$\alpha > \beta$$

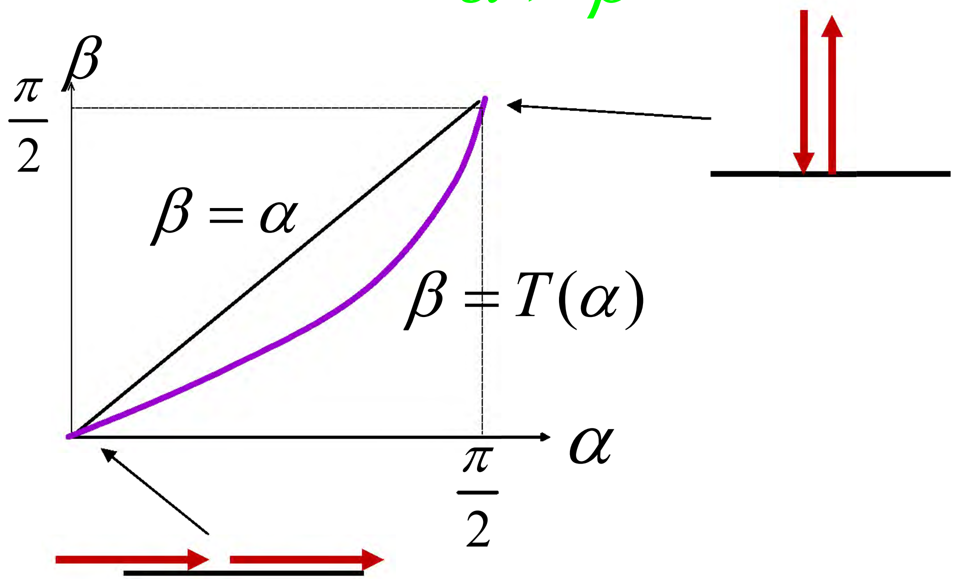

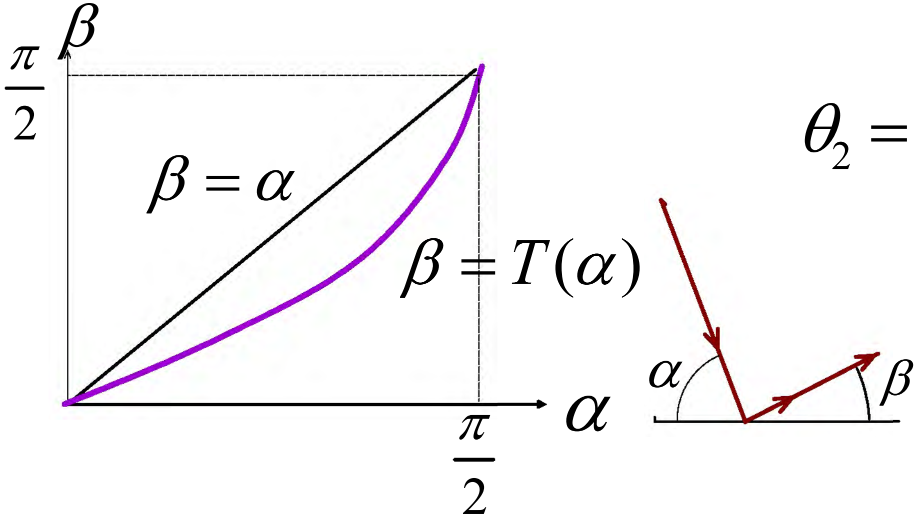

$$\theta_2 = \bar{T}(\theta_1) = T(\pi/2 - \theta_1)$$

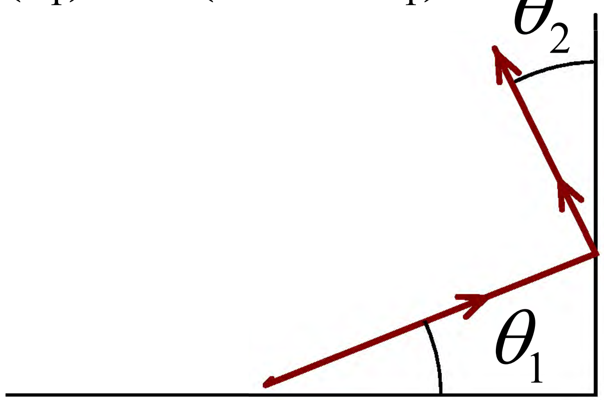

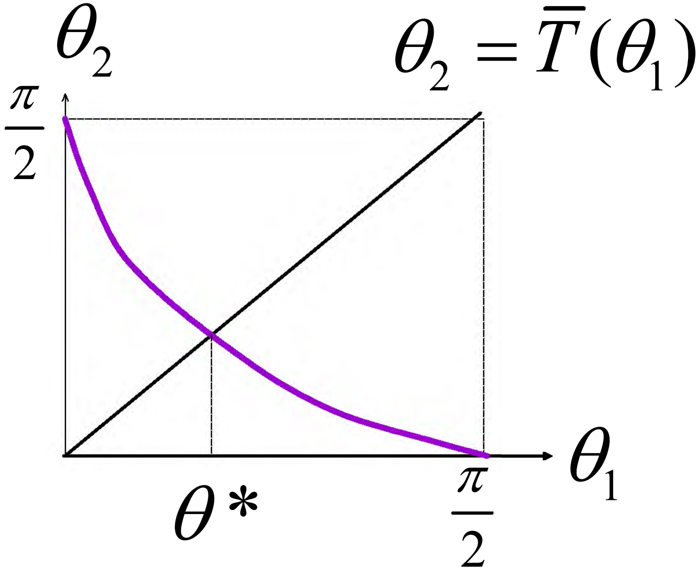

$$\theta_2 = \bar{T}(\theta_1) = T(\pi/2-\theta_1)$$

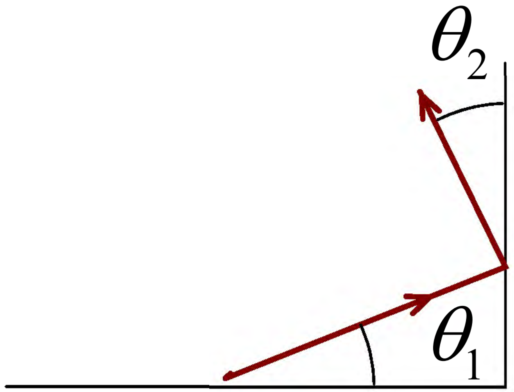

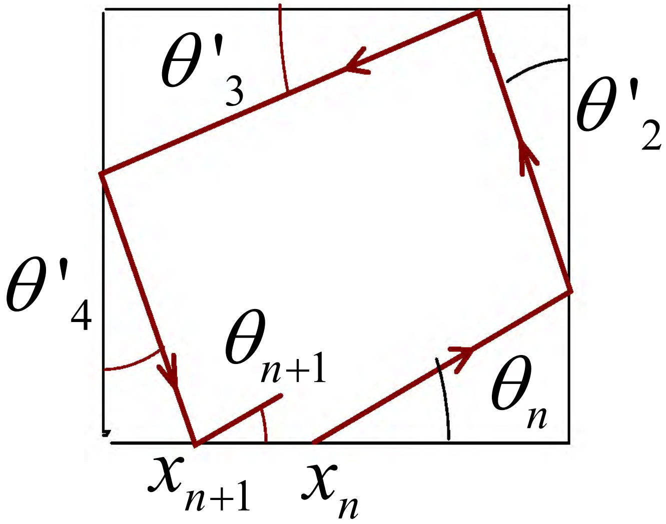

$$\theta_{n+1} = \bar{T}^4(\theta_n)$$

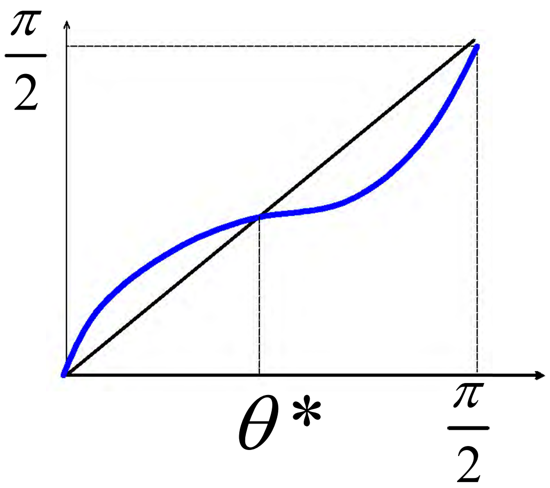

Numerically true (Mimura et.al.)

$$\begin{cases} \theta_{n+1} = \bar{T}^4(\theta_n) \\ x_{n+1} = G(\theta_n, x_n) \end{cases}$$

θ^*; stable

$$\theta_n \to \theta^* (n \to \infty)$$

$$\begin{cases} \theta_{n+1} = \bar{T}^4(\theta_n) \\ x_{n+1} = G(\theta_n, x_n) \end{cases}$$

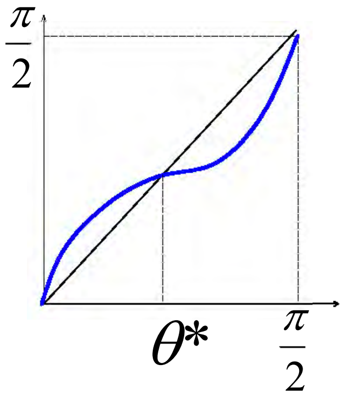

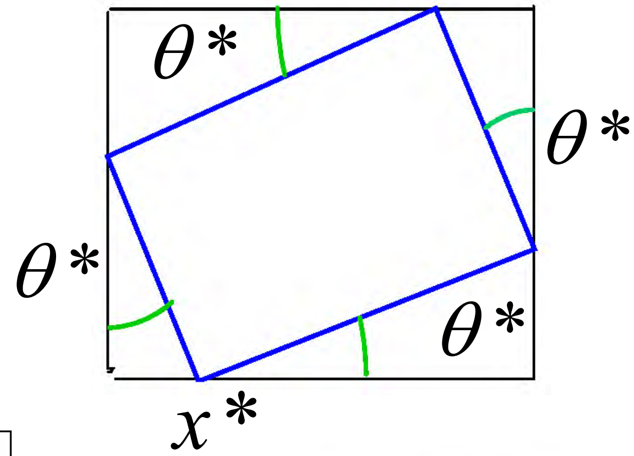

Prop. Suppose θ^* is stable.

If $\alpha > \beta = T(\alpha)$, then for θ near θ^*,

$$|G(\theta,x) - G(\theta,y)| \le q\,|x-y|$$

holds for $0 < q < 1$.

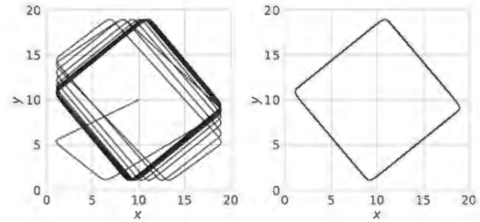

Fig. 1.9 Trajectories of the center of the disk of moving boundary model on square . Left: $0 \le t \le 10^4$, Right: $9.5 \times 10^3 \le t \le 10^4$.

$$\theta^* = \bar{T}^4(\theta^*),$$

$$x^* = G(\theta^*, x^*)$$

⇒ $\theta_n \to \theta^*,\ x_n \to {}^{\exists}x^*\ (n \to \infty)$

⇒ Unique existence of stable limit cycle

Remained problems

Discrete time model

$$\theta_{n+1} = \overline{T}^4(\theta_n)$$

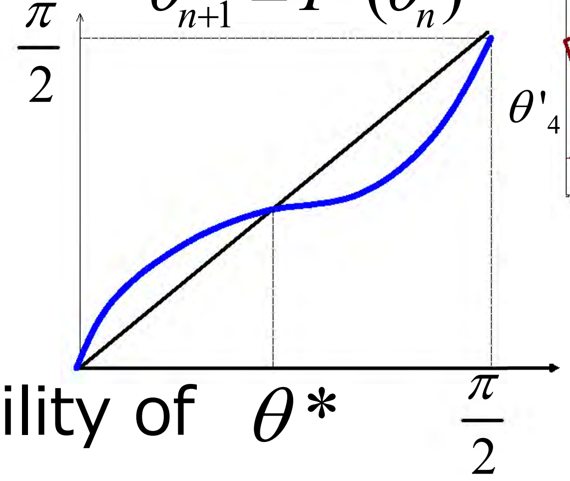

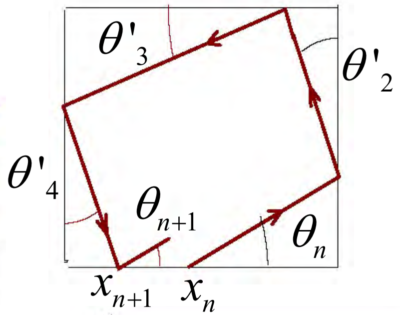

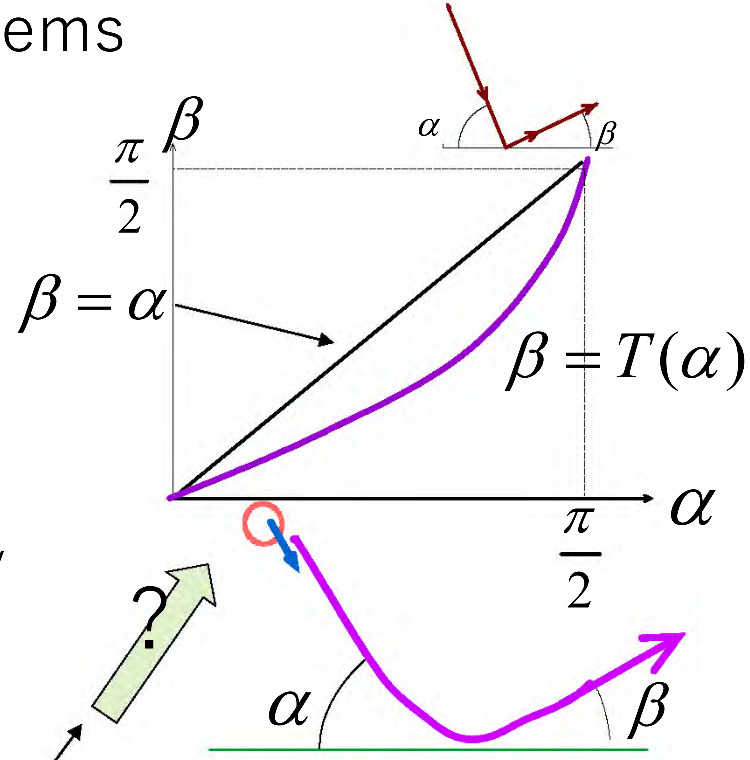

?

$\alpha > \beta$

unsatisfactory

?

? Stability of θ^*

Numerically true (Mimura et.al.)

$$\overline{T}(\theta) := T(\pi/2 - \theta)$$

MB model

$$\left\{ \begin{array}{lll} \dfrac{dP}{dt} & = & \displaystyle\int_{\partial\Omega_c} \gamma(u)\boldsymbol{n}dl, \\ u_t & = & \Delta u - u + f(\boldsymbol{x}, P), \end{array} \right.$$

ODE
particle model

$$\left\{ \begin{array}{lll} \dot{p} & = & \zeta, \\ \dot{q} & = & \xi + \dfrac{M_0}{\sqrt{2q}} e^{-2\alpha q}, \\ \dot{\zeta} & = & -(M_1|V|^2 + M_2\eta)\zeta, \\ \dot{\xi} & = & -(M_1|V|^2 + M_2\eta)\xi + \dfrac{M_0'}{\sqrt{2q}} e^{-2\alpha q}, \end{array} \right.$$

$$M_0 = 0$$

15. Ei, Masayasu Mimura and T. Miyaji, Reflection of a self-propelling rigid disk from a boundary, DCDS-A 2021, 14(3): 803-817
Special issue on recent topics in material, computer and life sciences. doi: 10.3934/dcdss.2020229

Proposition[15]

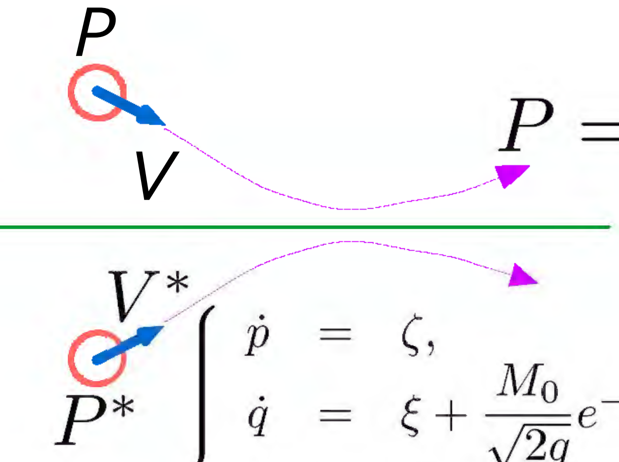

$$P=(p,q),\ V=(\zeta,\xi),\ P^*=(p,-q),\ V^*=(\zeta,-\xi)$$

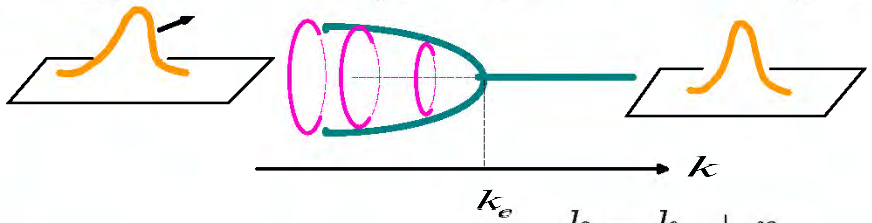

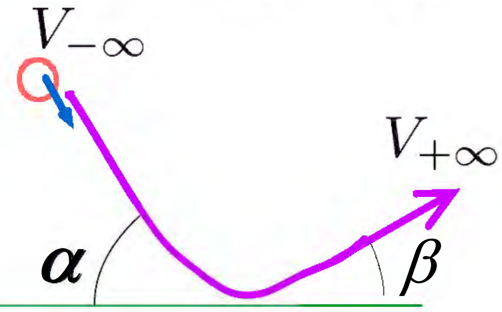

$$k=k_c+\eta$$

$$\left\{\begin{array}{lcl}\dot p &=& \zeta,\\ \dot q &=& \xi+\dfrac{M_0}{\sqrt{2q}}e^{-2\alpha q},\\ \dot\zeta &=& -(M_1|V|^2+M_2\eta)\zeta,\\ \dot\xi &=& -(M_1|V|^2+M_2\eta)\xi+\dfrac{M_0'}{\sqrt{2q}}e^{-2\alpha q},\end{array}\right. \Rightarrow \left\{\begin{array}{lcl}\dot q &=& r\sin\theta+\dfrac{M_0}{\sqrt{2q}}e^{-2\alpha q},\\ \dot r &=& -(M_1r^2+M_2\eta)r+\dfrac{M_0'\sin\theta}{\sqrt{2q}}e^{-2\alpha q},\\ \dot\theta &=& \dfrac{M_0'\cos\theta}{r\sqrt{2q}}e^{-2\alpha q}\end{array}\right. \quad \text{(E)}$$

$$V=r\boldsymbol{e}(\theta)$$

$$\boldsymbol{e}(\theta)=\begin{pmatrix}\cos\theta\\ \sin\theta\end{pmatrix}$$

$$(q,\zeta,\xi)\iff(q,r,\theta)$$

$$\theta_{-\infty}=\alpha>0,\ \theta_{+\infty}=\beta>0$$

(BC) $\displaystyle\lim_{t\to\pm\infty}(q(t),r(t),\theta(t))=\left(+\infty,\sqrt{\frac{-M_2\eta}{M_1}},\pm\theta_{\pm\infty}\right)$

$$V_{\pm\infty}=\sqrt{\frac{-M_2\eta}{M_1}}\boldsymbol{e}(\pm\theta_{\pm\infty})$$

1. For $\theta_{-\infty}\in[0,\pi/2]$, ${}^{\exists_1}\theta_{+\infty}\in[0,\pi/2]$ satisfying (E) and (BC).
2. If $\theta_{-\infty}\neq\pi/2$, $\dot q$ changes its sign from negative to positive just once.
3. If $M_0=0$, $\theta_{-\infty}\geq\theta_{+\infty}$ with equality only if $\theta_{-\infty}=0$ *or* $\pi/2$.

Relation between real phenomena and models

Real phenomena

1.3 Moving boundary model 3

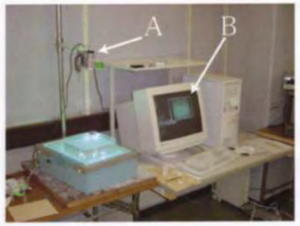

Fig. 1.1 The experimental facility by Kanda[4]. The experiment was recorded by the video camera at A and monitored by the display at B to produce a movie.

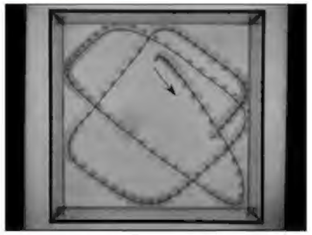

Fig. 1.2 A trajectory of a camphor disk of an experiment by [4].

more realistic but complicated models

(can not be analyzed, many black boxes)

+

Discrete time model

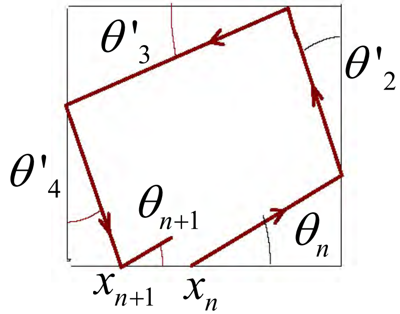

?

check experimentally

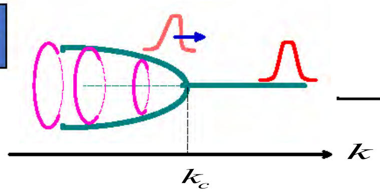

drift bifurcation

MB model

$$\begin{cases} \dfrac{dP}{dt} &= \displaystyle\int_{\partial\Omega_c} \gamma(u)\boldsymbol{n}dl, \\ u_t &= \Delta u - u + f(\boldsymbol{x}, P), \end{cases}$$

ODE

particle model

$$\begin{cases} \dot{p} &= \zeta, \\ \dot{q} &= \xi + \dfrac{M_0}{\sqrt{2q}}e^{-2\alpha q}, \\ \dot{\zeta} &= -(M_1|V|^2 + M_2\eta)\zeta, \\ \dot{\xi} &= -(M_1|V|^2 + M_2\eta)\xi + \dfrac{M_0'}{\sqrt{2q}}e^{-2\alpha q}, \end{cases}$$

実験との融合

実際の現象をより忠実に再現するためには

↑

モデル方程式の多変数化, 関数形の複雑化

実験で何が確認できるか.

物理現象: かなり詳細に計測可能
化学反応: 低分子ではかなり詳細に,
　　　　　高分子では定性的性質くらい
生命系:　On-Offの効果, 単調性くらい

生命系, あるいはそれに近い系: 定性的性質のみ仮定

・具体的な関数形を仮定できない
・ブラックボックスのまま扱う　⇒　現象でも確かに起きていることはないか？
・必要な変数の数も不明瞭
・・・・・・・・・・・・・・忠実な再現は困難

models with black boxes

$$\begin{cases} \dfrac{dP}{dt} &= \displaystyle\int_{\partial\Omega_c} \gamma(u)\boldsymbol{n}dl, \\ u_t &= \Delta u - u + f(\boldsymbol{x}, P), \end{cases}$$

u ; density of camphor expanding to water

generalization with black boxes

$$\begin{cases} \dfrac{dP}{dt} &= \displaystyle\int_{\partial\Omega_c} \gamma_1(U)\boldsymbol{n}dl, \\ U_t &= D\Delta U + F_0(U) + F_1(\boldsymbol{x}, P), \end{cases}$$

Rely on parts according to physical law

Corresponding to high molecular parts:
Generalize to vector values and treat as black box

$$u \in \boldsymbol{R} \Rightarrow U \in \boldsymbol{R}^N,\ D := diag\{d_1, \cdots, d_N\},\ d_j > 0$$

+

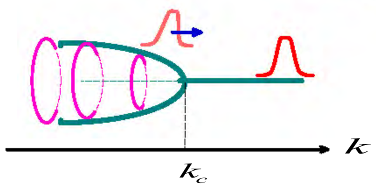

drift bifurcation

particle model

$$\begin{cases} \dot{p} &= \zeta, \\ \dot{q} &= \xi + \dfrac{M_0}{\sqrt{2q}} e^{-2\alpha q}, \\ \dot{\zeta} &= -(M_1|V|^2 + M_2\eta)\zeta, \\ \dot{\xi} &= -(M_1|V|^2 + M_2\eta)\xi + \dfrac{M_0'}{\sqrt{2q}} e^{-2\alpha q}, \end{cases}$$

例:樟脳(camphor)モデル

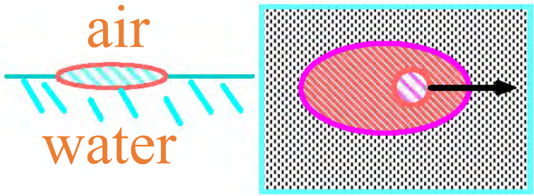

Iida, Kitahata, Nagayama 13

$$\begin{cases} \dfrac{dP}{dt} = \displaystyle\int_{\partial\Omega_c} \gamma_1(u)\boldsymbol{n}dl, \\ \dfrac{d\Theta}{dt} = \displaystyle\int_{\partial\Omega_c} \gamma_2(u)(\boldsymbol{r}\times\boldsymbol{n})dl, \\ u_t = \Delta u - u + f(\boldsymbol{x}, P, \Theta), \end{cases}$$

$$f(\boldsymbol{x}, \boldsymbol{x}_c, \theta_c) = \begin{cases} f_0, & \boldsymbol{x} \in \overline{\Omega}_c, \\ 0, & \boldsymbol{x} \in \Omega\backslash\overline{\Omega}_c, \end{cases}$$

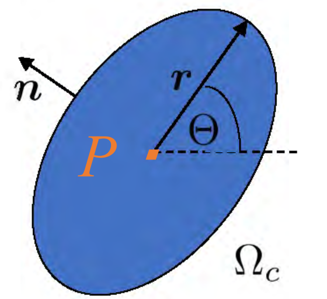

u；水中に展開した樟脳の濃度

$U \in \boldsymbol{R}^N$

$$\begin{cases} \dfrac{dP}{dt} = \displaystyle\int_{\partial\Omega_c} \gamma_1(U)\boldsymbol{n}dl, \\ \dfrac{d\Theta}{dt} = \displaystyle\int_{\partial\Omega_c} \gamma_2(U)(\boldsymbol{r}\times\boldsymbol{n})dl, \\ U_t = D\Delta U + F_0(U) + F_1(\boldsymbol{x}, P, \Theta), \end{cases}$$

物理法則に基づく部分は採用

化学反応系と考えられる部分は
ブラックボックス化して一般形に

樟脳片がない場合のゼロ解の大域的吸引性だけ仮定:実験により検証可能?

ブラックボックス部分の仮定

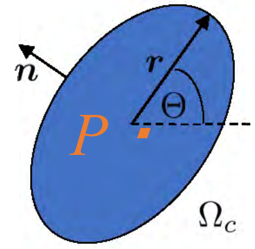

$$\begin{cases} \dfrac{dP}{dt} &= \displaystyle\int_{\partial\Omega_c} \gamma_1(U)\boldsymbol{n}dl, \\ \dfrac{d\Theta}{dt} &= \displaystyle\int_{\partial\Omega_c} \gamma_2(U)(\boldsymbol{r}\times\boldsymbol{n})dl, \\ U_t &= D\Delta U + F_0(U) + F_1(\boldsymbol{x}, P, \Theta), \end{cases}$$

U ; 水中に展開・昇華する樟脳に関連する項

樟脳片が固定された場合の定常解の線形安定性だけ仮定: 実験により検証可能?

$$U_t = D\Delta U + F_0(U) + F_1(\boldsymbol{x}, O, 0)$$

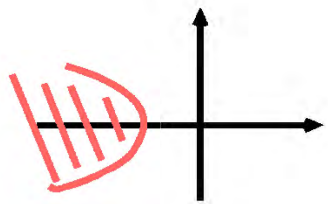

仮定: $^\exists S(\boldsymbol{x})$ s.t. $0 = D\Delta S + F_0(S) + F_1(\boldsymbol{x}, O, 0)$

$L := D\Delta + F_0'(S)$ $\quad \sigma(L) \subset \{Re(\lambda) < -\gamma_0\}$ $(^\exists\gamma_0 > 0)$

$$U(t, \boldsymbol{x}) \to S(\boldsymbol{x}) \ (t \to \infty)$$

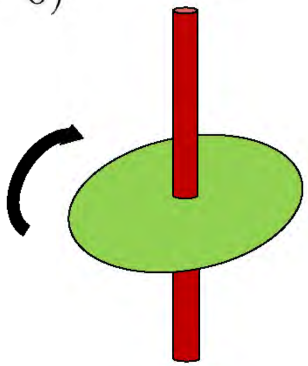

樟脳　Part II

$$
\begin{cases}
\dfrac{dP}{dt} &= \displaystyle\int_{\partial\Omega_c} \gamma_1(U)\boldsymbol{n}dl, \\
\dfrac{d\Theta}{dt} &= \displaystyle\int_{\partial\Omega_c} \gamma_2(U)(\boldsymbol{r}\times\boldsymbol{n})dl, \\
U_t &= D\Delta U + F_0(U) + F_1(\boldsymbol{x}, P, \Theta),
\end{cases}
$$

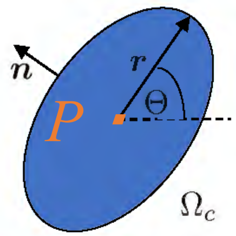

Ifγ_1 and γ_2 are sufficiently small, the camphor tip is asymptotically stable.

$$\Gamma_0 := \{r_0\boldsymbol{e}(\theta)\}$$

$$\Gamma_\varepsilon := \{(r_0 + \varepsilon h(\theta))\boldsymbol{e}(\theta)\}$$

$$0 < \varepsilon << 1,\ h(\theta) = \cos m\theta$$

微小変形

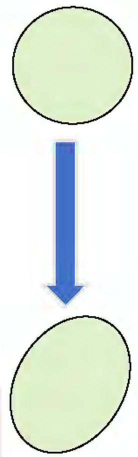

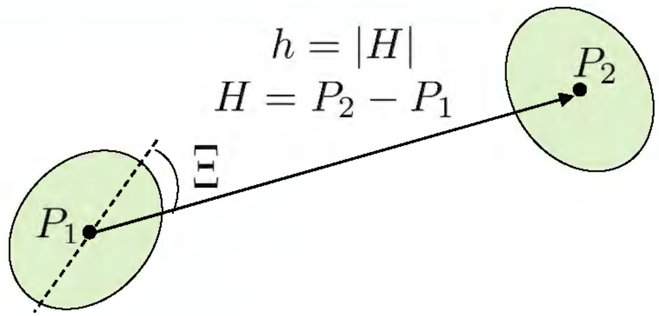

$$\frac{d}{dt}\Xi = \frac{\varepsilon}{\sqrt{h}}e^{-\alpha h}N_m \sin m\Xi$$

$$N_m < 0\ (N_m > 0) \Rightarrow \Xi \to 0\ (\pm\frac{\pi}{m})\ \text{as}\ t \to \infty$$

Equation of interaction

$$a_{33}\dot{\Theta}_1 = \langle\, \overline{L}\, \overline{S}_2, \overline{\Phi}_3^* \,\rangle_2$$

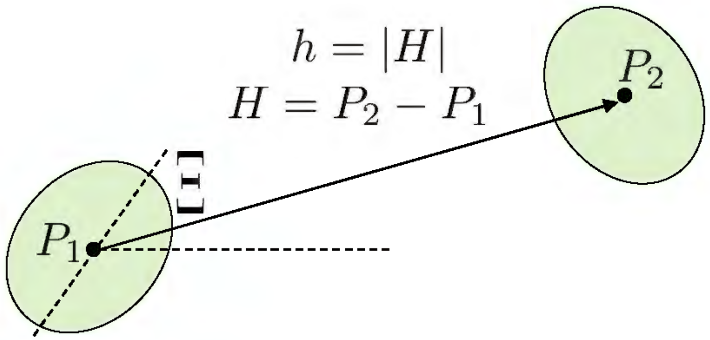

Theorem

$$\boxed{\frac{d\Xi}{dt} = \frac{\varepsilon}{\sqrt{h}} e^{-\alpha h} N_m \sin m\Xi + O(\varepsilon^2)}$$

$$\begin{aligned} N_m \quad := \quad & -\int_0^\infty \int_0^{2\pi} r \,\langle\, \boldsymbol{c}_0, \{F_0'(S_0(r)) - F_0'(0)\}\boldsymbol{\zeta}_1^*(r) \,\rangle\, e^{\alpha r \cos\theta} \cos m\theta d\theta dr \\ & -m r_0 \,\langle\, \boldsymbol{c}_0, \gamma_2'(W_0(r_0)) \,\rangle \int_0^{2\pi} e^{\alpha r_0 \cos\theta} \cos m\theta d\theta \end{aligned}$$

Note:

$$\Gamma_0 := \{r_0 \boldsymbol{e}(\theta)\}$$

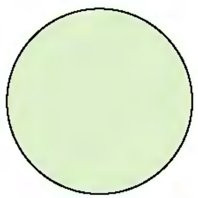

Circle with radius r_0

$$\Gamma_\varepsilon := \{(r_0 + \varepsilon \cos m\theta)\boldsymbol{e}(\theta)\}$$

Motion of Interaction

$$\boxed{\frac{d\Xi}{dt} = \frac{\varepsilon}{\sqrt{h}} e^{-\alpha h} N_m \sin m\Xi}$$

$$\Gamma_\varepsilon := \{(r_0 + \varepsilon \cos m\theta)\boldsymbol{e}(\theta)\}$$

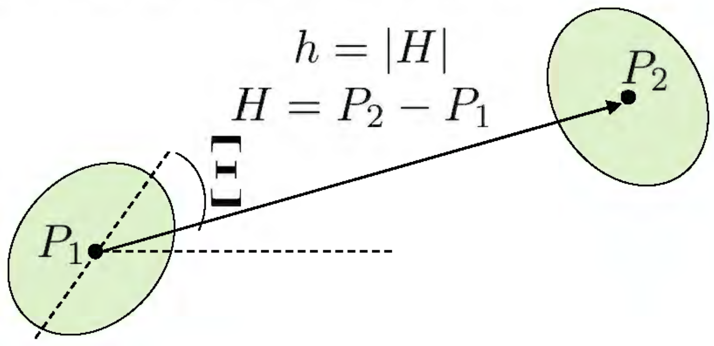

$N_m < 0,\ N_m > 0$

$$\boxed{\Xi \to 0,\ \pm\frac{\pi}{m}}$$

Ex. $m = 2$ (ellipse)

$$\Xi \to 0,\ \pm\frac{\pi}{2}$$

Apsis or minor axis

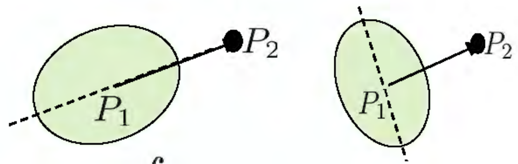

Note: $\Theta = \Theta_2 - \Theta_1$ appears in $O(\varepsilon^2)$

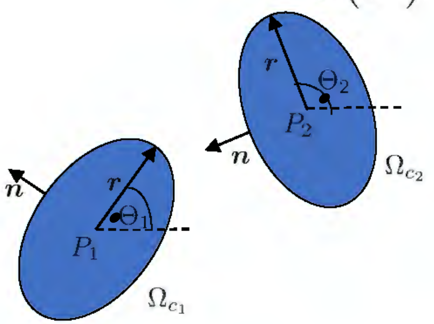

<u>Prop.</u>

$$\begin{cases} \dfrac{dP}{dt} &= \displaystyle\int_{\partial\Omega_c} \gamma_1(u)\boldsymbol{n}dl, \\ \dfrac{d\Theta}{dt} &= \displaystyle\int_{\partial\Omega_c} \gamma_2(u)(\boldsymbol{r}\times\boldsymbol{n})dl, \\ u_t &= \Delta u - u + f(\boldsymbol{x}, P, \Theta), \end{cases}$$

then

$$\boxed{N_m = 2\pi I_m(\alpha r_0) > 0,\ \Xi \to \frac{\pi}{m}}$$

m次の第1種変形ベッセル関数

E. Nagayama, Kitahata, Koyano 2018

Motion of interaction : Mode 2

$$\frac{d\Xi}{dt} = \frac{\varepsilon}{\sqrt{h}} e^{-\alpha h} N_2 \sin 2\Xi$$

$m = 2$ (ellipse)

$$N_2 > 0,\ \Xi \to \frac{\pi}{2}$$

$$\Gamma_\varepsilon := \{(r_0 + \varepsilon \cos 2\theta)\boldsymbol{e}(\theta)\}$$

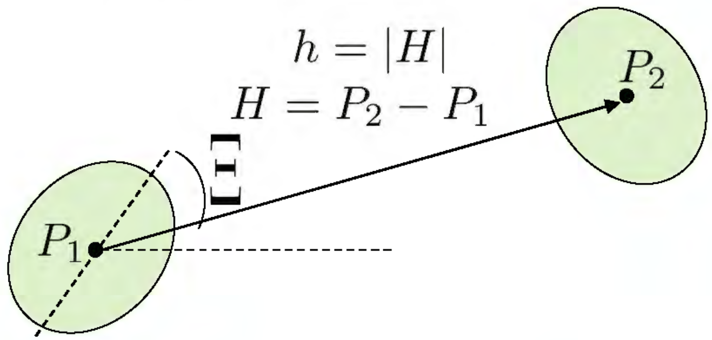

Note: $\Theta = \Theta_2 - \Theta_1$ appears in $O(\varepsilon^2)$

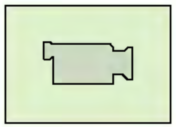

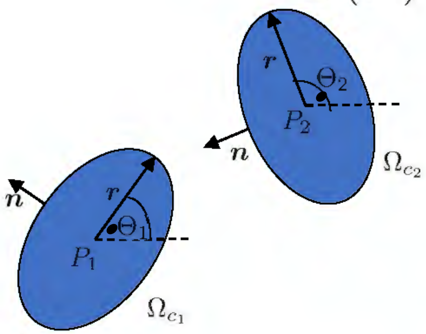

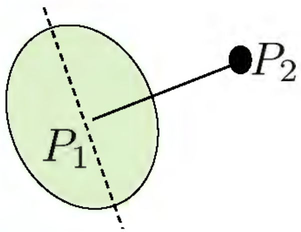

minor axis

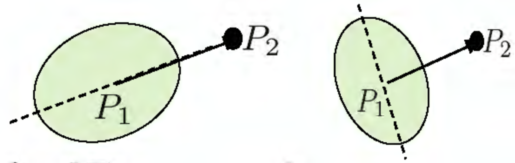

$$\begin{cases} \dfrac{dP}{dt} &= \displaystyle\int_{\partial\Omega_c} \gamma_1(u)\boldsymbol{n}\,dl, \\ \dfrac{d\Theta}{dt} &= \displaystyle\int_{\partial\Omega_c} \gamma_2(u)(\boldsymbol{r} \times \boldsymbol{n})\,dl, \\ u_t &= \Delta u - u + f(\boldsymbol{x}, P, \Theta), \end{cases}$$

Motion of interaction : Mode 3

$$\frac{d\Xi}{dt} = \frac{\varepsilon}{\sqrt{h}} e^{-\alpha h} N_3 \sin 3\Xi \quad \Rightarrow \quad N_3 > 0,\ \Xi \to \frac{\pi}{3}$$

$$\Gamma_\varepsilon := \{(r_0 + \varepsilon \cos 3\theta)\boldsymbol{e}(\theta)\}$$

$$\left\{ \begin{array}{lll} \dfrac{dP}{dt} & = & \displaystyle\int_{\partial\Omega_c} \gamma_1(u)\boldsymbol{n}dl, \\ \dfrac{d\Theta}{dt} & = & \displaystyle\int_{\partial\Omega_c} \gamma_2(u)(\boldsymbol{r}\times\boldsymbol{n})dl, \\ u_t & = & \Delta u - u + f(\boldsymbol{x}, P, \Theta), \end{array} \right.$$

$m = 3$

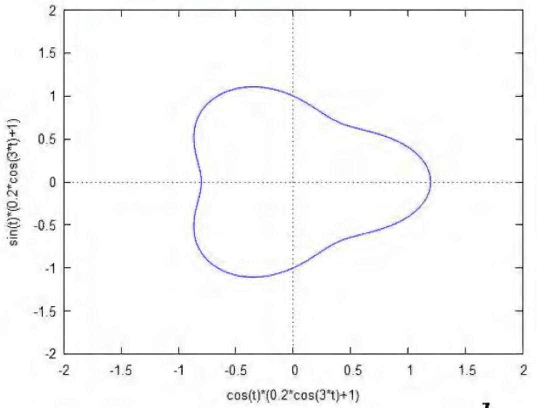

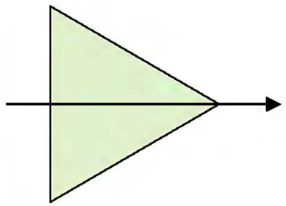

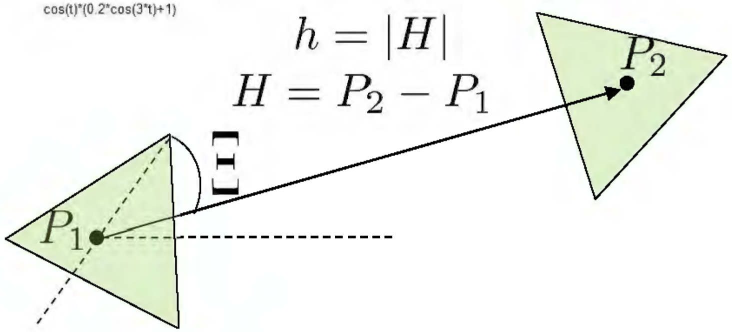

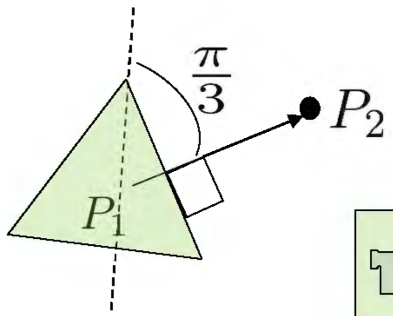

Repulsive interaction

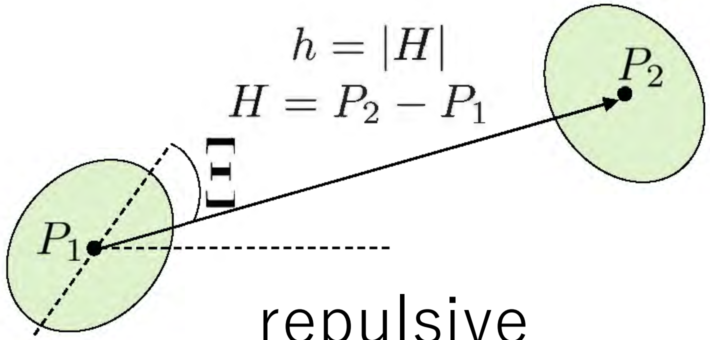

repulsive

experiment

$$
\begin{cases}
\dfrac{dP}{dt} = \displaystyle\int_{\partial\Omega_c} \gamma_1(u)\boldsymbol{n}dl, \\
\dfrac{d\Theta}{dt} = \displaystyle\int_{\partial\Omega_c} \gamma_2(u)(\boldsymbol{r}\times\boldsymbol{n})dl, \\
u_t = \Delta u - u + f(\boldsymbol{x}, P, \Theta),
\end{cases}
$$

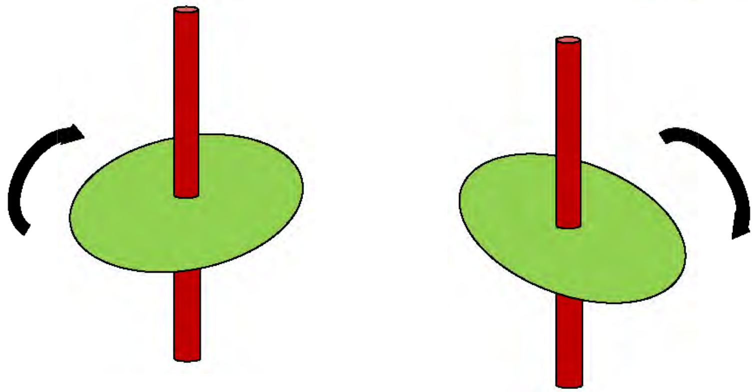

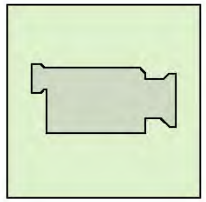

Fix centers $\Longrightarrow$ $\gamma_1 = 0$

Experiment

実験内容

＊楕円形樟脳粒を水に1つ浮かべて
自発回転しないことを確認

＊楕円形樟脳粒を純水に2つ浮かべて
向きの時間変化を観察

樟脳ろ紙同士の距離の変更は
軸の位置を変化させることで実現

楕円形樟脳粒同士の重心間距離を変化させて、
向きの揃う様子を観察

楕円形樟脳粒を適当な向きに固定しておいて、
離したあとの様子を観察（安定性のチェック）

楕円形の樟脳粒の作製

① 楕円形ろ紙に
樟脳メタノール溶液を
染み込ませる

② メタノールを揮発させる

樟脳も揮発していくが、
メタノールのほうが揮発が早い

③ 樟脳の染み込んだろ紙が完成！

樟脳ろ紙の乾燥過程での重量変化

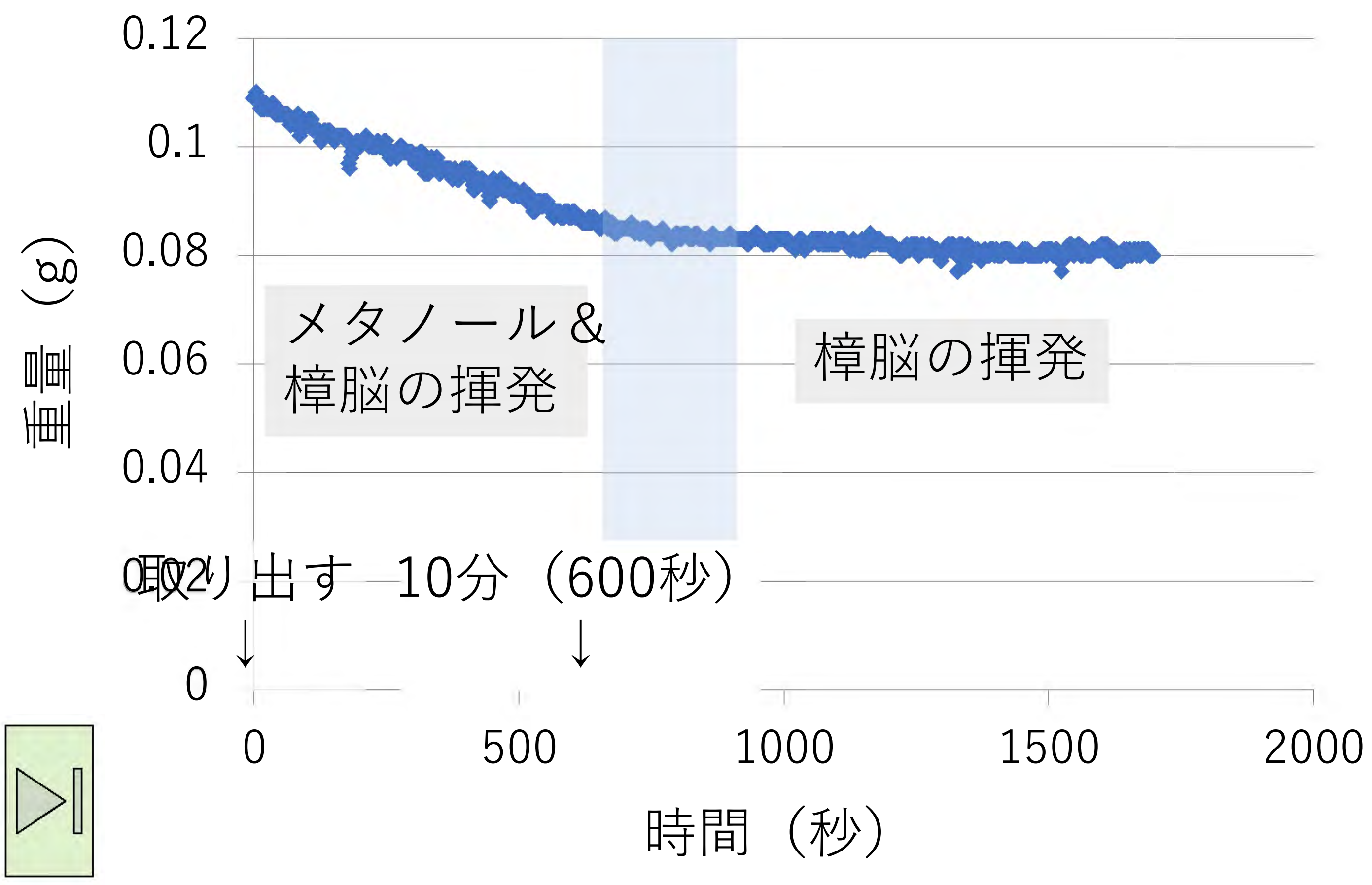

樟脳ろ紙を水面に浮かべた様子

ろ紙の穴に軸を通して
重心位置を固定
（※回転は可能）

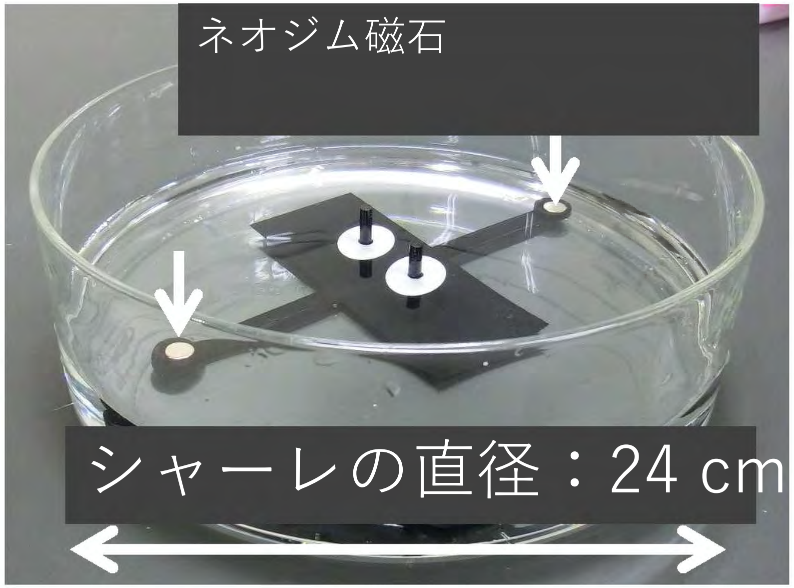

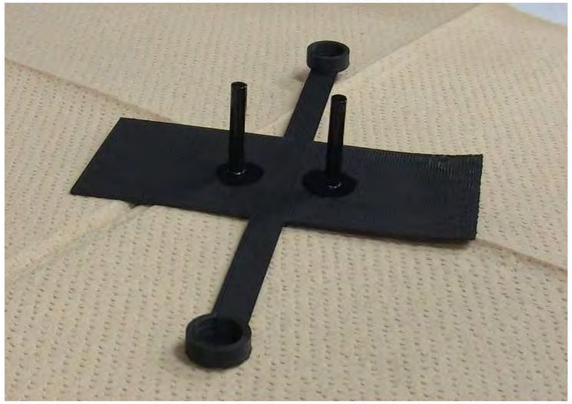

３Dプリンタで作製

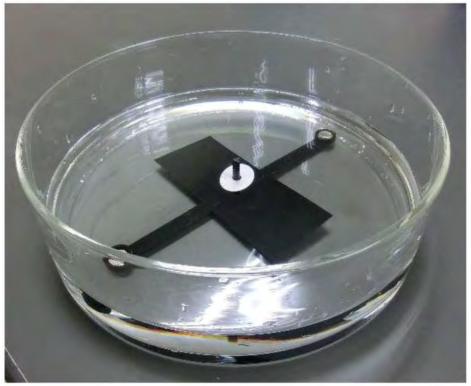

実験系の構築

光源を上から当てると
水面でよく反射してしまうので、
反射板（白い紙）を介して照らす

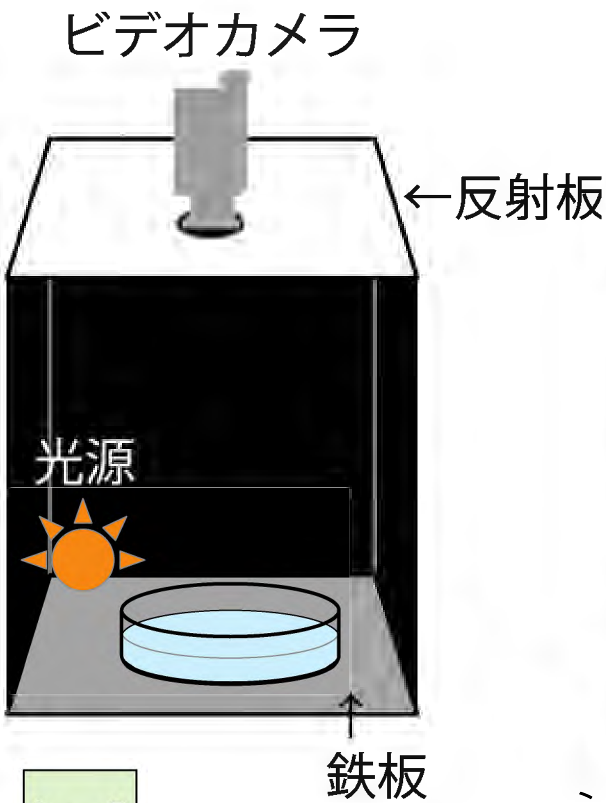

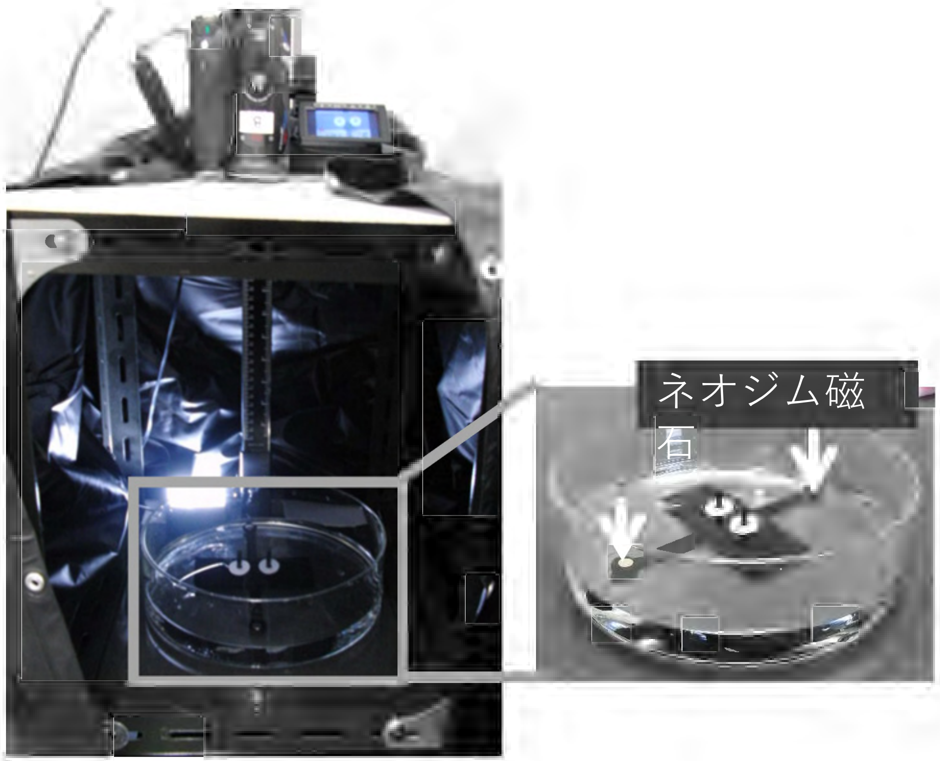

ネオジム磁石と鉄板が引き合うことで
３Ｄプリンタで作ったシステムが固定される

Check of the stationary state

Aspect 5:6

Aspect 3:4

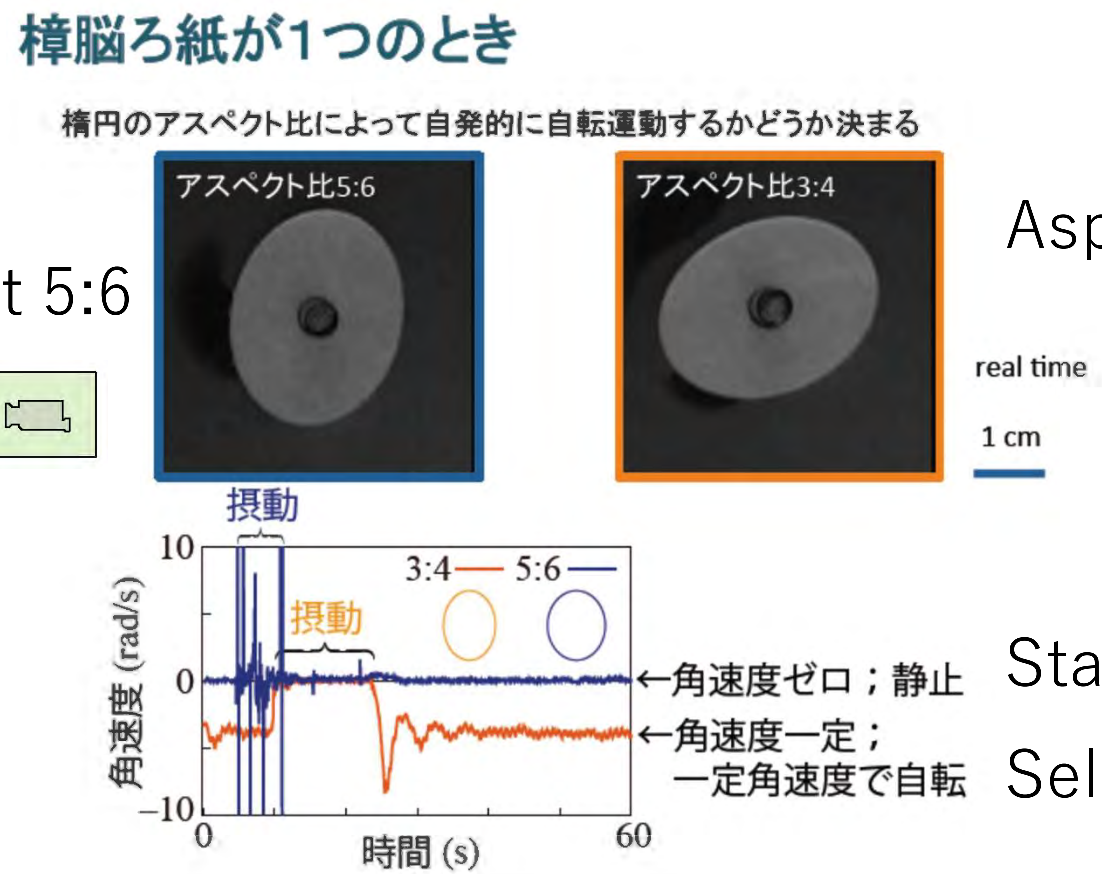

Stationary

Self rotating

Interaction of two camphors

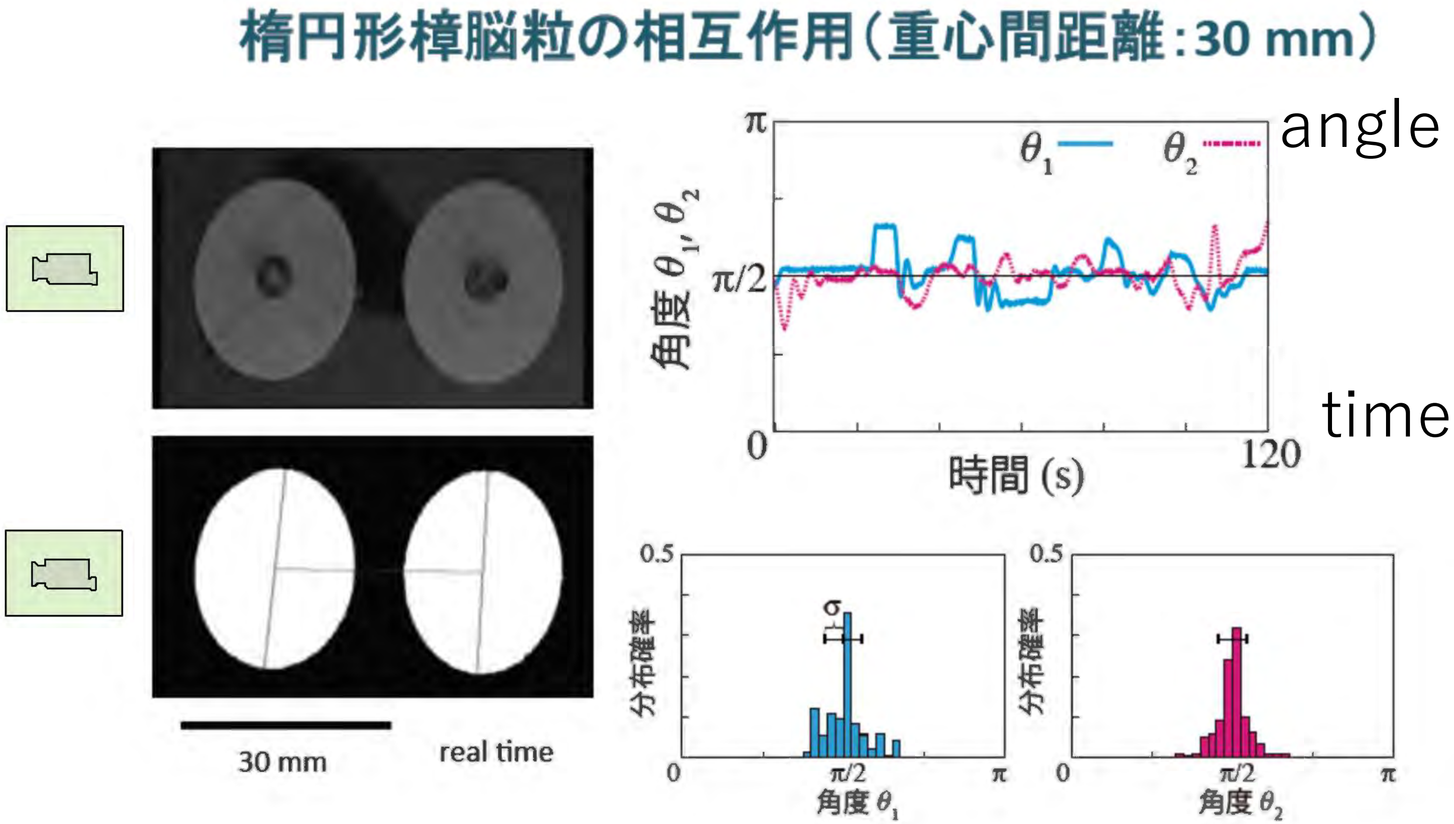

Check of the stability 1)

Arbitral initial states

安定性の確認1

適当な向きに固定しておいてから離す

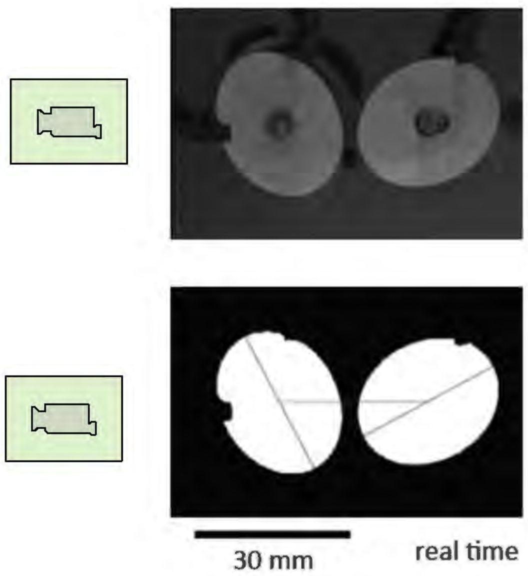

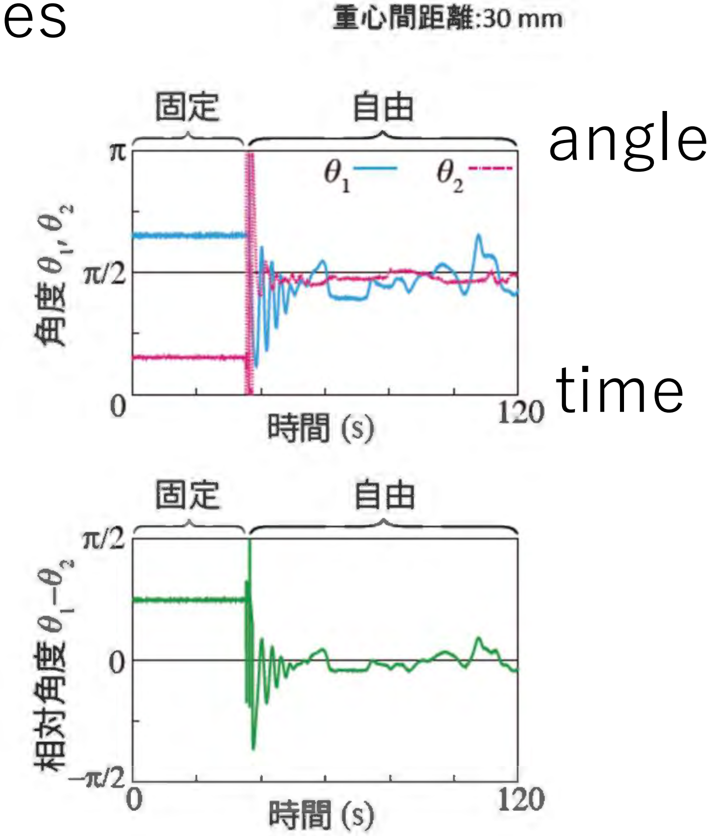

Check of the stability 2)

Adding perturbation

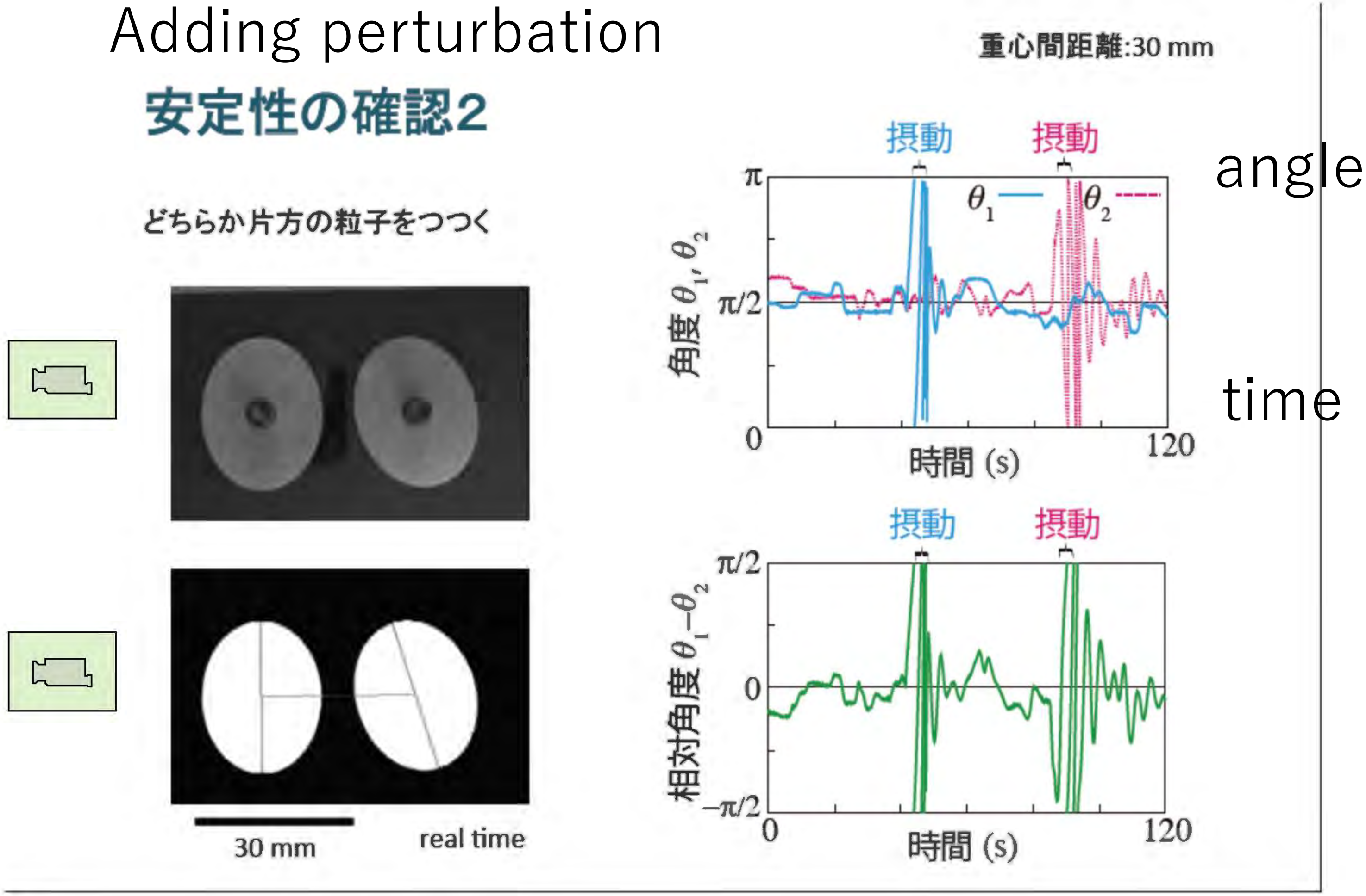

参考文献

[1] Xinfu Chen, S.-I. Ei and M. Mimura, SELF–MOTION OF CAMPHOR DISCS -MODEL AND ANALYSIS-, NETWORKS AND HETEROGENEOUS MEDIA Volume 4, Number 1 (2009), 1-18.

[2] J. Carr and R. L. Pego, Metastable patterns in solutions of $u_t = \varepsilon^2 u_{xx} + f(u)$, Comm. Pure Appl. Math., 42 (1989), 523-576.

[3] A. Doelman, R. A. Gardner and T. J. Kaper, Stability analysis of singular patterns in the 1-D Gray-Scott model, Physica D, 122 (1998), 1-36.

[4] 栄伸一郎「縮約理論」『非線形・非平衡現象の数理 4—パターン形成とダイナミクス』（三村昌泰編）第 4 章，東京大学出版会，2006 年.

[5] S.-I. Ei, The motion of weakly interacting pulses in reaction-diffusion systems, J.D.D.E. 14(1) (2002), 85-137. DOI: 10.1023/A:1012980128575

[6] S.-I. Ei, H. Ikeda and T. Kawana, Dynamics of front solutions in a specific reaction-diffusion system in one dimension, Japan J. Ind. Appl. Math. 25 (2008), 117-147.

[7] S.-I. Ei and T. Ishimoto, Dynamics and their interaction of spikes on smoothly curved boundaries for reaction-diffusion systems in 2D, Japan. J. Ind. Appl. Math. 30 (2013), no. 1, 69 - 90. https://doi.org/10.1007/s13160-012-0088-7 https://link.springer.com/article/10.1007

[8] S.-I. Ei and T. Ishimoto, Effect of boundary conditions on the dynamics of a pulse solution for reaction-diffusion

systems, NETWORKS AND HETEROGENEOUS MEDIA, Volume 8, Number 1, March (2013), pp. 191- 209. http://dx.doi.org/10.3934/nhm.2013.8.191

[9] S.-I. Ei, Y. Nishiura and K. Ueda, 2^n-splitting or Edge-splitting, Japan J. Ind. Appl. Math. 18(2) (2001), 181-205.

[10] S.-I. Ei, H. Kitahata, Y. Koyano and M. Nagayama, Interaction of non-radially symmetric camphor particles, Physica D 366 (2018), 10-26. https://doi.org/10.1016/j.physd.2017.11.004

[11] S.-I. Ei, M. Mimura and M. Nagayama, Pulse-pulse interaction in reaction-diffusion systems, Physica D 165 (2002), 176-198.

[12] S.-I. Ei, M. Mimura and M. Nagayama, Interacting Spots in reaction diffusion systems, DCDS 14 (2006), 31-62.

[13] S.-I. Ei and T. Ohta, Equation of motion for interacting pulses, Physical Review E vol. 50(6), 4672-4678, 1994.

[14] S.-I. Ei and J. Wei, Dynamics of metastable localized patterns and its application to the interaction of spike solutions for the Gierer-Meinhardt systems in two spatial dimension, Japan J. Ind. Appl. Math. 19(2) (2002), 181-226.

[15] G. Fusco and J. Hale, Slow motion manifold, dormant instability and singular perturbations, J. Dynamics and Differential Equations, 1 (1989), 75-94

[16] D. Henry, Geometric theory of semilinear parabolic equations, Lecture Notes in Mathematics 840, Springer-Verlag, 1981.

[17] K. Iida, H. Kitahata, M. Nagayama, Theoretical study on the translation and rotation of an elliptic camphor particle, Physica D 272 (2014) 39-50.

[18] H. Ikeda and S.-I. Ei, Front dynamics in heterogeneous diffusive media, Physica D 239 (2010), 1637-1649.

[19] Kota Ikeda, Shin-Ichiro Ei, Center Manifold Theory for the Motions of Camphor Boats with Delta Function, Journal of Dynamics and Differential Equations (2020), https://doi.org/10.1007/s10884-020-09824-9

[20] Y. Kan-on, Parameter dependence of propagation speed of travelling waves for competition-diffusion equations, SIAM J. Appl. Math. 26 (1995), 340-363

[21] 近藤滋, 波紋と螺旋とフィボナッチ, 秀潤社, 2013.

[22] K. Kawasaki and T. Ohta, Kink dynamics in one-dimensional nonlinear systems, Physica 116A (1982), 573-593.

[23] 三村昌泰, 枯草菌のコロニーパターンの多様性 (1), 連載第 1 回「数理モデルができるまで」, 数学セミナー 4 月号 (2020).

[24] 三村昌泰, 枯草菌のコロニーパターンの多様性 (2), 連載第 2 回「数理モデルができるまで」, 数学セミナー 5 月号 (2020).

[25] 三村昌泰, 宮路智行, 自己駆動粒子のビリヤード問題 (1), 連載第 7 回「数理モデルができるまで」, 数学セミナー 1 月号 (2021).

[26] 三村昌泰, 宮路智行, 自己駆動粒子のビリヤード問題 (2), 連載第 8 回「数理モデルができるまで」, 数学セミナー 2 月号 (2021).

[27] 森田 善久, 反応拡散方程式におけるフロント全域解, レクチャーノート, た応用数学勉強会 2019.

[28] 村川秀樹, Fast Reaction Limit of Reaction-diffusion Systems and Approximations to Nonlinear Diffusion Problems, 応用数学勉強会 2019 レクチャーノート.

[29] A. M. Turing, The Chemical Basis of Morphogenesis, Philosophical Transactions of the Royal Society of London, Series B, Biological Sciences, Vol. 237, 37-72（1952）.